The potential of Fluid Dynamic Absorbers for railway vehicle suspensions

Institute of System Dynamics and Control, German Aerospace Centre (DLR)

July, 2016.

By
Visakh V Krishna

Department of Aeronautical and Vehicle Engineering
KTH Royal Institute of Technology
SE-10044, Stockholm,Sweden.

Preface

This MSc thesis work is a part of my academic curriculum on rail vehicle engineering.

I am pursuing my master degree in vehicle engineering at the School of Engineering Sciences of KTH Royal Institute of Technology, Stockholm. I got the opportunity to conduct my thesis work at the Institute of System Dynamics and Control of DLR in Oberpfaffenhofen, Germany. It is primarily done in the field of rail vehicle suspension as a part of DLR's Next Generation Train initiative.

This experience is highly enriching and valuable in terms of the amount of knowledge I was able to gain over the entire thesis work. Moreover, I was able to obtain exposure on how it is to work in a research organization, co-ordinate with experts in different fields and proceed towards my goal.

Acknowledgement

I would like to thank Prof. Sebastian Stichel of the KTH Railway Group and Dr.-Ing. Andreas Heckmann, Institute of System Dynamics and Control, DLR for giving me this opportunity to work on the project.

I also thank Dr. Mats Berg and Dr. Carlos Casanueva for supporting and invoking interest in the field during my academic period in KTH.

I am also grateful to my colleagues Daniel, Gustav, Tillman, Andreas and my fellow interns for providing me with valuable inputs and help over the course of my thesis work.

Finally I would also like to extend my gratitude to my parents, my brother and all my friends for supporting and encouraging me over the course of the entire program.

Abstract

The main running objectives concerning the vertical dynamics of passenger rail vehicles are ride comfort and safety. The goal of this thesis is to employ the use of a Fluid Dynamic Absorber to minimize the vertical acceleration of the car body while minimizing the dynamic force fluctuations in the wheel rail contact. The Fluid Dynamic Absorber is a device which employs a tube with a varying cross section containing oscillating fluid. The device is characterized by two effects: The inertia effect of the oscillating fluid in the varying cross section and the damping effect due to the pressure losses during the fluid flow. It is introduced as a potential damping device for automobiles and also for earthquake resistant buildings. The work encompasses the creation of a linearized approximation of the non-linear model for parameter selection. Then, a non-linear model is built with the help of the Modelica language for use in time simulation of quarter-car models in the Dymola interface. A generalized design methodology for the device is then developed with the help of design procedures used for common tuned mass dampers and liquid column dampers. Finally, the non-linear model built using the Dymola interface is also exported for use in the full-car model in Simpack using Functional Mock-up Interface. A reduction of about 4% to 5% in the magnitude of the root mean square of the carbody acceleration was observed while the wheel-rail dynamic forces remained the same. Further improvement possibilities and the parameters influencing the vertical dynamic behavior of the vehicle are discussed.

Contents

List of Figures

List of Tables

1 Introduction

This chapter contains a brief introduction to the Next Generation Train (NGT) project and the Fluid Dynamic Absorber. The objectives of the thesis work are mentioned. The methodology employed along with a brief overview of the report contents are discussed. It also provides an overview of the tools and environments used over the course of the thesis work.

1.1 Background

The thesis work is concerned with bringing together the Next Generation Train project in the German Aerospace Centre (DLR) and the application of the Fluid Dynamic Absorber, a device aimed for use in vehicle suspensions.

1.1.1 Next Generation Train Project

The New Generation Train project [20] is an inter-disciplinary project undertaken by DLR with the objective of making the trains of the future more safe, efficient and eco-friendly.

Figure 1.1: Next Generation Train concept

The main objective is to raise the maximum running speed by 25 percent without compromising the safety. The requirements for the vehicles have been changing over the years.

The importance of life-cycle costs, energy costs, requirements of safety and the ride comfort standards are some of the main design points considered. The NGT project strives to bring DLR's expertise in rail vehicle engineering to focus on the whole rail vehicle system with focus on track and automatic train control systems as well.

With the changing requirements of the vehicles over the years, the importance of the life cycle costs increasing, rising energy costs, stringent requirements of safety and increasing standards of passenger comfort,

Primarily, attention is given to modular designs, intelligent system integration and a whole-system approach to the treatment of design to promote synergy between various sub-systems. The different areas of research included in the project can be classified as:

1. Lightweight construction in the Next Generation Train
2. Aerodynamics
3. Simulation of passenger flows
4. Lifecycle cost and High speed route evaluation
5. Simulating energy flows
6. System dynamics of wheels and rails.

The thesis is carried out in the domain of system dynamics of wheels and rails at the Institute of System Dynamics and Control at the Oberpfaffenhofen facility near Munich. The main vision of the NGT project is to incorporate unconventional methods and designs into the design of the rail vehicle and explore the associated improvements on the vehicle performance. The thesis starts with a primary focus on implementing the Fluid Dynamic Absorber for the multi body simulation of the NGT running gear.

1.1.2 Fluid Dynamic Absorber (FDA)

The Fluid Dynamic Absorber is a device proposed by the chair of fluid systems, TU Darmstadt as a potential damping device for use in earthquake resistant buildings [11] and automotive applications [22]. The device utilizes the phenomena of hydrostatic transmission to reduce the weight and the material required hence proving to be an improvement of the classical dynamic absorber [12]. [11] employs the device for the potential use for earthquake resistant buildings while clearly underlining the advantage of lower damping mass required compared to the existing designs of tuned mass dampers while not compromising with the damping process. The theory is briefly discussed with a parameter selection based on the J.P. Den Hartog criteria [12] for a common tuned mass damper. The theory is validated with help of a scaled down model of a building emphasizing the potential of the device and further improvements.

Taking the application of the Fluid Dynamic Absorber further in [22], the authors have discussed the twin objective optimization of road safety and comfort for a race car through the analysis of a quarter-car model. The results were exhibited with a pareto –curve with the criterion of comfort represented by the standard deviation in the carbody acceleration in the y-axis and the criteron of safety represented by the standard deviation of the dynamic force

in the tyre-road contact divided by the static load on the x-axis. While the pareto curve represents the trade-off between comfort and safety for different stiffness and damping values for a conventional suspension, the suspension configuration implemented with the addition of the Fluid Dynamic Absorber is able to lie outside the pareto-optimum generated with the conventional suspension.

This improvement is aimed to be implemented in the case of railway vehicle suspension as well, hence becoming the core motivation of the thesis statement.

1.2 Objective of the thesis

With the background of the NGT project and the Fluid Dynamic Absorber, the following points materialize as the objectives of the thesis work:

1. Perform a comprehensive fundamental linear analysis using quarter-car models in order to expose promising design configurations, application fields and component layoffs.
2. Perform a literature and internet survey on the state of the art design and application of hydraulic dampers in railway running gears.
3. Development and non-linear multibody analysis of one exemplary application to DLR's Next Generation Train running gear.

The thesis is also supposed to answer questions such as

- Can the device be applied in the suspension of high speed railway vehicles?
- What may promising applications look like? E.g. regarding suspension topology, component dimensions, etc.
- Which changes in today's running gear design are required to facilitate the introduction of the Fluid Dynamic Absorber?

1.3 Methodology and content description

The flow chart (Figure 1.2) represents the major phases of the methodology and corresponding tools used in each phase.The first two phases indicate the stages in which the device is understood, formulated and checked for consistency between the results found from the literature and the derived equations. The third and fourth phase indicate stages in which various parameters of the device are utilized and tuned for use in the rail vehicle suspension.

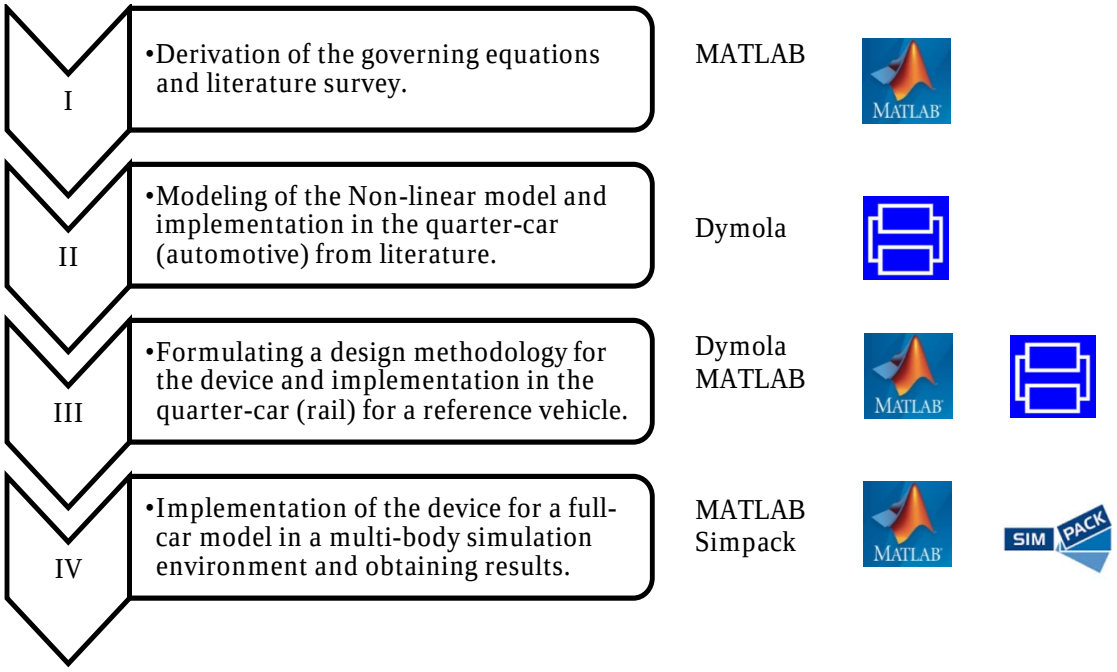

Figure 1.2: Methodology

Chapter 1 provides an introduction of the thesis work to be carried out.

Chapter 2 starts with a literature survey on conventional damping devices and existing High Speed Rail running gears. Then, the working principle of the Fluid Dynamic Absorber is understood. Comparison of the system of equations is done between a conventional suspension and a suspension with the Fluid Dynamic Absorber. By Section 2.3.4, the phase I as mentioned in Figure 1.2 is completed. Moving on further, the non-linear behavior of the Fluid Dynamic Absorber is designed in the Dymola environment. The chapter ends with the derivation of equations of motion for quarter-car model of rail vehicles, which will be used for linear analysis in the later chapters.

Chapter 3 employs the use of the Fluid Dynamic Absorber designed in Chapter 2 and the quarter-car model for the road vehicle from the literature survey [22] is constructed. Both linear analysis and non-linear time simulations are performed to validate the results obtained from the literature. With this chapter, phase II is completed.

Chapter 4 makes use of the observations from Chapter 3 and the design methodology of the device for use in rail vehicle suspensions is proposed. It is initially tested and verified on the quarter-car model of the Manchester benchmark model for time simulations. Then, it is applied on the quarter-car model of the Next Generation Train model for time simulations and results are discussed. This effectively concludes phase III.

In Chapter 5, the Functional Mock-up Interface is used to export a simplified model of the Fluid Dynamic Absorber from Dymola to the Simpack environment for performing time simulations on a full car model. Simulation cases are formulated and simulations performed. The results are further discussed, completing the objectives to conclude phase IV.

Chapter 6 mentions the activities performed to meet the thesis objectives and also discusses

the key conclusions at the end of the thesis work. Further, future possibilities and avenues for better design and improvement of the behavior of the device are discussed.

1.4 Overview of tools

A brief description about the tools used in the thesis and their capabilities are discussed. For preliminary investigation and simple models, MATLAB was used.

1.4.1 Dymola

Dymola (Dynamic Modelling Laboratory) is a modelling and simulation environment for modelling various kinds of physical systems. It supports hierarchical model construction, libraries to reuse components, connectors with physical relation definitions. Model libraries are available for different engineering domains. In the scope of this thesis work, the mechanics library has been dominantly used along with the combination of other libraries such as mathematical, interfaces, etc. The architecture of the Dymola environment and interface view is shown in Figure 1.3. The main feature of the modelling methodology is that the manual conversion of equations to a block diagram is replaced by the use of the automatic formula manipulation.

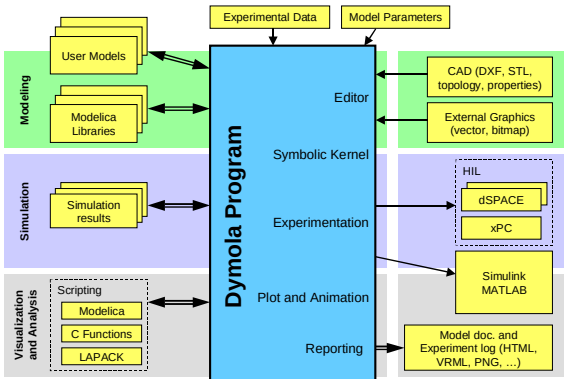

(a) Dymola architecture [19]

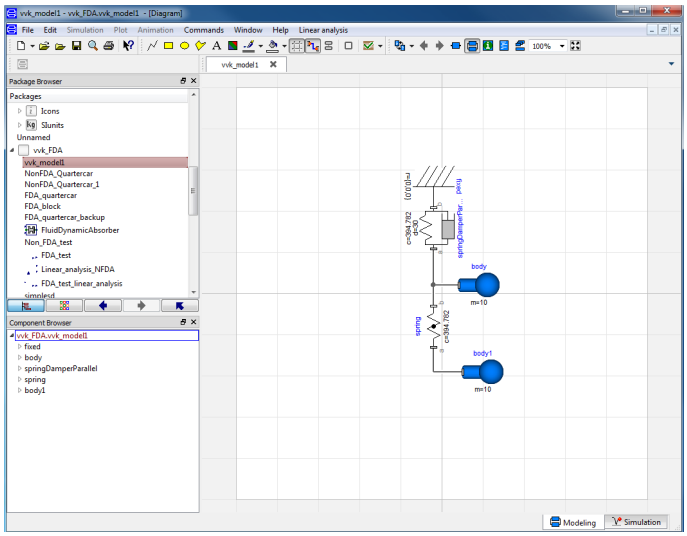

(b) Interface

Figure 1.3: Dymola

Dymola uses a modelling methodology comprising the object orientation and equations. The standard language used in formulating the physical relations between the objects is Modelica. It translates the Modelica equations and generates a corresponding C-code to run the simulation. This code can also be exported to other platforms like Simulink or used in Hardware-in-the-loop simulations. The script interface also allows managing simulation conditions and performing calculations. This feature is especially useful in case of parameter studies through multiple simulations.

Modelica [19] is an object-oriented language for modelling of large, complex and heterogeneous physical systems. It is a convenient standard language to use for multi-domain modelling like in the case of active systems for automotive and aerospace applications. The multi-domain feature also gives it a capability to be used in multi-level systems modelling and model-based systems engineering (MBSE). Any physical quantity can be represented as a physical quantity with appropriate units .The modelling process is improved because of the reusability of the components and that the manual manipulations are not required.

The Dymola environment has been actively used to model the non-linear Fluid Dynamic Absorber as will be seen in Section 2.4. Most of the quarter-car model simulations and analysis have been carried out in the Dymola environment.

1.4.2 Simpack

Simpack [28] is a multi-body simulation software used in the analysis and design of mechanical and mechatronic systems. It is mainly used in the automotive, railway and aerospace industries. Within these domains, Simpack can be used in different levels from the design of a single component to a complete system analysis. Apart from considering the internal dynamics, it can also include external conditions like aerodynamics, ground conditions, etc.

The applications of Simpack extend from simple eigen-value analysis to a full transient non-linear analysis. The MBS software is also capable of taking into account the high frequency vibrations in flexible bodies. One important aspect of Simpack in the rail domain is the ability to model wheel-rail contact and shock contact points (running over switches and crossings).

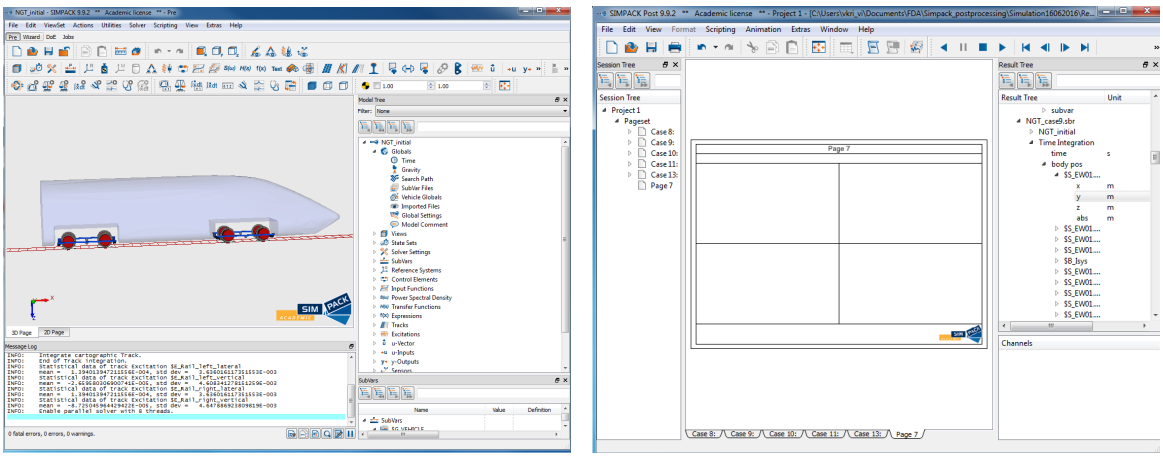

(a) Simpack working view (b) Simpack Post processor

Figure 1.4: Simpack

Simpack also has a lot of utilities like the comfort weighting filter standards (Wz, ISO, etc). Simpack is applied in the full-car simulation with the non-linear device and dynamic analysis performed and checked for improvements.

1.4.3 Functional Mock-up Interface

Functional Mock-up Interface (FMI) [30] is an independent standard to facilitate exchange of dynamic models and co-simulation. It was developed under the project MODELISAR under the leadership of Daimler AG. The primary goal of developing such a standard is to ease and support the exchange of simulation models between the Original Equipment Manufacturers (OEMs) and the suppliers.

While the development of tool-independent modelling languages (for e.g. Modelica) helps in model exchange between simulation tools, the modelling languages are to be supported in an interface which gives a possibility of making the exchange less complicated. A possible approach is to provide low-level interfaces to exchange these models easily.

As a result, Modelica tool providers (e.g. Dymola,AMESim), non-Modelica tool providers (e.g. Simpack) and some research institutes collaborated to form a standard interface defined as the Functional Mock-up Interface. This interface facilitates model exchange and co-simulation between various tools over various domains in a simpler way.

FMI is utilized to export the Modelica-built non-linear Fluid Dynamic Absorber model for quarter-car simulation from the Dymola environment to the non-Modelica based Simpack for a full-car simulation as will be discussed in more detail in the later Chapters.

Distribution of use

Table 1.1 gives a brief description of the operations performed with the respective tools in increasing complexity:

Table 1.1: Application of tools

MATLAB	• Preliminary investigation of data from literature survey • Transfer function generation of linear conventional suspension quarter-car models • Linearly approximated quarter-car system. • Parameter calculation of Fluid Dynamic Absorber. • Post processing of data obtained in Dymola simulations
Dymola	• Construction of the non-linear Fluid Dynamic Absorber model • Stochastically excited track tests of quarter-car models (both conventional and FDA) • Validation of device characteristics from literature • Validation of the linearly approximated system • Formulating the design methodology of the Fluid Dynamic Absorber for railway applications • Quarter-car parametric simulations. • Study of the improvements and identifying potential improvements in the quarter-car behaviour
Functional Mock-up Interface	• Creation of a simple approximated Functional Mock-up Unit of the non-linear Fluid Dynamic Absorber in Dymola. • Implementation of the imported Functional Mock-up Unit as a control element in the Simpack interface.
Simpack	• Simulation of full car model of the Next Generation Train running gear with conventional and the suspension with FDA. • Applying the comfort filters and calculating the standard comfort values.

2 Concept study

This chapter delves into the concepts involved in the thesis work. The vertical motion in conventional vehicle suspensions is studied. Then, the vertical motion with the application of a Fluid Dynamic Absorber is studied and compared with the former. The non-linear model is then designed in the Dymola environment as a component to be used in time simulations. Further, the system of equations for a quarter-car rail vehicle suspension is derived.

The quarter-car model comprises of a full car model divided symmetrically such that the model consists of a quarter of the mass and the suspension elements. The quarter-car model does not contain the geometrical effects of the carbody or the representation of the lateral or the longitudinal effects. But it provides a simple approach to study the multi-body dynamics in the vertical direction.

The literature survey over different domains was conducted before starting with the concept study. Fundamental concepts on dynamic analysis techniques and modelling procedures of vehicles from [3] and [8] were studied. The theory of tuned mass dampers and their applications were studied from [12], [18] [31] and [25]. These references will be cited throughout the corresponding sections.

2.1 Conventional suspension

The quarter-car model in case of a simple conventional suspension for a car (without secondary suspension) is studied initially to contrast with the suspension with the Fluid Dynamic Absorber. (See Figure 2.1)

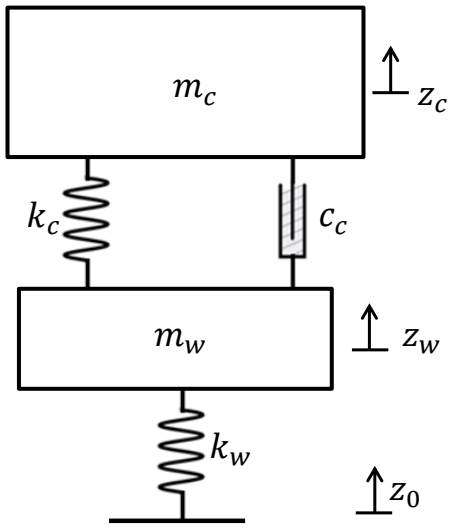

Figure 2.1: Quarter-car model with conventional suspension

where:
m_c is the mass of the carbody in the suspension model
m_w is the mass of the wheel
z_c, z_w represent their displacements respectively
z_0 represents the displacement generated by the surface irregularities
k_c and k_w represent the spring stiffness of the carbody suspension and the wheel respectively
c_c represents the damper coefficient of the suspension system.

The individual free body diagrams and their corresponding force components are shown in Figure 2.2

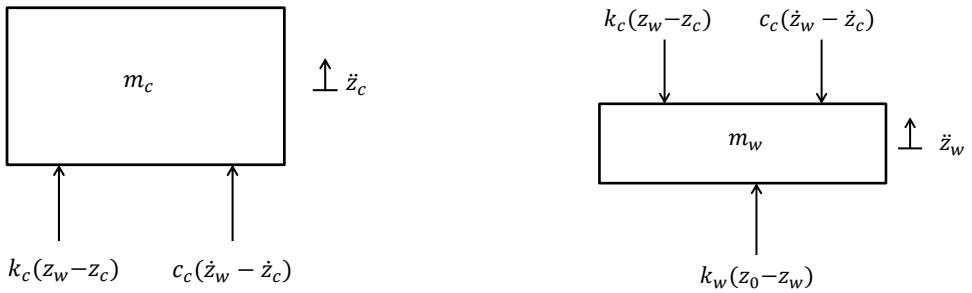

(a) Carbody (b) Tyre

Figure 2.2: Free Body diagrams

Solving the system for equilibrium, the following equations are derived:

$$\begin{bmatrix} m_c & 0 \\ 0 & m_w \end{bmatrix} \begin{bmatrix} \ddot{z}_c \\ \ddot{z}_w \end{bmatrix} + \begin{bmatrix} c_c & -c_c \\ -c_c & c_c \end{bmatrix} \begin{bmatrix} \dot{z}_c \\ \dot{z}_w \end{bmatrix} + \begin{bmatrix} k_c & -k_c \\ -k_c & k_c + k_w \end{bmatrix} \begin{bmatrix} z_c \\ z_w \end{bmatrix} = \begin{bmatrix} 0 \\ k_w z_0 \end{bmatrix} \tag{2.1}$$

2.2 Hydraulic damper

The hydraulic damper is a device used to damp the motion of oscillating masses linked by the suspension. They reduce the kinetic effects of running over an irregular surface, improving ride quality and reducing the force on the track. It is introduced as a part of both the primary and secondary suspensions of a rail vehicle to damp spring oscillations. The damper works by the principle of absorbing excess energy stored in the springs and dissipate it in the form of heat. The damping values are chosen according to the weight of the vehicle after considering both the loaded and unloaded scenarios.

2.2.1 Construction

The basic elements in a hydraulic damper are (See Figure 2.3 and Figure 2.4)

- Main piston consists of the primary valving components and is responsible for the major contribution to the damping forces.
- Gas separator/Separating piston is a piston that separates the gas from the oil.

- Pressure tube/Main piston tube is the cylindrical cross section that contains the main piston
- Reserve tube is the outer cylinder in a twin-tube damper and holds the extra fluid from the main tube during the oscillations of the main piston.

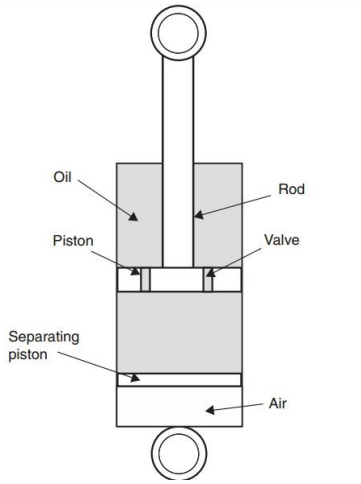

Figure 2.3: Monotube hydraulic damper [26]

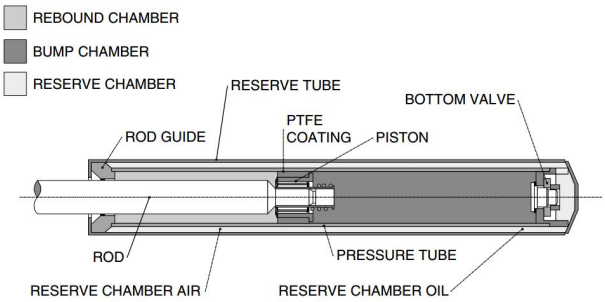

Figure 2.4: Twin-tube hydraulic damper [24]

Monotube damper [26] (Figure 2.3) is a gas-pressurized shock absorber consisting of a single tube. This tube, also called the pressure tube has two pistons- Working piston and Separating piston. They move relatively inside the pressure tube in response to track/road irregularities. The two pistons separate the gas and the liquid components in the cylinder. The monotube damper comparatively requires larger length compared to a twin-tube damper with similar performance. This generally makes it difficult for application in vehicle suspensions because of the spatial constraints. But, the monotube damper can be mounted from both the directions unlike a twin-tube damper. The pressure of the gas inside the monotube damper can be as high as 260-360 psi. This high pressure can also partly bear the weight of vehicle which is not the case for a twin-tube damper.

A basic twin-tube damper [24] (Figure 2.4) consists of two nested cylindrical tubes, the pressure tube and the reserve tube. There is a compression valve at the bottom end of the device. The valve controls the movement of the fluid between the tubes. When the piston

oscillates, the hydraulic fluid moves between the tubes through the valves, converting the kinetic energy into heat. The damping caused by flow through the valves is non-linear. But the cross section at the valves is changed with the flow rate. This compensates for the non-linear behavior and gives a linear damping force [32] within the operating speeds as seen in Figure 2.5. This gives rise to a damping force of the form:

$$F_d = C \times \dot{x} \tag{2.2}$$

where C is a constant damping coefficient and $\dot{x}$ is the relative velocity between the ends of the damper.

A small variation of the twin-tube damper is the Gas cell tube. The construction of this device is similar to the twin-tube damper but its reserve tube also contains low pressure Nitrogen. This reduces the foaming/aeration of the hydraulic fluid as a result of twin-tube over-heating. Most of the modern day vehicle suspensions apply this device for damping.

2.2.2 Dampers in railway vehicles

In Figure 2.5, working principle of a typical damper used in the secondary suspension of rail vehicles is described [16]. The basic dimensions and performance can be seen in Table 2.1 [16].

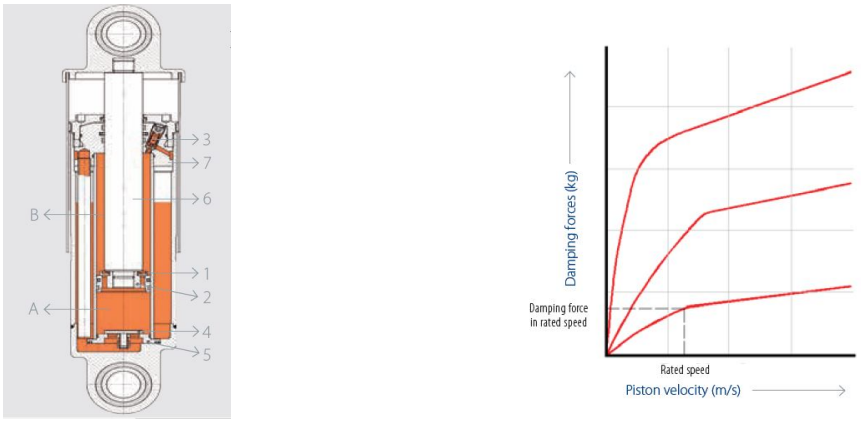

(a) Damper cross section (b) Performance curve

Figure 2.5: Model SDS- Knorr Bremse [16]

Table 2.1: Model SDS-Knorr Bremse - Data [16]

Application	Functional Principle	Stroke	Diameter	Damping force
Secondary and Primary damper: Vertical and Horizontal	Uni-directional oil flow, light design	50-300 mm	116 mm	up to 10 kN @ 0.1 m/s

Tension stroke: The check valve (1) in the piston (2) closes, and the oil is forced through the damping valve (3), thus the damping force is generated. Simultaneously, the check valve (4) in the cylinder bottom (5) opens, and space (A) below the piston is filled with oil.

Compression stroke: The check valve (4) in the cylinder bottom (5) closes. The oil from space (A) flows into space (B) through the opened check valve (1) of the piston (2). Due to the movement of the piston rod into the cylinder, the volume (A) decreases and the oil is again forced through the damping valve (3). Thus damping is accomplished.

From the performance curve in Figure 2.5b, it can be seen that the damping is approximately linear up to the rated speeds. This damper can be used for vertical and horizontal damping in rail vehicles.

Space availability in running gears

The dimensional constraints of the Fluid Dynamic Absorber were determined after considering the space available for a conventional damper. For this purpose, typical dimensions of dampers and the space availability in the existing running gears were studied. The Fluid Dynamic Absorber is applied in parallel to the secondary suspension as will be explained in Section 4.2. The product catalogues of bogies currently available in the market for High Speed Trains [1], [7] and [27] were used for the purpose.

Since the physical dimensions of the dampers were not explicitly given in the catalogues, approximate dimensions are obtained by comparing the wheel diameter and the damper in the scaled-down engineering diagrams given in Appendix A. The space availability for the FDA is checked for a maximum lateral dimension of 0.15 m. The vertical dimensions, available for the FDA assembly are given by the term FDA-L in Table 2.2. Cases where it is possible to add an extra FDA in parallel are indicated with $\times 2$.

Table 2.2: Comparison of space available in running gear for High Speed Trains

Model	**Operating speed (km/h)**	**Application**	**FDA-L (m)**
Alstom CL 334	360	P150	0.35×2
Siemens SF 500 TDG	350	ICE3	0.35×2
Alstom CL 511	320	P150	0.45
Bombardier Flexx fit	160-280	ICE1	0.35
Siemens SF 600 TDG	250	DB-VT605	0.3
Alstom CL 624	225-250	Trenitalia, RENFE	0.4
Bombardier Flexx link	160-250	REGINA	0.35
Alstom CL 623	225	West Coast Mainline (UK)	N/A
Siemens SF 5000 ETDG	200	Desiro	0.3
Alstom CL 347	200	X40/Coradia Duplex	0.4
Alstom X 200	160-200	Coradia Nordic	0.35
Alstom CL 541	160-200	Coradia Polyvalent	0.35

2.3 Fluid Dynamic Absorber

The construction of the Fluid Dynamic Absorber is depicted in Figure 2.6. In [22], the device is situated parallel to the suspension. The upper-frame of the Fluid Dynamic Absorber is attached to the carbody while the piston is connected to the wheel with a spring k_{pi}. To understand the mechanism of the device and integrate it with the quarter-car model, the following principles are used.

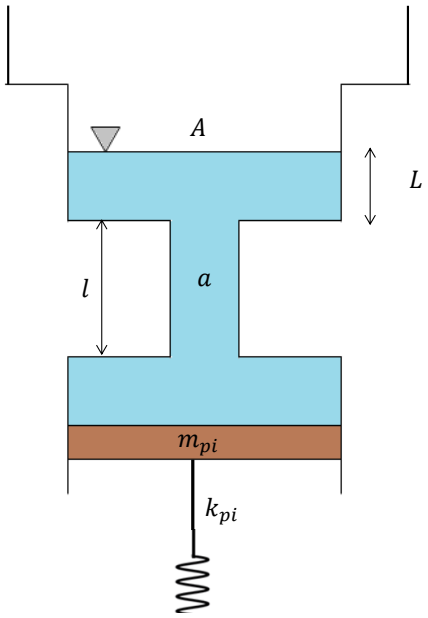

Figure 2.6: Fluid Dynamic Absorber

2.3.1 Fluid mechanics

Fluid mechanics and the related concepts were studied from [23], [5] ,[10], [14] and [29]. The principles used from the literature in the context of the Fluid Dynamic Absorber are explained. The damping and the inertial transmission effects by the device are the consequences of:

Bernoulli's theorem

The Bernoulli theorem [23] states, " For a perfect incompressible liquid, flowing in a continuous stream, the total energy of a particle remains the same, while the particle moves from one point to another."(See Figure 2.7)

It can be put mathematically as:

$$\frac{v^2}{2} + gz + \frac{p}{\rho} = constant. \tag{2.3}$$

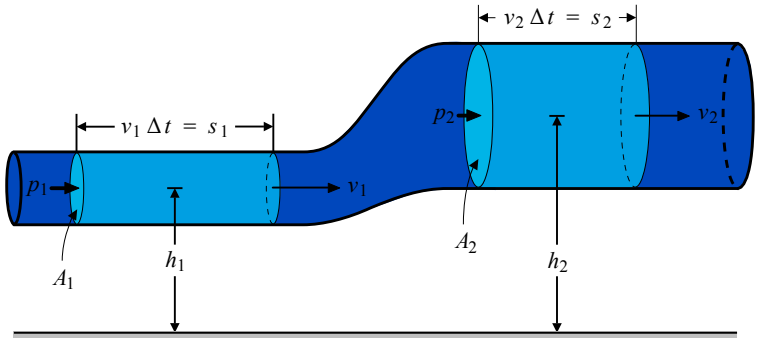

Figure 2.7: Bernoulli's principle

Continuity equation

The continuity equation is a consequence of the principle of conservation of mass for a fluid flowing through varying cross sections. For a fluid with constant density flowing from cross section 1 with area A_1 and velocity v_1 to cross section A_2 with velocity v_2, it can be described as:

$$A_1 v_1 = A_2 v_2 \tag{2.4}$$

Pressure loss

During fluid flow when it encounters abrupt change in cross-section, frictional surfaces or orifices, there is a drop in the pressure due to the change in the flow behavior of the fluid leading to the formation of eddies (in case of cross section changes) or shear stress exerted by the walls due to friction (in case of frictional surfaces) [5].

The local pressure loss due to a sudden enlargement of the cross section from Figure 2.8b can be written as :

$$h_L = \frac{k_L u_1^2}{2g} \quad where \quad k_L = (1 - \frac{A_1}{A_2})^2. \tag{2.5}$$

The local pressure loss due to sudden contraction of the cross section from Figure 2.8a is written as:

$$h_L = \frac{0.44 u_2^2}{2g}. \tag{2.6}$$

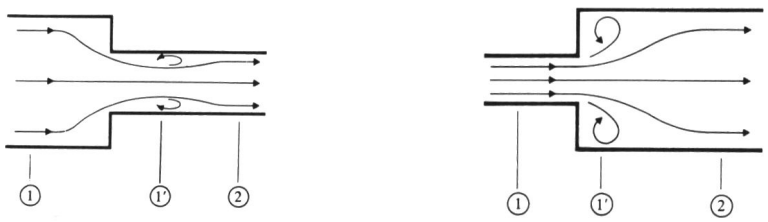

(a) Sudden contraction (b) Sudden expansion

Figure 2.8: Flow losses in pipes [5]

The pressure loss due to friction for laminar flow is described by the Hagen-Poiseuille equation as:

$$\Delta p_{loss} = \frac{32\mu L u}{d^2}. \tag{2.7}$$

where:
μ is the dynamic viscosity of the fluid ($kgm^{-1}s^{-1}$)
u is the velocity of the fluid at the cross section.(m/s)
h_L is the headloss in (m)
L is the length of the pipe (m)
g is the acceleration due to gravity (m/s^2)
The total pressure loss over a given length of the pipe can be summed up and the represented by a pressure loss factor ζ such that:

$$\Delta p_{totalloss} = \frac{\rho u^2 \Sigma \zeta}{2}. \tag{2.8}$$

2.3.2 Quarter-car model with Fluid Dynamic Absorber

The model of the suspension with the FDA is described in Figure 2.9

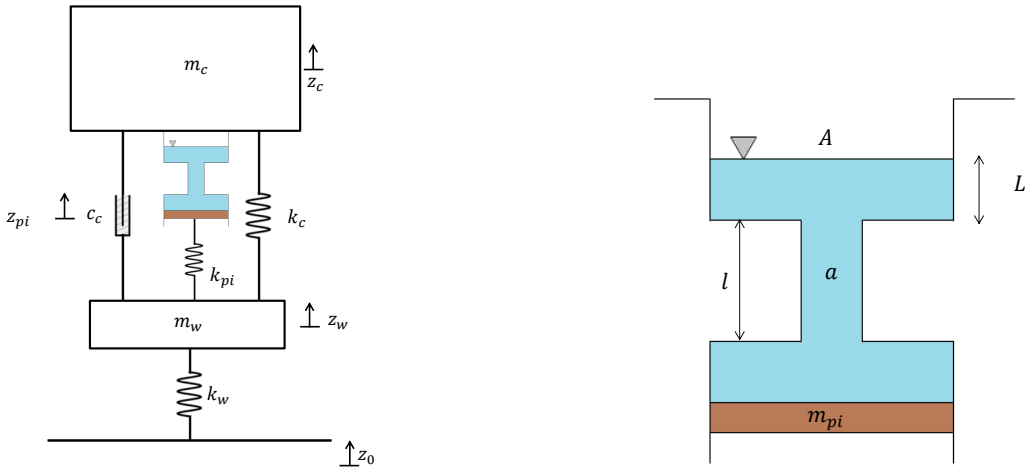

(a) Quarter-car model

(b) FDA construction

Figure 2.9: Fluid Dynamic Absorber [22]

where
z_{pi} represents the displacement of the plunger of the Fluid Dynamic Absorber.
A and L represent the area and the length of the enlarged cross-section respectively.
a and l represent the area and the length of the smaller cross-section respectively.
k_{pi} represents the spring stiffness between the FDA and the wheel.

The individual Free-body diagrams are described below:

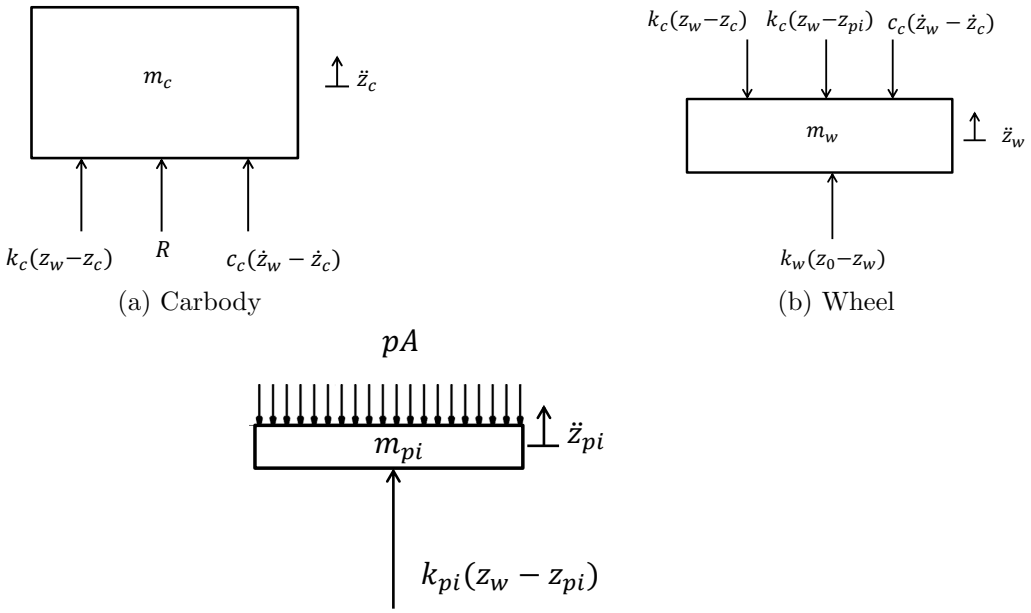

(a) Carbody

(b) Wheel

(c) FDA plunger

Figure 2.10: Freebody diagrams

R represents the reaction force from the Fluid Dynamic Absorber on the car body (acts on the FDA frame) and pA represents the pressure exerted by the fluid on the surface of the plunger. Based on the Free body diagrams (Figure 2.10), the following equations describe the motion of the carbody, FDA plunger and the wheel respectively:

$$m_c\ddot{z}_c + k_c(z_c - z_w) + c_c(\dot{z}_c - \dot{z}_w) - R = 0, \tag{2.9}$$

$$m_{pi}\ddot{z}_{pi} + pA + k_{pi}(z_{pi} - z_w) = 0, \tag{2.10}$$

$$m_w\ddot{z}_w + c_c(\dot{z}_w - \dot{z}_c) + z_w(k_c + k_w + k_{pi}) - z_c k_c - z_{pi}k_{pi} = k_w z_0. \tag{2.11}$$

Investigating further to calculate R and pA, the equations of motion within the Fluid Dynamic Absorber are analyzed: 3 surfaces are marked as shown in Figure 2.11 where: ρ is the density of the fluid; z_{F1} is the displacement of the fluid at surface 1; z_{F2} is the displacement of the fluid at surface 2; m_F is the mass of the accelerated fluid at the control volume (ρal).

The ratios between the areas and lengths are denoted as:

$$\frac{A}{a} = \alpha \tag{2.12}$$

$$\frac{L}{l} = \beta \tag{2.13}$$

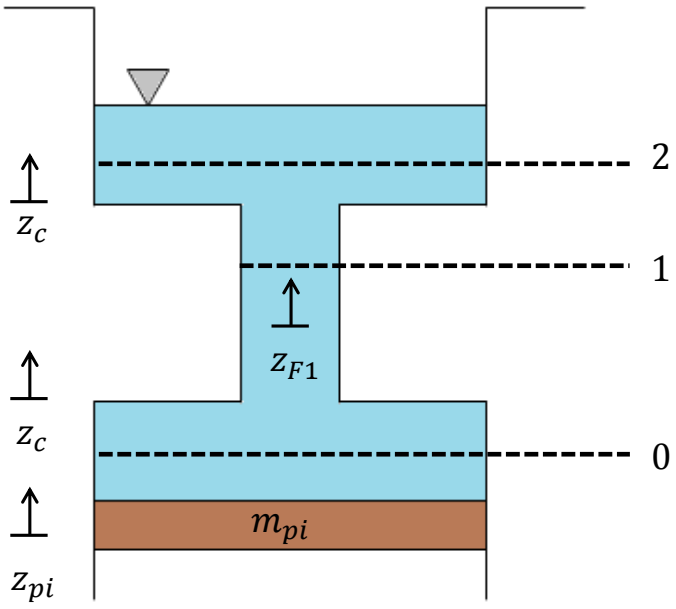

Figure 2.11: Cross sections of FDA

Applying the equation of continuity between surfaces 0 and 1 gives

$$A\dot{z}_{pi} - (A-a)\dot{z}_c = a\dot{z}_{F1}, \tag{2.14}$$

$$\dot{z}_{F1} = \alpha\dot{z}_{pi} + (1-\alpha)\dot{z}_c. \tag{2.15}$$

Applying the equation of continuity between surfaces 1 and 2 results in

$$a\dot{z}_{F1} + (A-a)\dot{z}_c = A\dot{z}_{F2} \tag{2.16}$$

Substituting the value of $\dot{z}_{F1}$ from Equation (2.15), we get

$$\dot{z}_{F2} = \dot{z}_{pi}. \tag{2.17}$$

At the uppermost surface, the pressure acting on the liquid is equal to the atmospheric pressure

$$pA = p_{fluid}A + p_{loss}A. \tag{2.18}$$

Here
p_{fluid} represents the hydraulic pressure which can be calculated by integrating the Bernoulli Equation over the length of the FDA.
p_{loss} represents the head losses due to the friction factor, expanding/contracting cross sections.
Calculating p_{fluid} ignoring the pressure components due to gravity and change in kinetic energy (See Figure 2.12a for reference) gives

$$p_{fluid} = 2\int_0^L \rho\ddot{z}_{F2}dl + \int_0^l \rho\ddot{z}_{F1}dl \tag{2.19}$$

Substituting values for $\ddot{z}_{F1}$ and $\ddot{z}_{F2}$ from Equations (2.15) and (2.17), we get:

$$p_{fluid} = \rho l[\ddot{z}_{pi}(\alpha+2\beta) + \ddot{z}_c(1-\alpha)]. \tag{2.20}$$

Multiplying p_{fluid} with A and substituting further with the mass of the control fluid(m_F):

$$p_{fluid}A = m_F[\ddot{z}_{pi}(\alpha^2 + 2\alpha\beta) + \ddot{z}_c(\alpha - \alpha^2)] \tag{2.21}$$

The total force acting on the plunger is therefore

$$pA = m_F[\ddot{z}_{pi}(\alpha^2 + 2\alpha\beta) + \ddot{z}_c(\alpha - \alpha^2)] + p_{loss}\alpha a \tag{2.22}$$

Substituting the value of pA in Equation (2.10)

$$[m_{pi} + m_F(2\alpha\beta + \alpha^2)]\ddot{z}_{pi} + (\alpha - \alpha^2)m_F\ddot{z}_c + k_{pi}(z_{pi} - z_w) = -p_{loss}\alpha a \tag{2.23}$$

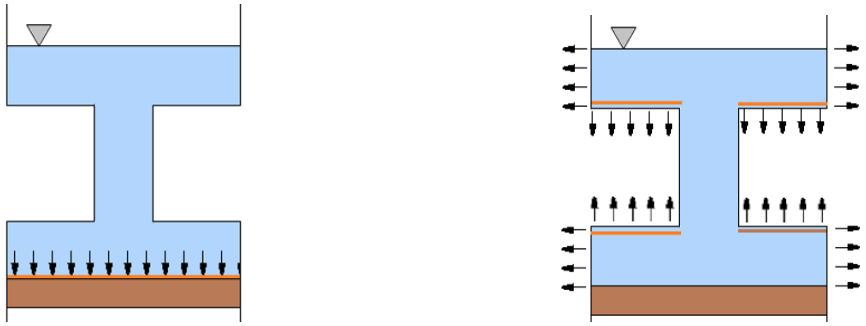

(a) Hydraulic pressure (b) Frame reaction

Figure 2.12: Pressure force and FDA Frame reaction

Calculating the force R acting on the FDA frame attached to the carbody (m_c):

Analyzing the pressure acting on the FDA frame in Figure 2.12b, the arrows depict the direction of the pressure acting on the FDA frame. It can be noticed that the horizontal pressure components cancel out each other while there is a difference in the vertical components. The horizontal lines at the expansion and contraction depict the cross section acted upon by the residual vertical pressure.The area is given by $A - a$ or $a(\alpha - 1)$.
The difference in the pressure can be calculated by integrating the Bernoulli equation over the length l:

$$\Delta p_{(length=l)} = \rho l \ddot{z}_{F1}. \tag{2.24}$$

Substituting the value for $\ddot{z}_{F1}$ from Equation (2.15) we get

$$\Delta p_{(length=l)} = \rho l(\alpha\ddot{z}_{pi} + (1 - \alpha)\ddot{z}_c). \tag{2.25}$$

The force acting on the FDA frame after adding the pressure loss is

$$R = (A - a)\rho l(\alpha\ddot{z}_{pi} + (1 - \alpha)\ddot{z}_c) + Ap_{loss}. \tag{2.26}$$

Substituting the mass of the control fluid (m_F) yields

$$R = -m_F(\ddot{z}_{pi}(\alpha - \alpha^2) + \ddot{z}_c(1 - \alpha)^2) + p_{loss}\alpha a. \tag{2.27}$$

Substituting the value of R in Equation (2.9) then gives

$$[m_c + m_F(1 - \alpha)^2]\ddot{z}_c + (\alpha - \alpha^2)m_F\ddot{z}_{pi} + k_c(z_c - z_w) + c_c(\dot{z}_c - \dot{z}_w)p_{loss}\alpha a. \tag{2.28}$$

The frame reaction R and the hydraulic pressure pA have been evaluated and input in the equations of motion of the bodies (Equations (2.28) , (2.23), (2.11).) Calculating the pressure loss using equations (2.5) and (2.6) yields

$$p_{loss} = 0.5 sign(\dot{z}_{pi} - \dot{z}_c)\rho\alpha^2(\dot{z}_{pi} - \dot{z}_c)^2\Sigma\zeta, \tag{2.29}$$

where the pressure loss factor accounted to expansion losses and contraction losses is calculated as

$$\Sigma\zeta = 0.44 + (1 - \frac{a}{A})^2. \tag{2.30}$$

Here the pressure loss due to the friction factor is not taken into account since its value is very small as compared to the entry and the exit losses. The *sign* function takes into account the direction of action of the damping force since the value $(\dot{z}_{pi} - \dot{z}_c)^2$ is always positive. This expression is a source of non-linearity in the system of equations. In the next section, the approach to linearize the pressure loss is discussed.

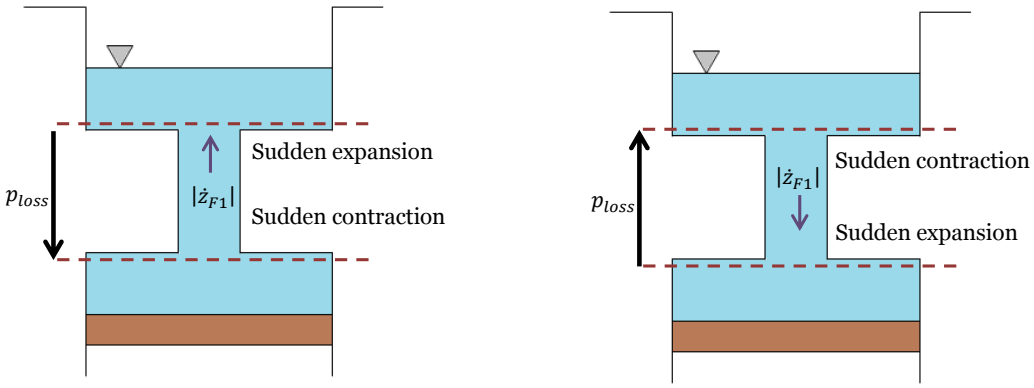

(a) Net upward direction

(b) Net downward direction

Figure 2.13: Pressure loss direction with respect to flow

2.3.3 Linearization of pressure loss

The non-linear force due to the pressure losses $p_{loss}\alpha a$ from Equation (2.29) can be linearized to $c_{fda}(\dot{z}_{pi} - \dot{z}_c)$ and hence be considered as an equivalent linear damper with a damper coefficient c_{fda} as described below.

Quadratic damping

Equation (2.29) represents a case of quadratic damping. It is generally of the form [29]:

$$F_d = -sign(\dot{x})C_q\dot{x}^2 \tag{2.31}$$

The force due to quadratic damping vs velocity is shown in Figure 2.14 [29]:

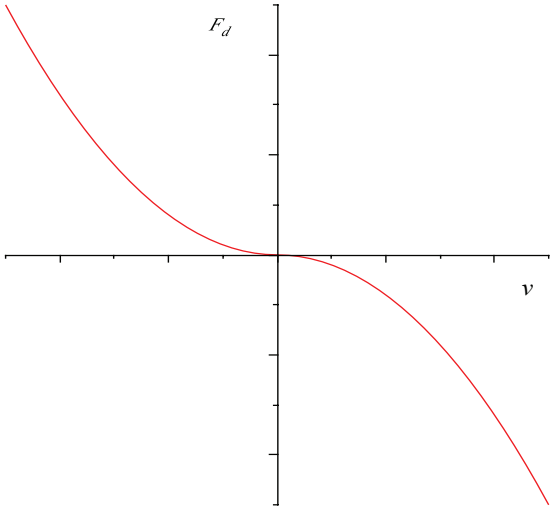

Figure 2.14: Quadratic damping

Energy method linearization

[29] describes the method to calculate the equivalent viscous damping coefficient for a quadratic damper for small displacements. For this purpose, the energy dissipated by the quadratic damper per cycle is taken to be equal to the energy dissipation of a linear damper with damping coefficient $C_{linearequivalent}$. Equating the expressions, the value of $C_{linearequivalent}$ is determined. Using the concept of Equivalent Viscous Damping the following expressions are obtained:
The Energy lost per cycle in a damper for a harmonically excited system is

$$W_d = \oint F_d dx. \tag{2.32}$$

For a linear viscous damper with damping coefficient C let:

$$x = X sin(\omega t - \phi), \tag{2.33}$$

where:
x is the displacement of the mass
X is the amplitude of the vibration
ω is the angular frequency of the vibration
ϕ is the phase difference.

$$\dot{x} = \omega X cos(\omega t - \phi) \tag{2.34}$$

$$W_d = \oint C\dot{x}dx = \oint C\dot{x}^2 dt \qquad \text{since } dx = \dot{x}dt \tag{2.35}$$

$$W_d = C\omega^2 X^2 \int_0^{\frac{2\pi}{\omega}} cos^2(\omega t - \phi)dt = \pi C\omega X^2 \tag{2.36}$$

For quadratic damping where C_q is the quadratic damping coefficient, evaluating the work done per cycle gives

$$W_d = \oint C_q \dot{x}^2 dx \tag{2.37}$$

$$W_d = 4C_q\omega^3X^3\int_0^{\frac{\pi}{2\omega}} cos^3(\omega t-\phi)dt = \frac{8}{3}C_q\omega^3X^3 \tag{2.38}$$

Comparing the work done per cycle for the linear damping case (Equation (2.36)) with the quadratic damping case as assumed

$$\pi C\omega X^2 = \frac{8}{3}C_q\omega^2X^3, \tag{2.39}$$

yields the linear equivalent damping coefficient for a quadratic damper with quadratic damping coefficient C_q

$$C_{linearequivalent} = \frac{8C_q\omega X}{3\pi}. \tag{2.40}$$

In the case of the Fluid Dynamic Absorber, from Equation (2.29)

$$C_q = 0.5\rho\alpha^2\Sigma\zeta, \tag{2.41}$$

and

$X = (Z_{pi}-Z_c)$ i.e. the amplitude of the difference in plunger and carbody displacements. (2.42)

Hence

$$C_{linearequivalent} = c_{fda} = \frac{4\rho A\omega\alpha^2(Z_{pi}-Z_c)}{3\pi}\Sigma\zeta. \tag{2.43}$$

2.3.4 System equations

The equations describing the system with the effects of the Fluid Dynamic Absorber can hence be written as:

$$\begin{bmatrix} m_c+m_F(1-\alpha^2) & (\alpha-\alpha^2)m_F & 0 \\ (\alpha-\alpha^2)m_F & m_{pi}+m_F(2\alpha\beta+\alpha^2) & 0 \\ 0 & 0 & m_w \end{bmatrix}\begin{bmatrix}\ddot{z}_c\\ \ddot{z}_{pi}\\ \ddot{z}_w\end{bmatrix}+\begin{bmatrix} c_{fda}+c_c & -c_{fda} & -c_c \\ -c_{fda} & c_{fda} & 0 \\ -c_c & 0 & c_c \end{bmatrix}\begin{bmatrix}\dot{z}_c\\ \dot{z}_{pi}\\ \dot{z}_w\end{bmatrix}$$
$$+\begin{bmatrix} k_c & 0 & -k_c \\ 0 & k_{pi} & -k_{pi} \\ -k_c & -k_{pi} & k_c+k_{pi}+k_w \end{bmatrix}\begin{bmatrix}z_c\\ z_{pi}\\ z_w\end{bmatrix} = \begin{bmatrix}0\\0\\k_wz_0\end{bmatrix} \tag{2.44}$$

Comparison

Comparing the matrix Equations (2.44) and (2.1), it can be noticed that the carbody with the Fluid Dynamic Absorber has an additional inertial mass of $m_F(1-\alpha)^2$ which at the same time is subjected to an inertia force proportional to the acceleration of the plunger making up the inertia effect due to fluid transmission. This inertial mass is highly dependent on the value of α and is considerably higher than the actual fluid mass in the device hence giving potential savings in weight.

At the same time c_{fda} contributes to the damping effect which is also dependent on the value of α and dependent on the amplitude and the angular frequency of the plunger movement making simple linear analysis comparatively difficult as opposed to a conventional suspension. These two effects will be modelled and studied in the later sections.

2.4 Modelling in Dymola

The steps involved in the development of the non-linear model of the Fluid Dynamic Absorber in Dymola are described in this section.

2.4.1 Methodology

Figure 2.15 describes the approach taken to design a force element in Modelica.

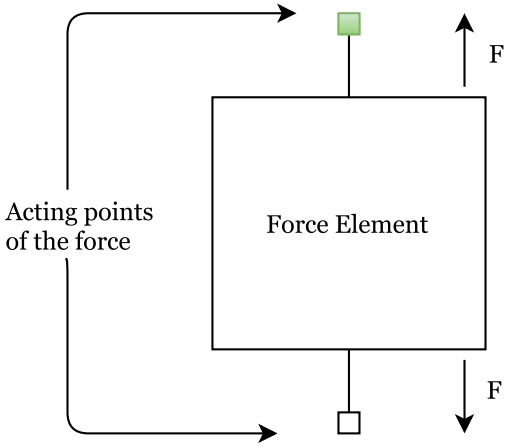

Figure 2.15: Force element construction

This is a simplified representation of the requirement of the device. It is required to have two state points (or flanges as it is called in Modelica) and they might be connected to similar state points containing a mass, fixed point or the state point of another force element in the system. This approach ensures that this model has re-usability and can be used as a building block in other multi-body systems as well.

The flanges are one of the simplest models in the Modelica library and are called by bigger models like springs. It follows the hierarchy based modelling procedure in Modelica. These state points are to be governed by a set of algorithms. For any point connected to one of these points the same kinetic properties must hold all time. In Figure 2.16a the displacement, velocity and the acceleration at flange a of the spring and flange b of the mass must be equal at all points of time. Apart from the uniform kinetic properties, another rule is *flow*. The quantity associated with flow should be such that the sum of all components of the particular quantity should be zero at the particular state point/ flange. In the case of the force element described in Figure 2.16a the sum of the forces acting on a particular statepoint/flange is equal to zero.

These sets of rules are not only useful in the mechanics domain. They can also be applied in the case of electrical circuits as shown in Figure 2.16b. At flange A of the resistor R_1, the sum of all the currents is equal to zero making it a flow property while the voltage is the same at flange A of R_1 and flange B of R_2.

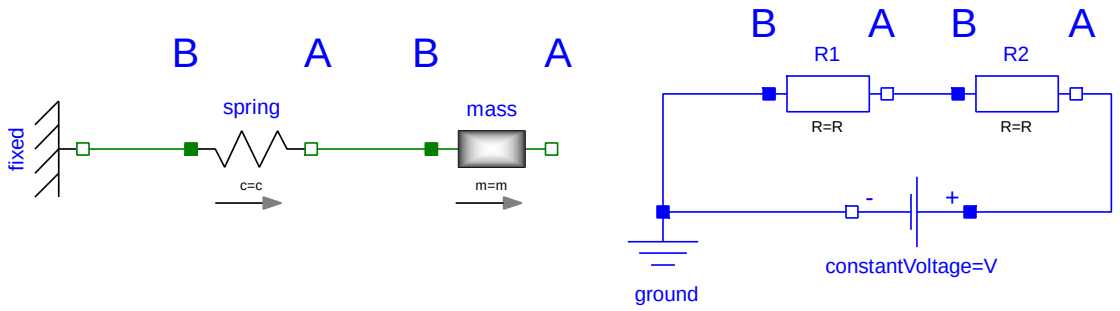

(a) Spring mass example

(b) Resistor example

Figure 2.16: Dymola element examples

It is possible to model the force elements for more than one degree of freedom by assigning state variables for the respective directions. The simplest case is to model for a single direction and assign the direction of action with the help of another component in the modelica library called 'prismatic joint'.

2.4.2 Modelling Fluid Dynamic Absorber

From Figure 2.17 is obvious that the values R and pA from Section 2.3 are not equal and hence there is a residual force in the Fluid Dynamic Absorber. Its effect can be explained by the accelerating fluid inside the absorber which results in an internal force of the device and does not act directly on the carbody or the piston. So the Fluid Dynamic Absorber will have to be modelled as a force element with two differing forces acting on both its ends unlike a spring or a damper which applies equal magnitude of force in both directions with respect to its kinetic properties.

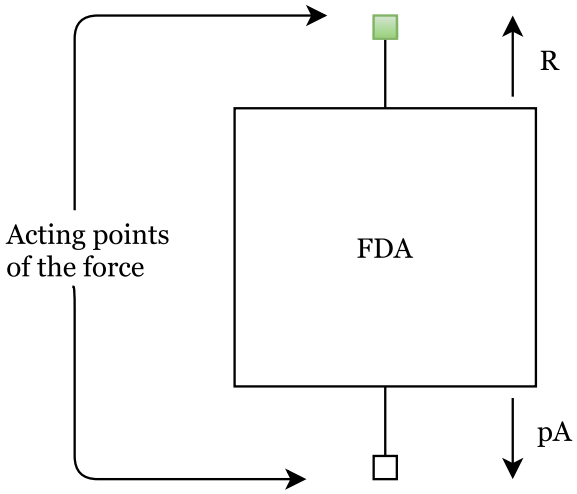

Figure 2.17: Fluid Dynamic Absorber element schematic diagram

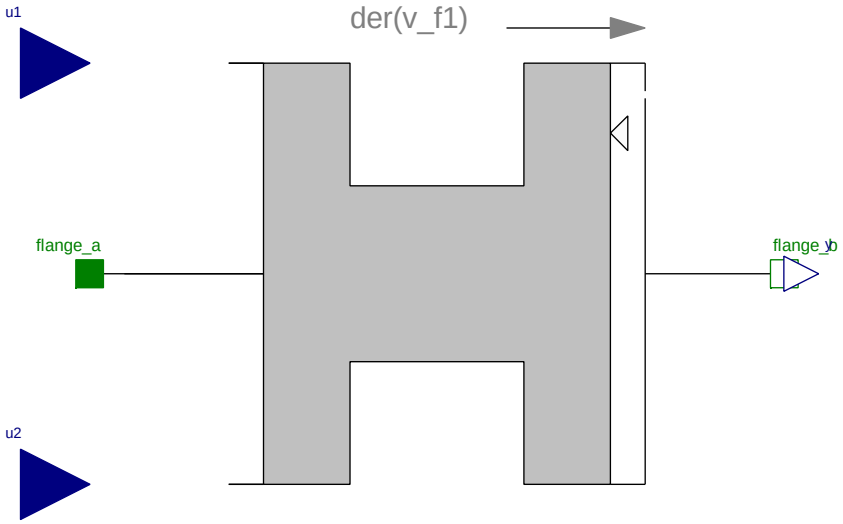

Figure 2.18: Fluid Dynamic Absorber model

As discussed in Section 1.4.1, Modelica can solve a system of equations on its own. This makes it possible to represent the equations derived in Chapter 2 in Modelica language. These equations are declared inside the force-element definition and the reaction forces R and pA are calculated in an iterative manner over the time simulation period. A limitation is that only differential equations of the first order can be coded in the Modelica environment. A total of 22 equations are written in the Modelica language and the force R is applied to flange b and force pA is applied to flange a. The full Modelica code of the Fluid Dynamic Absorber model can be viewed in appendix D.

Since the equations require the absolute velocities of the carbody and the piston as opposed to the relative motion between the piston and the carbody, it is input to the Fluid Dynamic Absorber element with help of absolute velocity sensors (*carbody_v* and *piston_v*) . The

prismatic joint (FDA_P) takes care that the kinematics and the forces are applied in the given direction (in this case 1,0,0 = x-direction.) Figure 2.19 compares the schematic diagram of a Fluid Dynamic Absorber with its Dymola counterpart.

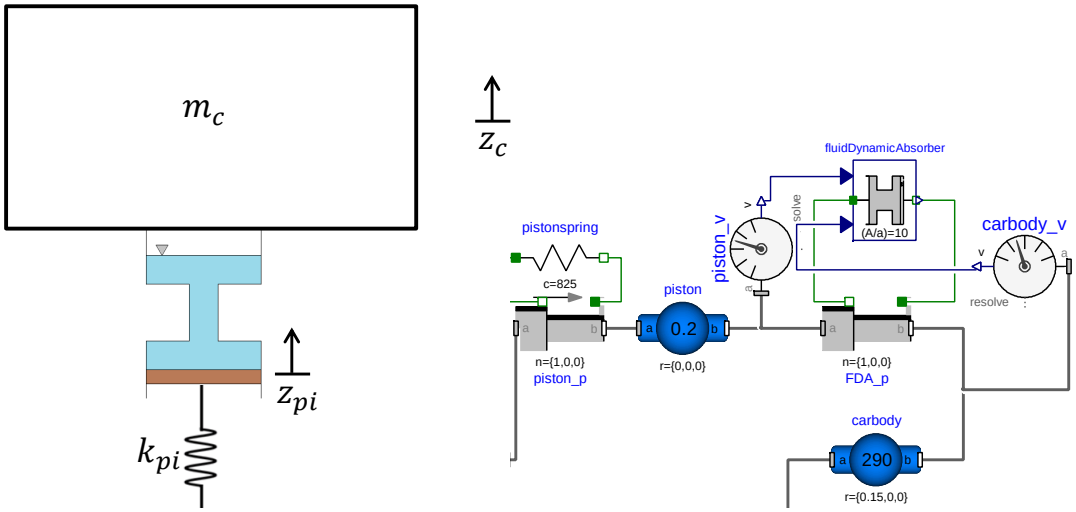

(a) Diagram (b) Dymola implementation

Figure 2.19: FDA attached to the carbody

Sign() function

The $sign()$ function derived in Equation (2.29) presents a case of steep change in values due to the direction based action of quadratic damping. This can result in errors during the run-time or increase the simulation time. A continuous function differentiable at all the points can solve this issue. For this purpose referring to the technique proposed in [4], the $sign()$ function can be substituted with an $arctan()$ function. The argument of the arctan function should be multiplied with a high number so that the value fluctuates between 1 and –1 as much as possible. For this purpose a constant atf (arctan factor) is created with an initialization of a high value as seen in the equation

$$sign(x) \simeq arctan(x \times atf) \times \frac{2}{\pi}. \tag{2.45}$$

The remaining parts of the Fluid Dynamic Absorber including the piston stiffness spring and the piston mass are constructed using generic models from Dymola's mechanics library. This model can now be added to the library and used as a sub-component in any of the mechanical systems.

2.5 Equations of motion for rail vehicle suspensions

The equations of motion of the quarter-car models of rail vehicles are derived in this section and will be used in the later sections to build a linearized model.

2.5.1 Conventional suspension for rail vehicles

The equations of motion can be derived applying the free body diagram concepts as in Section 2.1 and with reference from [3]. The rail vehicle suspension typically consists of a bogie in between the wheel and the carbody as well. Figure 2.20 shows a quarter-car rail model with conventional suspension:

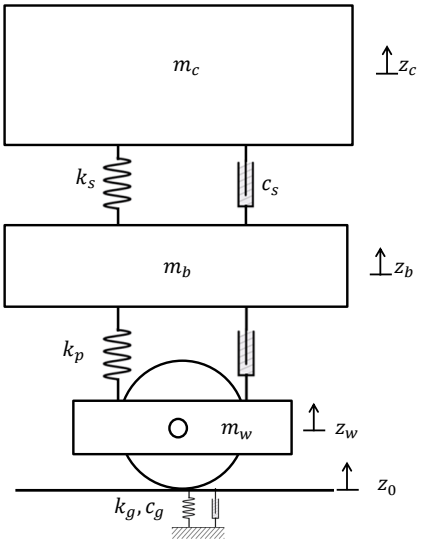

Figure 2.20: Quarter-car rail model with conventional suspension

where:
m_c is the mass of the carbody
k_s and c_s are the stiffness and the damping values of the secondary suspension respectively
m_b is the mass of the bogie-frame
k_p and c_p are the stiffness and the damping values of the primary suspension respectively
m_w is the mass of the wheelset
z_c, z_b, z_w, z_0 are the displacements of the carbody,bogie-frame,wheelset and the wheel-rail surface respectively.
The equations of motion for the quarter-car model are:

$$\begin{bmatrix} m_c & 0 & 0 \\ 0 & m_b & 0 \\ 0 & 0 & m_w \end{bmatrix} \begin{bmatrix} \ddot{z}_c \\ \ddot{z}_b \\ \ddot{z}_w \end{bmatrix} + \begin{bmatrix} c_p & -c_p & 0 \\ -c_p & c_p + c_s & -c_s \\ 0 & -c_s & c_s + c_g \end{bmatrix} \begin{bmatrix} \dot{z}_c \\ \dot{z}_b \\ \dot{z}_w \end{bmatrix} + \begin{bmatrix} k_p & -k_p & 0 \\ -k_p & k_p + k_s & -k_s \\ 0 & -k_s & k_s + k_g \end{bmatrix} \begin{bmatrix} z_c \\ z_b \\ z_w \end{bmatrix} = \begin{bmatrix} 0 \\ 0 \\ k_g z_0 + c_g \dot{z}_0 \end{bmatrix} \quad (2.46)$$

Here, k_g andc_g describe the stiffness and the damping value at the rail-wheel contact.

2.5.2 FDA as a part of the primary suspension

The quarter-car model of the rail vehicle with the Fluid Dynamic Absorber applied in parallel to the primary suspension is illustrated in Figure 2.21

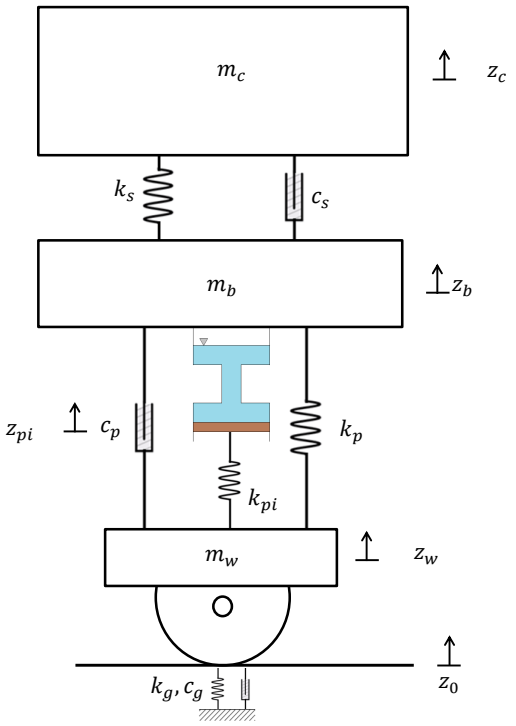

Figure 2.21: Quarter-car rail model with FDA parallel to primary suspension

Applying the derivation procedure as in Section 2.3.4 , the equations of motion are derived as:

$$\begin{bmatrix} m_c & 0 & 0 & 0 \\ 0 & m_b + m_F(1-\alpha)^2 & m_F(\alpha - \alpha^2) & 0 \\ 0 & m_F(\alpha - \alpha^2) & m_{pi} + m_F(2\alpha\beta + \alpha^2) & 0 \\ 0 & 0 & 0 & m_w \end{bmatrix} \begin{bmatrix} \ddot{z}_c \\ \ddot{z}_b \\ \ddot{z}_{pi} \\ \ddot{z}_w \end{bmatrix} +$$

$$\begin{bmatrix} c_s & -c_s & 0 & 0 \\ -c_s & c_{fda} + c_s + c_p & -c_{fda} & -c_p \\ 0 & -c_{fda} & c_{fda} & 0 \\ 0 & -c_p & 0 & c_p + c_g \end{bmatrix} \begin{bmatrix} \dot{z}_c \\ \dot{z}_b \\ \dot{z}_{pi} \\ \dot{z}_w \end{bmatrix}$$

$$+ \begin{bmatrix} k_s & -k_s & 0 & 0 \\ -k_s & k_p + k_s & 0 & -k_p \\ 0 & 0 & k_{pi} & -k_{pi} \\ 0 & -k_p & -k_{pi} & k_p + k_{pi} + k_g \end{bmatrix} \begin{bmatrix} z_c \\ z_b \\ z_{pi} \\ z_w \end{bmatrix} = \begin{bmatrix} 0 \\ 0 \\ 0 \\ k_g z_0 + d_g \dot{z}_0 \end{bmatrix} \quad (2.47)$$

2.5.3 FDA as a part of the secondary suspension

The quarter-car model of the rail vehicle with the Fluid Dynamic Absorber applied in parallel to the secondary suspension is illustrated in Figure 2.22

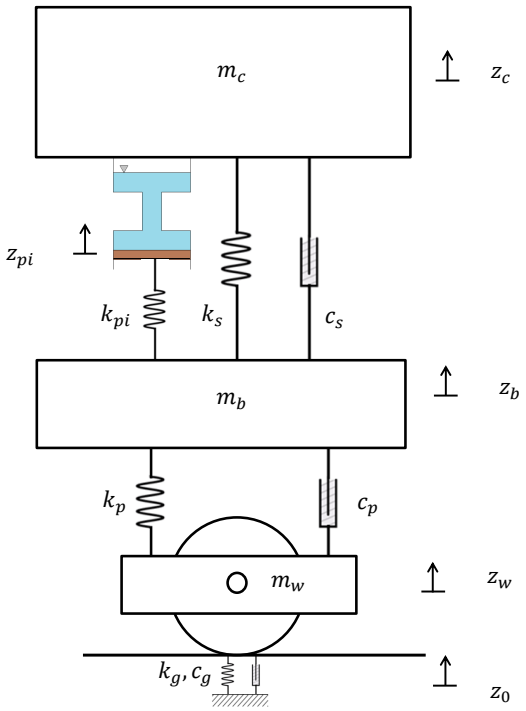

Figure 2.22: Quarter-car rail model with FDA parallel to secondary suspension

Applying the derivation procedure as in Section 2.3.4 , the equations of motion are derived as:

$$\begin{bmatrix} m_c + m_F(1-\alpha)^2 & m_F(\alpha-\alpha^2) & 0 & 0 \\ m_F(\alpha-\alpha^2) & m_{pi} + m_F(2\alpha\beta+\alpha^2) & 0 & 0 \\ 0 & 0 & m_b & 0 \\ 0 & 0 & 0 & m_w \end{bmatrix} \begin{bmatrix} \ddot{z}_c \\ \ddot{z}_{pi} \\ \ddot{z}_b \\ \ddot{z}_w \end{bmatrix} + \begin{bmatrix} c_s + c_{fda} & -c_{fda} & -c_s & 0 \\ -c_{fda} & c_{fda} & 0 & 0 \\ -c_s & 0 & c_s + c_p & -c_p \\ 0 & 0 & -c_p & c_p + c_g \end{bmatrix} \begin{bmatrix} \dot{z}_c \\ \dot{z}_{pi} \\ \dot{z}_b \\ \dot{z}_w \end{bmatrix} + \begin{bmatrix} k_s & 0 & -k_s & 0 \\ 0 & k_{pi} & -k_{pi} & 0 \\ -k_s & k_{pi} & k_{pi} + k_s + k_p & -k_p \\ 0 & 0 & -k_p & k_p + k_g \end{bmatrix} \begin{bmatrix} z_c \\ z_{pi} \\ z_b \\ z_w \end{bmatrix} = \begin{bmatrix} 0 \\ 0 \\ 0 \\ k_g z_0 + d_g \dot{z}_0 \end{bmatrix} \quad (2.48)$$

3 Quarter-car model (Automotive)

In the previous chapter, the concepts behind the working principle of the Fluid Dynamic Absorber were understood. The device was employed for a road vehicle in [22] and studied. This chapter validates the work done in Chapter 2 with the literature results. A quarter-car model is then built for the case employing the non-linear Fluid Dynamic Absorber and its behavior studied through time simulations. Further, the frequency response function of the non-linear model is studied.

3.1 Literature results

The literature [22] contains information on the transfer functions and the improvement with the application of the Fluid Dynamic Absorber on the quarter-car (automotive) model. Figure 3.1 depicts the transfer function curve for the carbody and the wheel respectively.

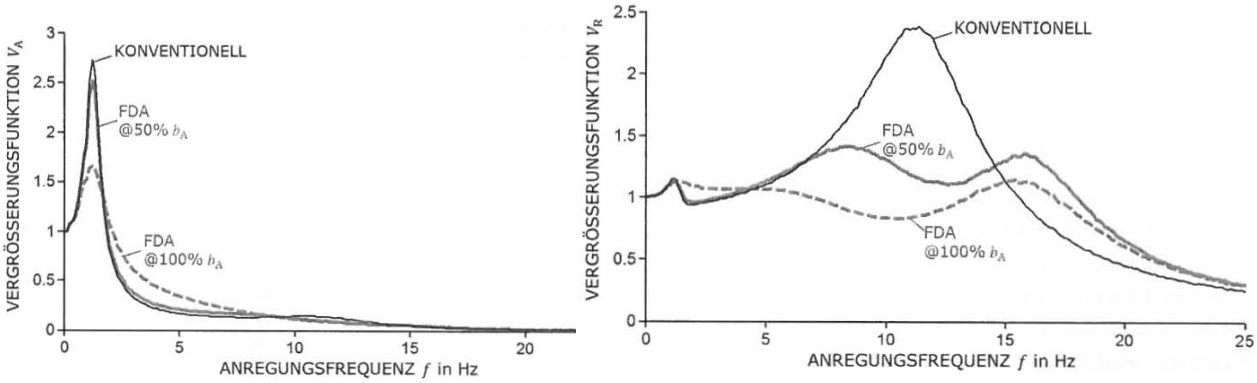

(a) Carbody transfer function

(b) Wheel transfer function

Figure 3.1: Transfer function from [22]

One notable point was that the damping co-efficient of the Fluid Dynamic Absorber was taken as a constant value throughout the whole frequency range (0 to 25 Hz).

3.2 Validation of literature results

The first step is confirming whether the derived relations and the assumptions taken during the quarter-car analysis in Chapter 2 match with the transfer functions obtained in literature. For this purpose, scripts were prepared in MATLAB with the case of a conventional suspension and the suspension with the Fluid Dynamic Absorber. The systems are then checked for the response for a frequency range between 0 and 100 Hz. The linearized damping coefficient derived in Section 2.3.3 could not be calculated because of the unavailability

of parameter $Z_{pi} - Z_c$ (which can be determined by a time simulation) in the equation. So the damping coefficient is taken as the value used in literature (720Ns/m).
Figure 3.2 depicts the transfer function curve for the carbody and the wheel respectively as generated in MATLAB.

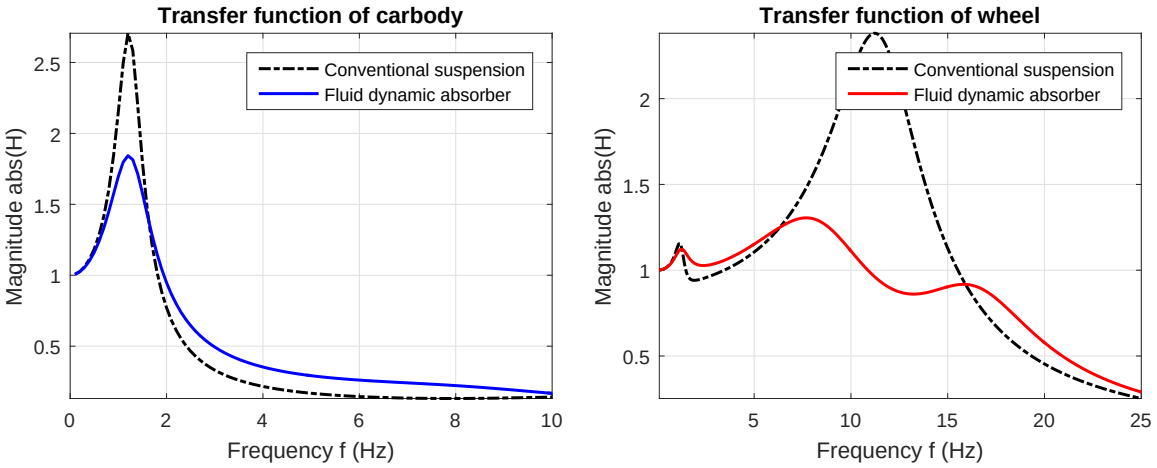

(a) Carbody transfer function

(b) Wheel transfer function

Figure 3.2: Transfer function from derived equations

It can be seen from Figure 3.2 that the transfer functions correspond with each other although there is a difference seen in the transfer function of the wheel. This exercise is indicative of the validity of the derived equations (from Chapter 2). Simultaneously, scripts for preliminary linear analysis of the quarter-car vehicle with a conventional suspension for rail vehicles have been prepared.

In Section 2.3.3, the equivalent linear damping coefficient of the Fluid Dynamic Absorber has been derived in Equation (2.36). This clashes with the assumption of a constant equivalent damping coefficient of the Fluid Dynamic Absorber in the literature since the damping coefficient can be clearly seen as a function of the frequency.

An approach to a better estimation of the response of the suspension along with the Fluid Dynamic Absorber would be to model the non-linear model first and observe the response in a time simulation.

3.3 Construction of non-linear model

Figures 3.3a and 3.3b represent the construction of the quarter-car models with and without the Fluid Dynamic Absorber. The data inputs to the parameters are described in Table 3.1. These values are taken from the literature. The damping effect due to the Fluid Dynamic Absorber is not linearized.

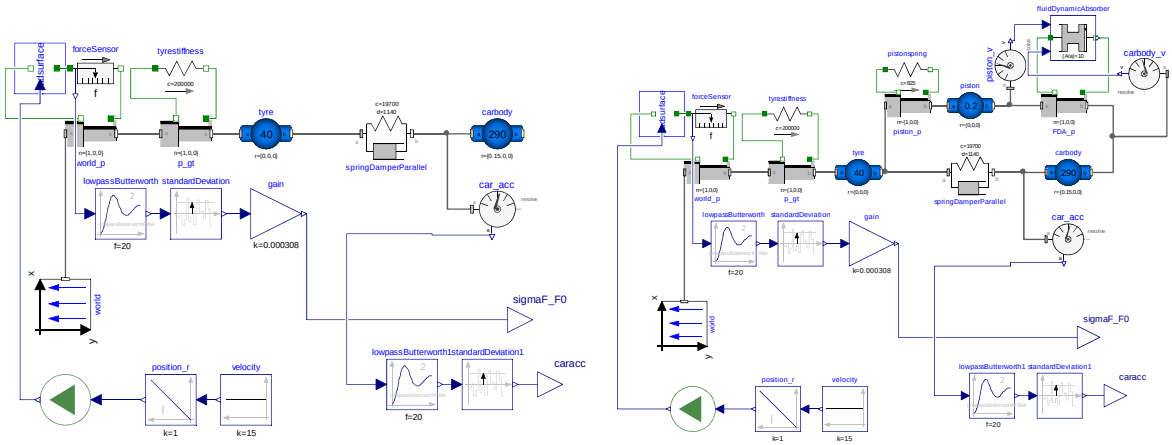

(a) Conventional (b) Fluid Dynamic Absorber

Figure 3.3: Quarter-car models

Table 3.1: Parameters of Quarter-car model (automotive)

Parameters	**Value**
Mass of the Carbody (m_c)	290 kg
Mass of the wheel (m_w)	40 kg
Tyre stiffness (k_w)	200 kN/m
Suspension stiffness (k_c)	19.7 kN/m
Suspension damping (c_c)	1140 Ns/m
FDA Parameters	
length of control volume (l)	0.145m
Length of enlarged portion (L)	0.127m
Length ratio (β)	0.88
Enlarged area (A)	$0.05^2\pi m^2$
Area ratio (α)	10
Fluid density (ρ)	880 kg/m^3
Piston stiffness (k_{pi})	84 kN/m
FDA stiffness (c_{fda})	720 Ns/m

3.4 Time simulation

The quarter-car model in the literature was simulated on 'rough road'. A suitable excitation to the tyre is required to both observe the carbody acceleration and the dynamic force on the wheel.

3.4.1 Road model

The modelling of the road surface has been taken from [2] which estimates the road surface in the form of a spring-damper model as shown in Figure 3.4.

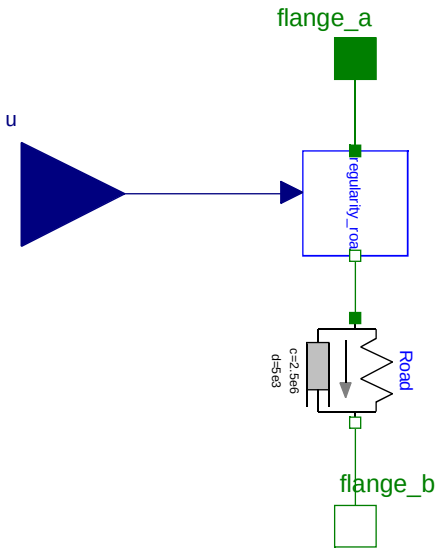

Figure 3.4: Road model

The road/track irregularities can be modelled in the form of power spectral densities (PSD)[28]. It is a linearized method of analysis. The power spectra are calculated with help of Fourier transforms of signals. The power spectrum is the square of the Fourier transform. As a result the phase information is lost but importantly it gives an estimation of the amount of the power content corresponding to the specific frequency of excitation. The power spectral densities are generally empirically fitted data of real time measured data of road/track irregularities and are helpful in modelling the conditions in a multi-body simulation context. Commercially available softwares like Simpack maintain a library of different types of road/track conditions and are employed in different time-simulations.

The road irregularities contain the appropriate power spectral densities as given in Table C.1. All the PSD's are utilized to generate appropriate curves to mimic the road irregularities corresponding to each of the conditions. Using the noise package utilities in Dymola maintained by the Institute of System Dynamics and Control, stochastic signals with the various power spectral densities were modelled as a separate component for use in the quarter-car simulation.

The quarter-car is modelled and mounted on the road model (with stochastically excited time-dependent signals.)

3.4.2 Simulation results

The quarter-car models in Figure 3.3b and Figure 3.3a were simulated with a simulation time of 50s at a speed of 54km/h as mentioned in [22] on the bad unfortified road conditions to check the running behavior.

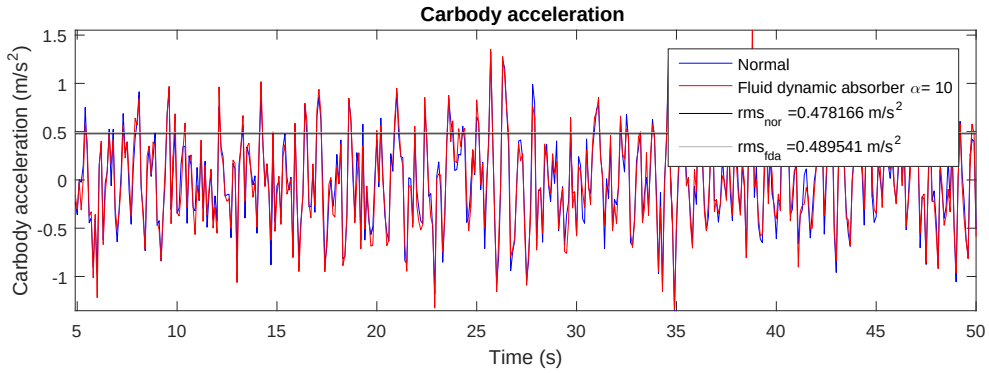

Figure 3.5: Carbody acceleration for quarter-car model based on [22]

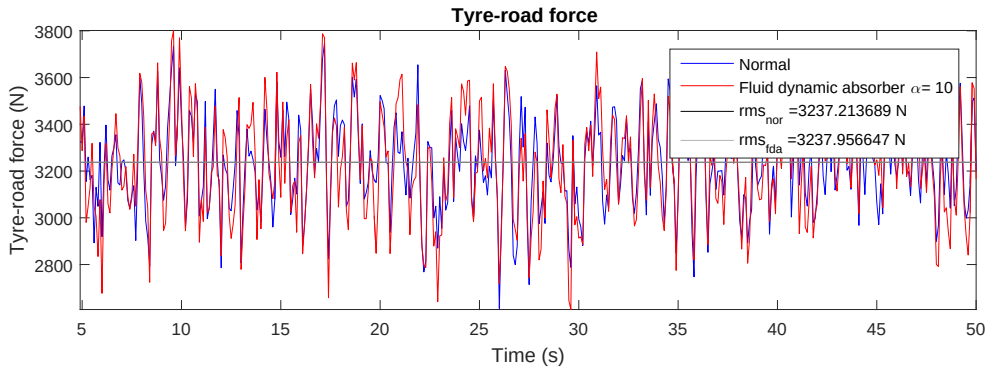

Figure 3.6: Tyre-road force for quarter-car model based on [22]

As can be seen from the results in Figures 3.5 and 3.6, the addition of the Fluid Dynamic Absorber does not give an improvement in the carbody acceleration and the dynamic forces have almost remained the same. This, therefore leaves a lot of room for improvement. The potential improvements as suggested in the literature [22] hence do not match with the results obtained from the simulation of the non-linear model.

A possible reason is the difference in the road conditions taken in the literature from the ones taken in the simulation. This behavior dependence of the suspension according to the road conditions is due to the non-linear damping behavior of the Fluid Dynamic Absorber. This, therefore exposes a fundamental challenge in the design process of the dynamic absorber. Its dependence on the boundary conditions has to be accounted.

3.5 Frequency Response Function

A direct outcome of the simulation result from Section 3.4 is that the method of using the transfer function to determine the characteristics of the system cannot be applied on the suspension. This is primarily because of the non-linear behavior of the Fluid Dynamic Absorber. An alternative method to observe how the system behaves as a function of frequency is through the use of chirp signal excitation. The chirp signal is a swept sine wave with frequency varying along the time between two values. [9] discusses in detail the

various methods to generate swept-sine signals for the plant excitation (Plant refers to the system that is excited).

Chirp package

The generation of the chirp signal was performed in accordance to the Modelica package described in [9] . It describes the proper scheduling of excitation frequency and amplitude. It is termed as a black-box approach wherein correlation methods are applied to the acquired input and output data. The excitation signals can be termed to be quasi-harmonic excitation signals i.e the stimulus is based on a sinusoidal function with the frequency being dependent on time. It can be termed as:

$$u(t) = A(t, f(t))sin(2\pi F(t)), \tag{3.1}$$

where

$$F(t) = \int_0^t f(\tau)d\tau. \tag{3.2}$$

is the integral of the instantaneous frequency f.
F(t) indicates the number of elapsed periods of the sine function.

The frequency range is specified in the package with the starting frequency and the ending frequency. The frequency can be varied across the range using three approaches.

1. Linear variation.
$$f_{linear} = f_{start} + k_l.t. \tag{3.3}$$
2. Exponential variation
$$f_{exponential} = f_{start}.k_e^t. \tag{3.4}$$
3. Constant period ratio variation
$$f_{const.periodratio} = \frac{f_{start}}{1 - f_{start}.ln(k_c).t}. \tag{3.5}$$
where k_l, k_e and k_c are the respective varying constants.[9]

The main objective is to vary the frequency in such a way that the system is able to reach the steady state throughout the given frequency range. The third approach allows for sufficient time at higher frequencies as compared to the linear and the exponential variation as shown in Figure 3.7

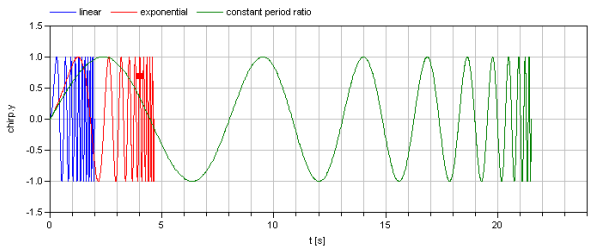

Figure 3.7: Chirp signals with variation (a) Linear (b) Exponential and (c) Constant period ratio [9]

It has a frequency progression equidistantly distributed over the logarithmic frequency scale. This type of excitation ensures that sufficient time is provided to study the steady state response at the particular value of excitation frequency.

Here, a simpler approach is employed where the amplitude is kept constant throughout the increasing frequency for a particular case. Then the normalized response (*response*/*gain*) of the carbody and the tyre for cases with different gain in amplitude values are compared. This way, the effect of the exciting vibrations on the frequency response can be studied. The simulation cases shown in Table 3.2 were modelled to study. The simulation is run for a time of 1440s from 0 to 30 Hz. The input signal is of the form in Figure 3.8

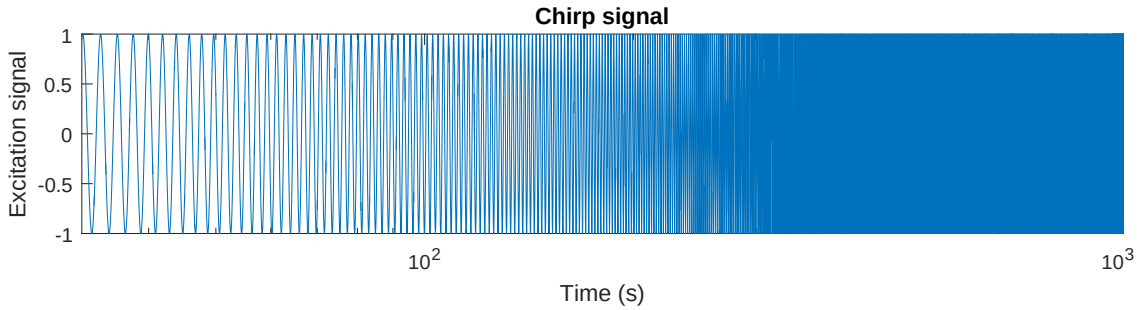

Figure 3.8: Chirp signal

Table 3.2: Cases with the respective gain in excitation amplitude

Case	**Gain in excitation amplitude**
1	1
2	5
3	10
4	20
5	50

The obtained frequency response is divided by the gain value to show the normalized response values (i.e. response value divided by gain). Figures 3.9 and 3.10 show the normalized responses for different cases as a function of frequency for both the carbody and the tyre.

Inference

The normalized response of the system is different for different amplitudes of excitation.This negates the constant assumption of the damping effect from [22]. Figures 3.9 and 3.10 depict the requirement to count the effect of excitation amplitude to determine the behavior of the system with respect to excitation frequencies. It would have not been so in the case of conventional linear suspension where the normalized response would remain the same for different amplitudes of excitation. To generate a transfer function for the linearized system, this system dependency on excitation amplitudes should be accounted. The strategy to achieve the same is by building a linearized approximation with help of principles

mentioned in Section 2.3.3 and generate the excitation specific transfer function which can be considered as a quasi-transfer function.

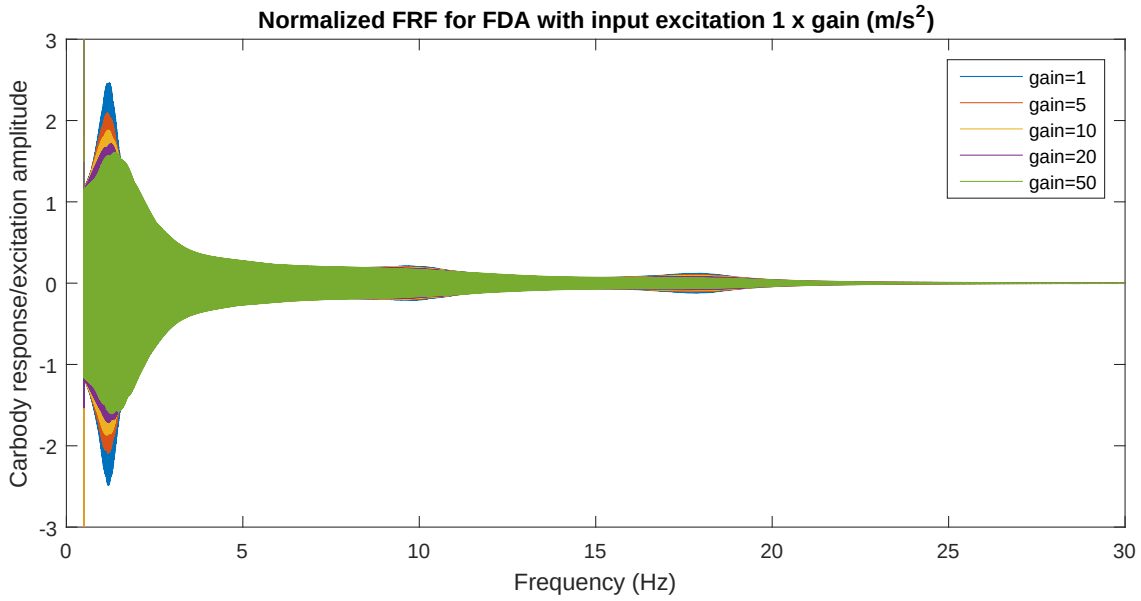

Figure 3.9: Frequency response function of carbody

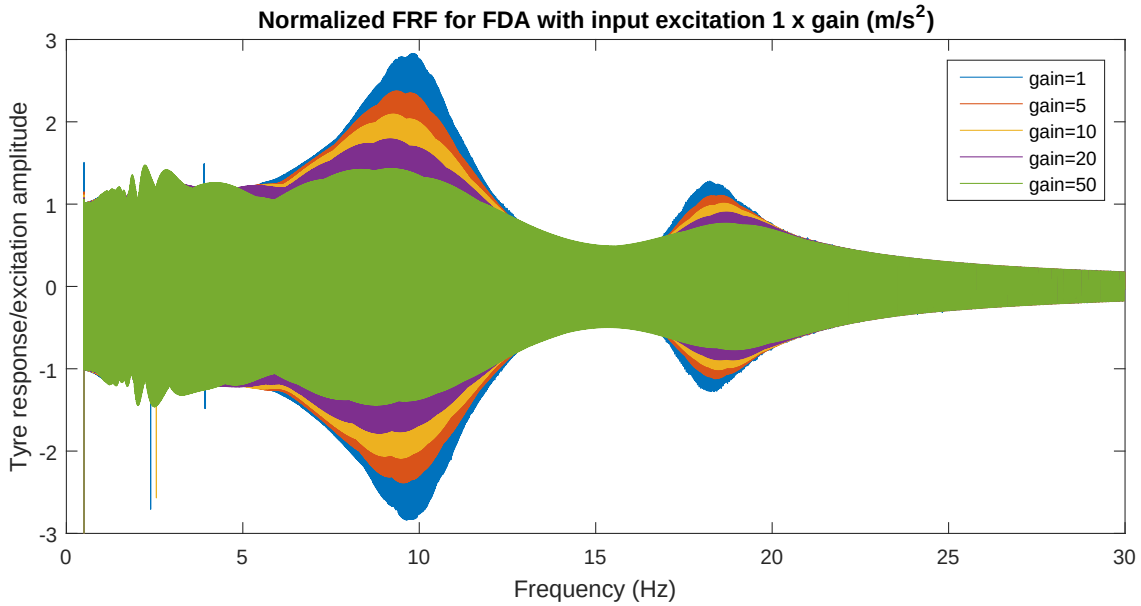

Figure 3.10: Frequency response function of tyre

4 Quarter-car model (Rail)

In this chapter, a design methodology for a Fluid Dynamic Absorber is formulated. The application of the device is discussed in the context of rail vehicles and is employed in rail vehicle quarter-car models. Two models, the Manchester benchmark model and the NGT running gear are studied. The design methodology is also validated.

4.1 Design methodology of a Fluid Dynamic Absorber

Parameters

The Fluid Dynamic Absorber design consists of the parameters as seen in Figure 4.1.

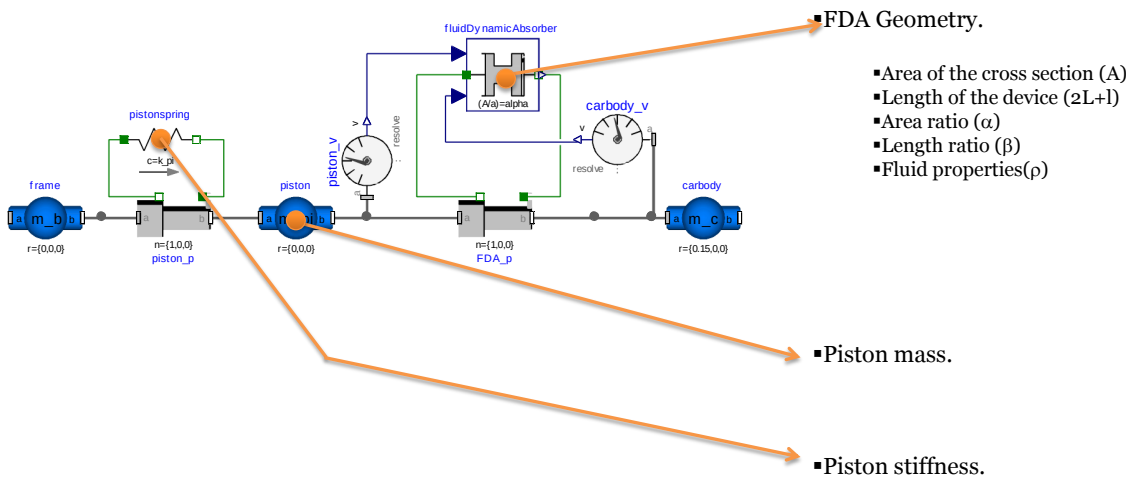

Figure 4.1: Fluid Dynamic Absorber parameters

The parameters can be divided into two categories as shown in Table 4.1

The parameters constrained by space are initially assigned with values comparable with the dimensions of rail vehicle dampers currently available in the market [33] [13] [21]. This makes sure that the absorber design can be conveniently placed in the present suspension systems. The density of the damper fluid is assumed as the standard value used in the normal viscous dampers as 880 kg/m^3.

Table 4.1: Paremeter classification

Spatial constraint influenced	**Independent of spatial constraints**
• Area of the cross section (A) • Stroke length ($2L + l$) • Length ratio (β)	• Area ratio (α) • Fluid properties (ρ) • Piston mass (m_{pi}) • Piston stiffness (k_{pi})

The parameters area ratio (α), piston mass (m_{pi}) and piston stiffness (k_{pi}) that are not spatially restrained are to be optimally calculated. The piston mass (m_{pi}) value's contribution is negligible compared to the inertial contribution which is a function of the area ratio (α). The value can hence be fixed to a similar value as seen in [22].

The value of area ratio (α) is a critical parameter since a lower value can result in less damping effect while a higher value can result in over-damping. Similarly, the value of the piston stiffness (k_{pi}) is also critical since a high stiffness value will make the piston follow the motion of the frame (Figure 4.1) while a low stiffness value will make the piston follow the motion of the carbody. So the design methodology should result in an optimal combination of the these two parameters for a given set of values of the remaining ones.

Analogy with liquid mass damper

Figure 4.2 illustrates the construction of a liquid mass damper.[10] describes the construction and the design methodology of the liquid mass damper. This device is identical to the Fluid Dynamic Absorber but does not have the inertia effect due to the varying cross section. The pressure loss due to the varying cross section area in the dynamic absorber is similar to the pressure loss in liquid mass damper (i.e. both are cases of quadratic damping)

The parameters for the liquid mass damper are calculated based on the criteria described in [10] which is built on the Den Hartog criteria for tuned mass dampers described in [12]. The only modification needed in the methodology for application in the Fluid Dynamic Absorber is the additional area ratio (α).

Optimization approach

The working principle of a liquid mass damper, its tuning properties and its design methodology are discussed and derived in detail in [10]. The optimization approach of the liquid mass damper is discussed here in brief. In Figure 4.2

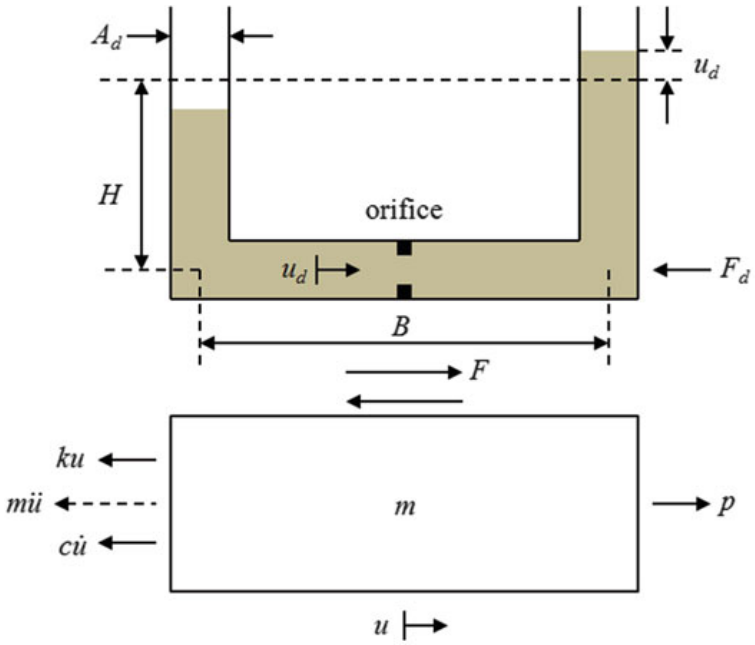

Figure 4.2: Liquid mass damper [10]

u is the displacement of the body being damped;
A_d is the cross section of the tube containing the liquid;
u_d denotes the displacement of the fluid column in the tube relative to the body;
B and H denote the dimensions of the tube as seen in Figure;
F_d denotes the force due to damping at the orifice;
F is the reaction force between the liquid mass damper and the body;
p denotes the external exciting force on the body;
β denotes $\frac{B}{B+2H}$.

The system of equations are derived as:

$$\begin{bmatrix} m+m_d & \beta m_d \\ \beta m_d & m_d \end{bmatrix} \begin{bmatrix} \ddot{u} \\ \ddot{u}_d \end{bmatrix} + \begin{bmatrix} c & 0 \\ 0 & c_{eq} \end{bmatrix} \begin{bmatrix} \dot{u} \\ \dot{u}_d \end{bmatrix} + \begin{bmatrix} k & 0 \\ 0 & k_d \end{bmatrix} \begin{bmatrix} u \\ u_d \end{bmatrix} = \begin{bmatrix} p \\ 0 \end{bmatrix} \tag{4.1}$$

where after linearization similarly as in Section 2.3.3

$$F_d \approx c_{eq}.u_d \tag{4.2}$$

Using the linear system of Equations (4.1), the transfer function of the body is calculated. Then, the parameters k_d and c_{eq} are modified using numerical simulations such that the two peaks in the transfer function have equal values and a smooth transition as shown in Figure 4.3

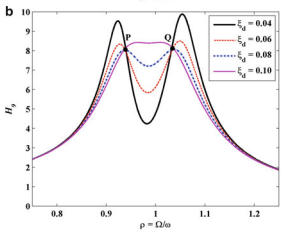

Figure 4.3: Transfer functions for different values of damping [10]

From the above case, an analogy with the Fluid Dynamic Absorber can be drawn where:

- k_d is equivalent to k_{pi} of the FDA
- c_{eq} is equivalent to the c_{fda} derived for the FDA
- β is equivalent to the β for the FDA

  The only difference is that the FDA has an additional inertia effect and its c_{fda} is dependent on the value of area ratio α as well.

Formulation of design methodology

The optimization approach desribed in Section 4.1 can be used to generate a set of parameters for a linearly approximated model to generate the optimal transfer function in MATLAB using the linear approximation of the damping effect. (Equation (2.43)).

$$c_{fda} = \frac{4\rho A\omega\alpha^2(Z_{pi} - Z_c)}{3\pi}\Sigma\zeta$$

Since the linearized damping coefficient is dependent on the excitation frequency and the relative piston amplitude relative to the carbody, this value can be input from an initial non-linear time simulation in Dymola. The dependency on frequency can be accounted for by generating a separate damping coefficient in the linearized model of equations for each frequency value. This way the linear approximation of the model can be obtained by the input of the excitation factors (piston amplitude) from the initial non-linear time simulation. Figure 4.4 describes a schematic diagram of the proposed methodology.

Hence, for the design of a Fluid Dynamic Absorber for the given conditions, two models are required: a non-linear time simulation model (Dymola) and a linearized approximation of a model for parameter calculation.

Table 4.2: Design methodology models

Model	MATLAB model	Dymola model
Purpose	Optimal Parameter calculator	Initial boundary condition input and time simulation
Nature	Linearized approximation	Stochastically excited Non-linear model
	Input from non-linear model: Relative amplitude of carbody and piston ($Z_{pi} - Z_c$). It represents the effect of excitation amplitude.	Calculates ($Z_{pi} - Z_c$)

Using the two models above, the flow chart (Figure 4.4) depicts the design methodology. The design methodology described also holds for other applications of the Fluid Dynamic Absorber. The resulting design varies with different applications, dimensional constraints and excitation conditions. This design methodology will be implemented and studied for the rail vehicle models.

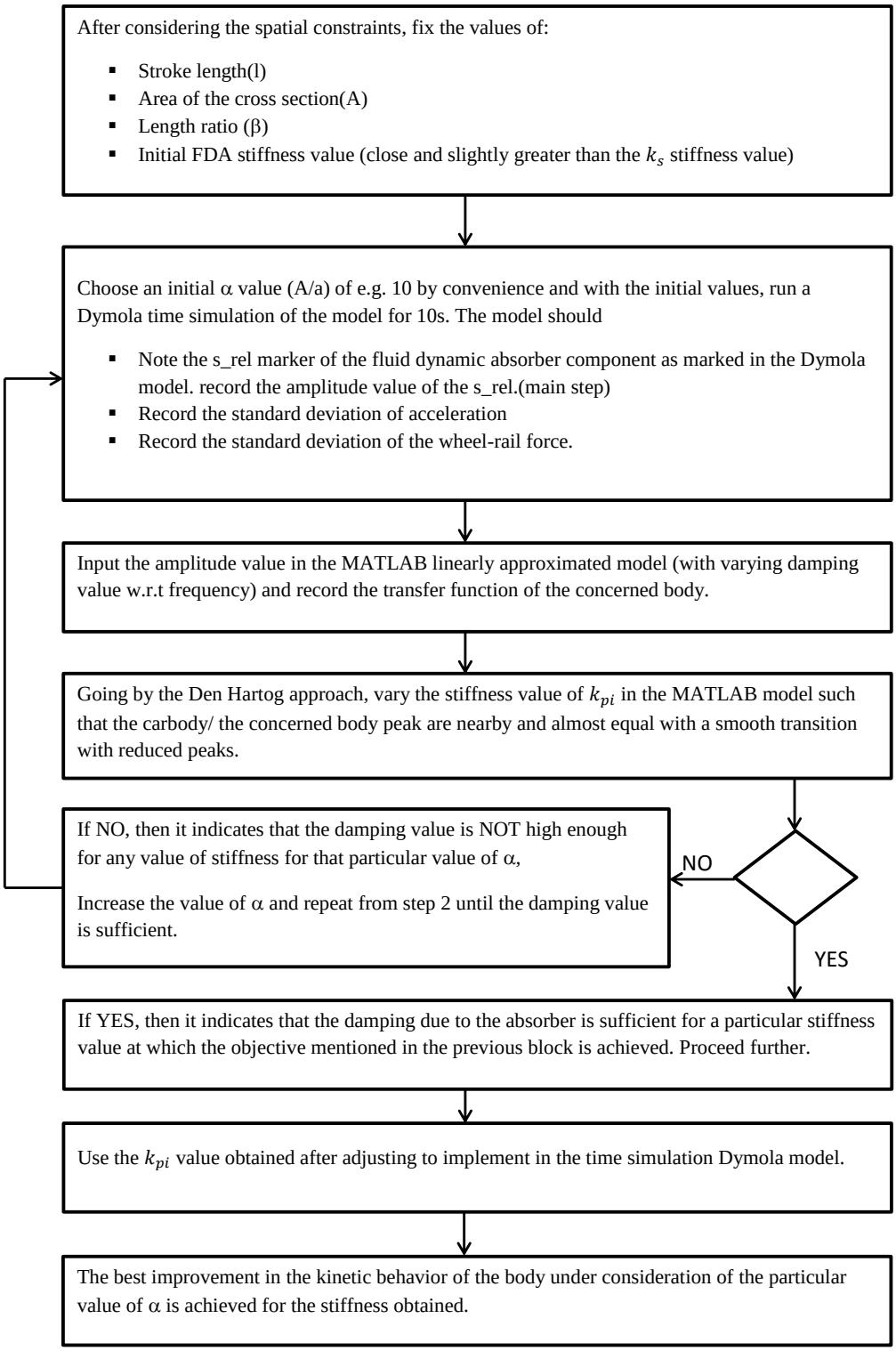

Figure 4.4: Design methodology

4.2 Point of application

The previous section described the design methodology for a Fluid Dynamic Absorber. From the rail vehicle point of view, this device can either be applied in the primary or the secondary suspension. With the system equations for quarter-car vehicle with FDA attached to primary suspension (Section 2.5.2) and secondary suspension (Section 2.5.3), a linearized approximation of the system was built using MATLAB.

The damping effect is primarily dependent on the relative piston displacement. There is a greater degree of displacement between the frame and the carbody (separated by a softer secondary suspension) than the displacement between the wheelset and the frame (separated by a stiff primary suspension). Moreover, the effect of the Fluid Dynamic Absorber is negligible on the unsprung wheel mass as compared to the sprung masses as seen in Figure 4.5 and Figure 4.6.

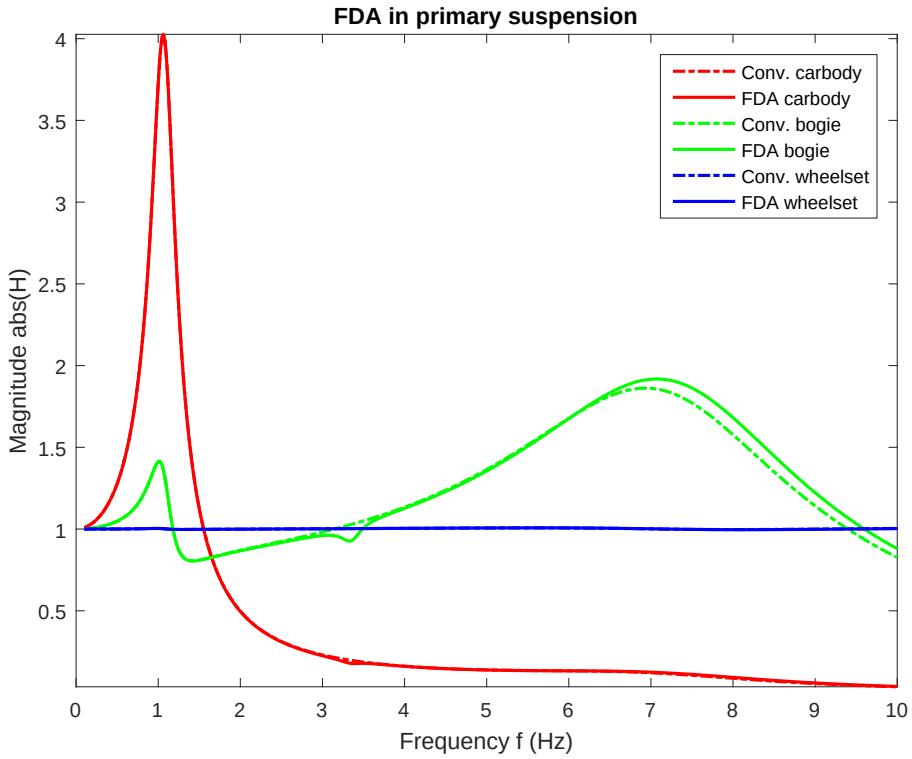

Figure 4.5: Transfer function of vehicle bodies when FDA is applied to primary suspension

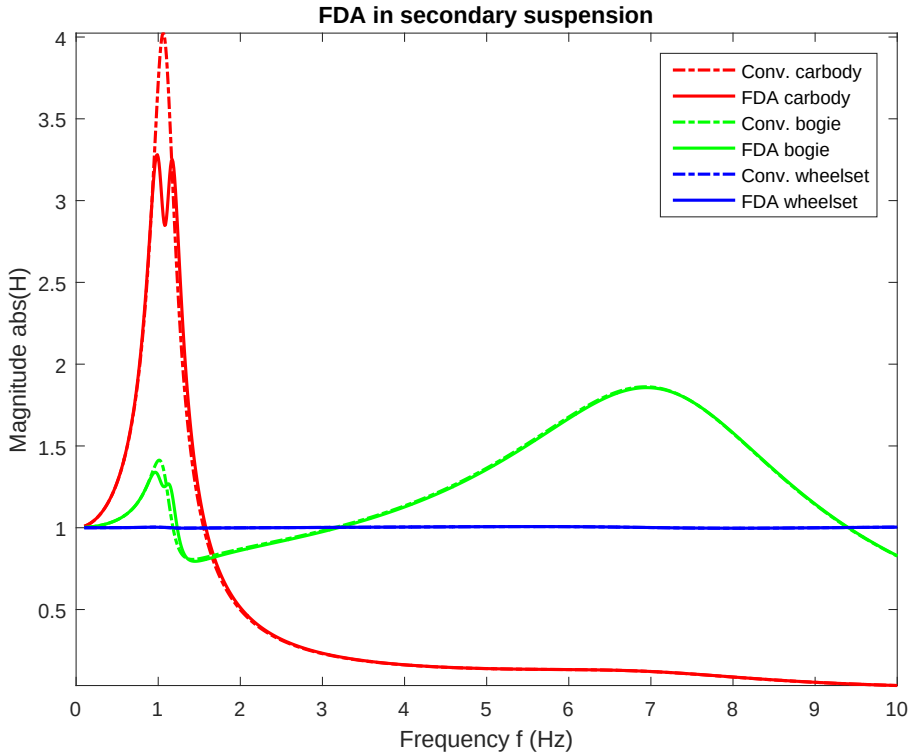

Figure 4.6: Transfer function of vehicle bodies when FDA is applied to secondary suspension

Hence the Fluid Dynamic Absorber can contribute to a greater improvement when applied in parallel to the secondary suspension.

4.3 Manchester benchmark model

The Manchester Benchmark model [15] is a standard model used in the computer simulation of rail vehicle dynamics. It is used by suspension designers investigating vehicle dynamic behavior to compare the characteristics of different software packages. It facilitates the explanation of the approach to the modelling process and various approximations adopted in each of the packages. Two benchmark models are provided.

4.3.1 Modelling

Benchmark vehicle 1 is chosen for the quarter-car modelling in this case. It is a general passenger coach with two bogies and a simple primary suspension. Based on the vehicle specifications of the model specified in [15] the parameters for the quarter-car model are calculated and shown in Table 4.3.

Table 4.3: Quarter-car parameters : Manchester benchmark model 1

Parameter	**Value**
Mass of the wheel	1813 kg
Mass of the bogie frame	1307.5 kg
Primary stiffness	2.4×10^6 N/m
Primary damping	8000 Ns/m
Secondary stiffness	4.3×10^5 N/m
Secondary damping	20000 Ns/m
Mass of the carbody	8000 kg

Track model

The railway track for the quarter-car model is modelled according to track model B from [6] as shown in Figure 4.7. Since the vertical direction is investigated,a 1-Dimensional model as in Figure 4.7b is applied.

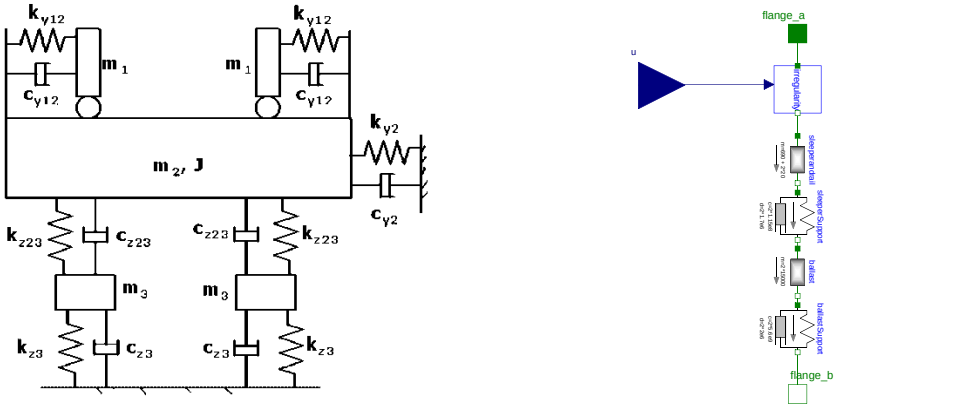

(a) From [6] (b) Designed for simulation

Figure 4.7: Track B model

The values of the parameters are given in Table 4.4:

Table 4.4: Track B parameters [6]

k_{z23} MN/m	c_{z23} kNs/m	k_{z3} MN/m	c_{z3} kNs/m	m_1 kg	m_2 kg	m_3 kg	J kgm^2
115	1700	5600	2000	20	690	15000	300

The irregularities were generated using the power spectral density function for a standard German track [3]. Figure 4.8 depicts the time simulation quarter-car model of the Manchester benchmark in the Dymola interface with a) conventional suspension b) suspension with the Fluid Dynamic Absorber.

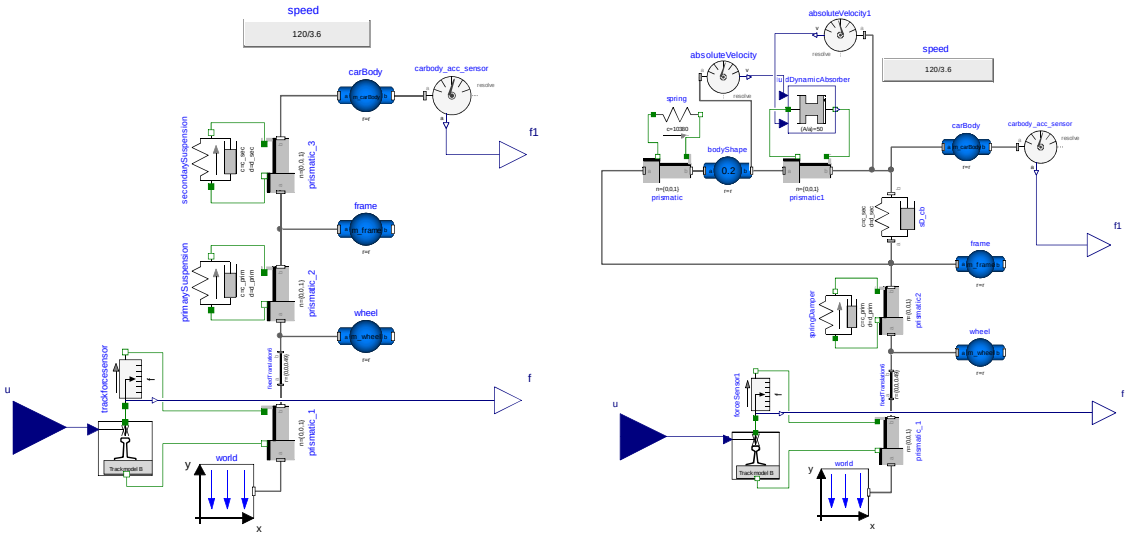

(a) Conventional suspension (b) With FDA in secondary suspension

Figure 4.8: Manchester Benchmark quarter-car model

4.3.2 FDA parameters for Manchester Benchmark model

Applying the design procedure from Section 4.1:

1. The spatial constraints are chosen analogous to damper dimensions from [13], [33], [21] and [16]. The bogie designs of some typical High Speed Train running gear are given in catalogues [7] and [27]. The dimensions represent the maximum limit since the effect of the Fluid Dynamic Absorber increases with the volume of oscillating fluid. (Table 4.5)

   Table 4.5: Spatial parameters of FDA for railway secondary suspension

Spatial parameter	**Values**
Stroke length $(2L + l)$	0.732 m
Radius at larger cross section (R)	0.071 m
Length ratio (β)	0.72

2. The initial value for area ratio α=10 can be used as the starting point. A Dymola simulation is run for the initial values. The value of relative amplitude of carbody and piston $(Z_{pi} - Z_c)$ is obtained from the initial simulation :(s_{rel}). The value is taken as 0.0015m.

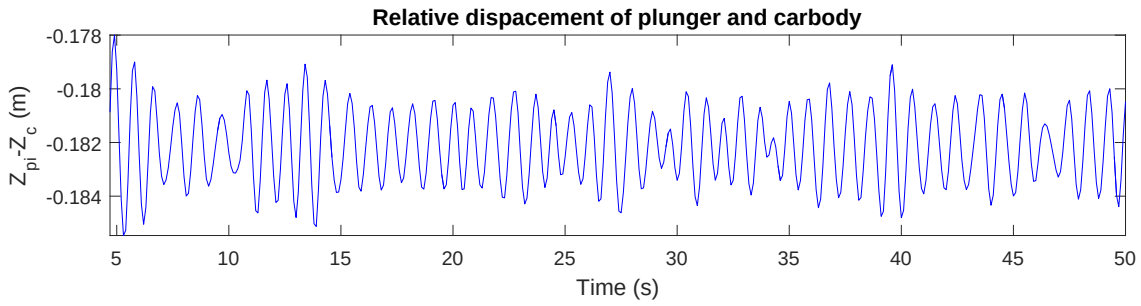

Figure 4.9: s_{rel} : $(z_{pi} - z_c)$

3. The value of $(Z_{pi} - Z_c)$ is input in the linearized MATLAB approximation.

4. Using the value of$(Z_{pi} - Z_c)$, the optimal piston stiffness is calculated as 2320 N/m using numerical simulations of the linearized model [10]. The transfer functions of the linearized approximation can be seen in Figure 4.10, Figure 4.11, Figure 4.12 and Figure 4.13.

5. Seeking further improvement ,the Area ratio (α) was increased to 20, 50 and then 100.

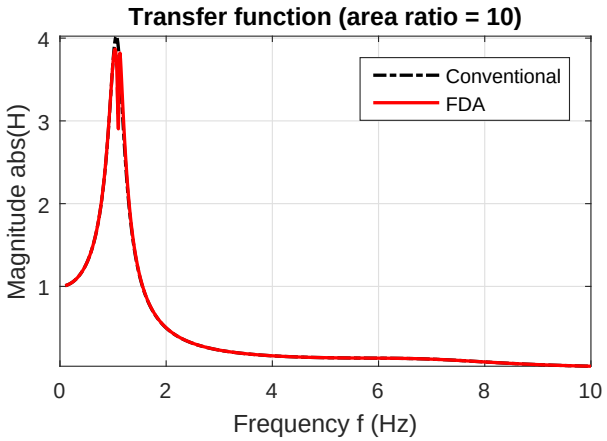

Figure 4.10: Carbody transfer function(α= 10)

From Figure 4.10 it can be concluded that the damping is not sufficient, giving rise to sharp peaks with the optimal stiffness value (2320 N/m). From the transfer function, it is visible that the addition of the Fluid Dynamic Absorber does not give significant improvement for the given value of Area ratio (α). The area ratio (α) should be increased for more damping.

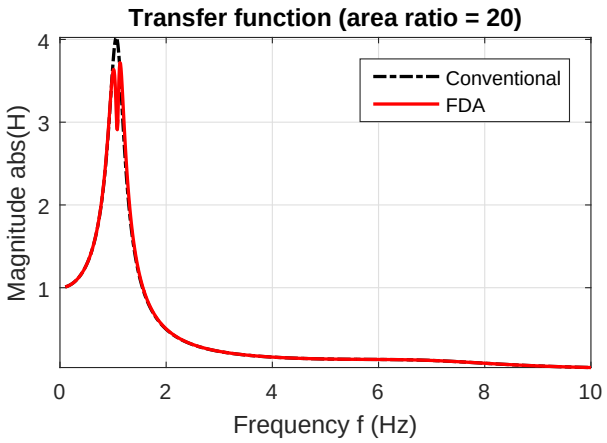

Figure 4.11: Carbody transfer function(α= 20)

From Figure 4.11 it can be concluded that the damping is still not sufficient, giving rise to sharp peaks with the optimal stiffness value (4200 N/m). From the transfer function, it is visible that for the given value of Area ratio (α), the transfer function has decreased and needs further reduction. Area ratio (α) should be increased for more damping.

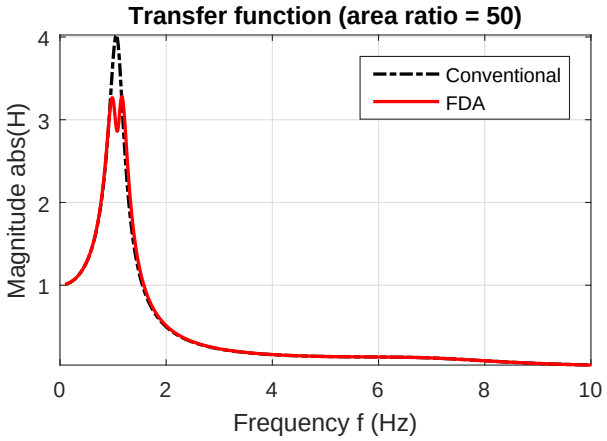

Figure 4.12: Carbody transfer function(α= 50)

From Figure 4.12 it can be concluded that the damping has reduced the peaks by a good extent with the optimal stiffness value (10300 N/m). From the transfer function, it is visible that for the given value of Area ratio (α), the transfer function has substantially decreased and can be improved more. Area ratio (α) can be increased more for even smoother peaks.

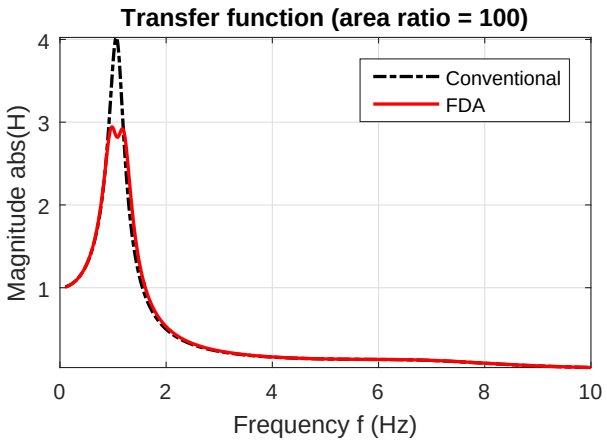

Figure 4.13: Carbody transfer function(α= 100)

From Figure 4.12 : The damping has reduced the peaks by an optimum extent with the optimal stiffness value (21500 N/m). The Area ratio (α) is an optimum value for optimum damping. Increasing the value can lead to over-damping. It represents the optimum combination of parameters.

It can be seen from the previous steps that the area ratio (α) can theoretically be increased till infinity. But an important consideration is the nature of the flow of the fluid. The system of equations concerning the fluid behavior in the Fluid Dynamic Absorber only holds as long as the flow inside the device is laminar which will not be the case at higher values of (α) . The value of the Reynolds number can act as an indicator for the purpose.

Another step to be taken into consideration is the manufacturability of small cross sections. In the above case, further investigation is limited to (α) =100 since greater area ratios will require smaller cross sections.

6. The cases with Area ratio (α) = 50 and Area ratio (α) = 100 are taken and implemented for time simulation in Dymola for a period of 50 s and carbody accelerations are evaluated. The parameters of the Fluid Dynamic Absorber calculated from the design methodology are:

Table 4.6: Parameters of FDA for different area ratios for Manchester benchmark model

Area ratio (α)	50	100
Length of the stroke ($2L + l$)	0.732 m	0.732 m
Length ratio (β)	0.72	0.72
Radius of the larger cross section (R)	0.071 m	0.071 m
Piston spring stiffness (k_{pi})	10300 N/m	21500 N/m
Piston mass (m_{pi})	0.2 kg	0.2 kg

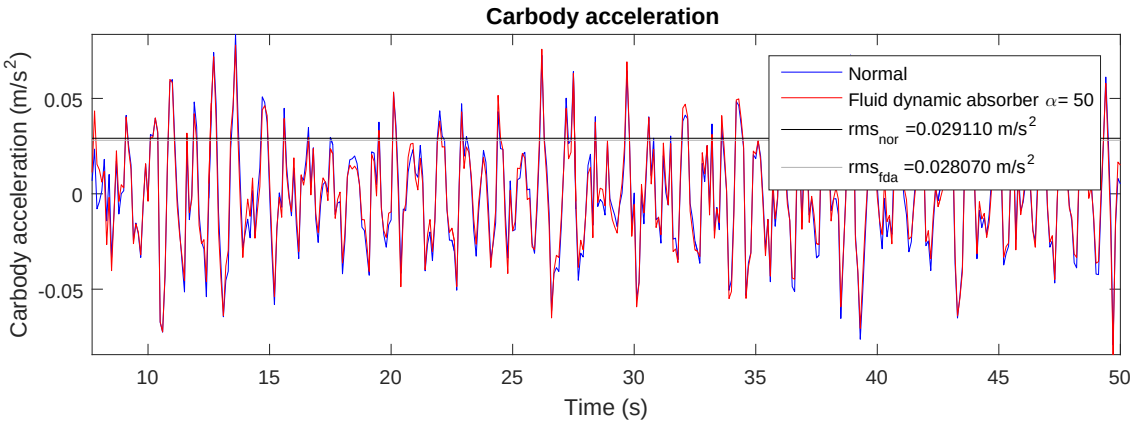

Figure 4.14: Carbody acceleration for α =50

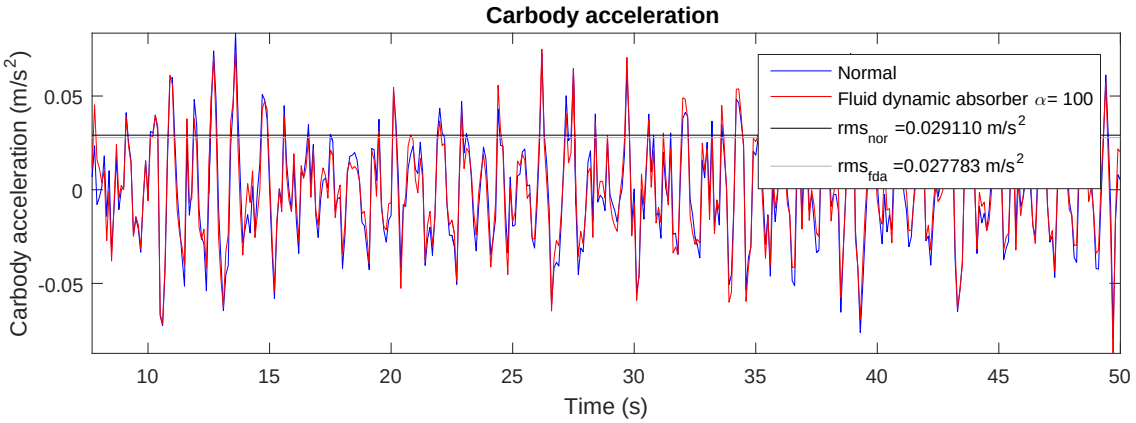

Figure 4.15: Carbody acceleration for α =100

Table 4.7: Rms(z)acceleration: Carbody

Area ratio (α)	Conventional (m/s^2)	FDA (m/s^2)	Percent change
50	0.0291	0.0281	-3.4%
100		0.0278	-4.5%

This combination of parameters represents the best configuration for minimum car-body acceleration .

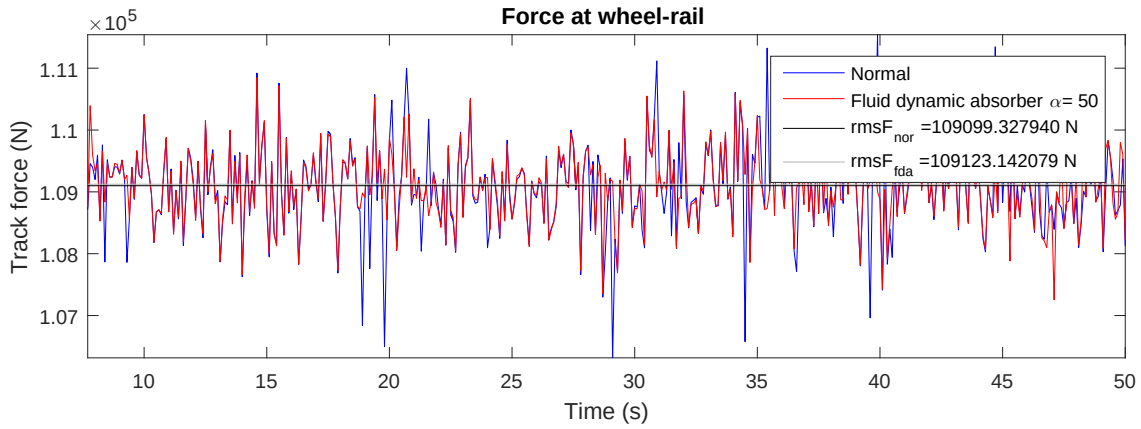

Figure 4.16: Wheel-rail force for α =50

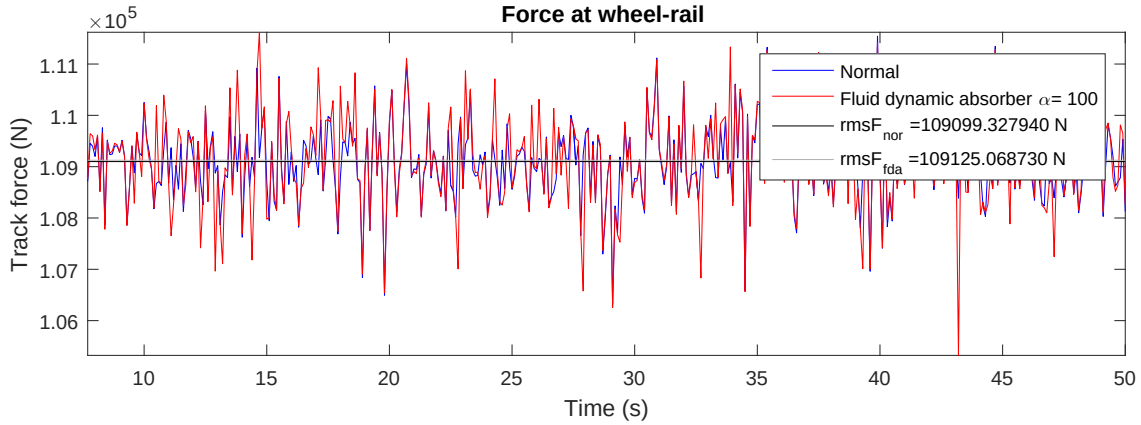

Figure 4.17: Wheel-rail force for α =100

The static load (F_0)is calculated as the weight of the quarter-car model on the track due to gravity. For a conventional suspension it is 108981 N and with Fluid Dynamic Absorber it is 109043 N.

Table 4.8: Wheel-rail force

$rms(Conv.)$ (N)	$\frac{rms(F)}{F_0}$	Area ratio (α)	$rms(FDA)$(N)	$\frac{rms(F)}{F_0}$
109099	1.001	50	109123	1.0007
		100	109152	1.0007

The wheel-rail forces do not change a lot in all the cases. But the addition of the Fluid Dynamic Absorber gives a reduction in the carbody acceleration by 3% to 4%.

4.3.3 Verification of the design methodology

The design methodology employed in the Manchester benchmark model needs to be verified. The two methods that can be employed are shown in Figure 4.18.

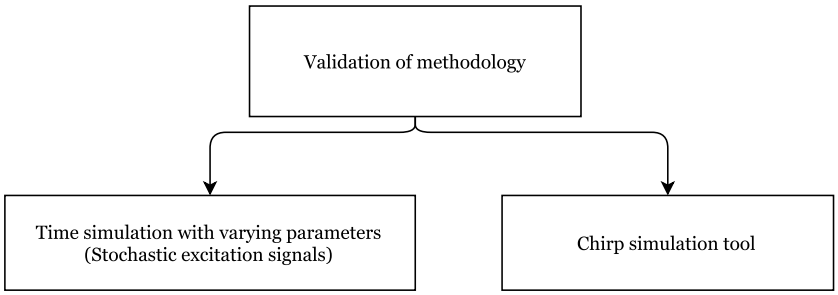

Figure 4.18: Validation of methodology

The case for area ratio (α)= 50 is verified using these methods.

Time simulation with varying parameters

The time simulation model is run with the following parameters:

Table 4.9: Time simulation with varying parameters

Area ratio (α)	50
Density of fluid	880 kg/m^3
Length of stroke	0.732 m
Length ratio (β)	0.72
Radius of larger cross section (R)	0.071m
Piston mass (m_{pi})	0.2 kg

The model is run for multiple cases with piston spring stiffness varied from 6000 N/m to 1.2×10^6 N/m. From the results obtained in the design methodology, the carbody acceleration should be minimum when the piston spring stiffness equals (k_{pi}) = 10300 N/m. The observations from the simulations were plotted as in Figure 4.19:

The root mean square mean value of displacement for the conventional suspension is marked with the triangle while that for the calculated value by the MATLAB approximation with the circle. Since, the calculated value using the MATLAB approximation gives the lowest value in time simulation as well, it means that the transfer function ($H|\frac{z_c}{z_0}|$) generated using the linearized approximation agrees with the behavior calculated in the non-linear time-simulations. Hence the methodology is validated with time simulation of varying piston stiffness (k_{pi}).

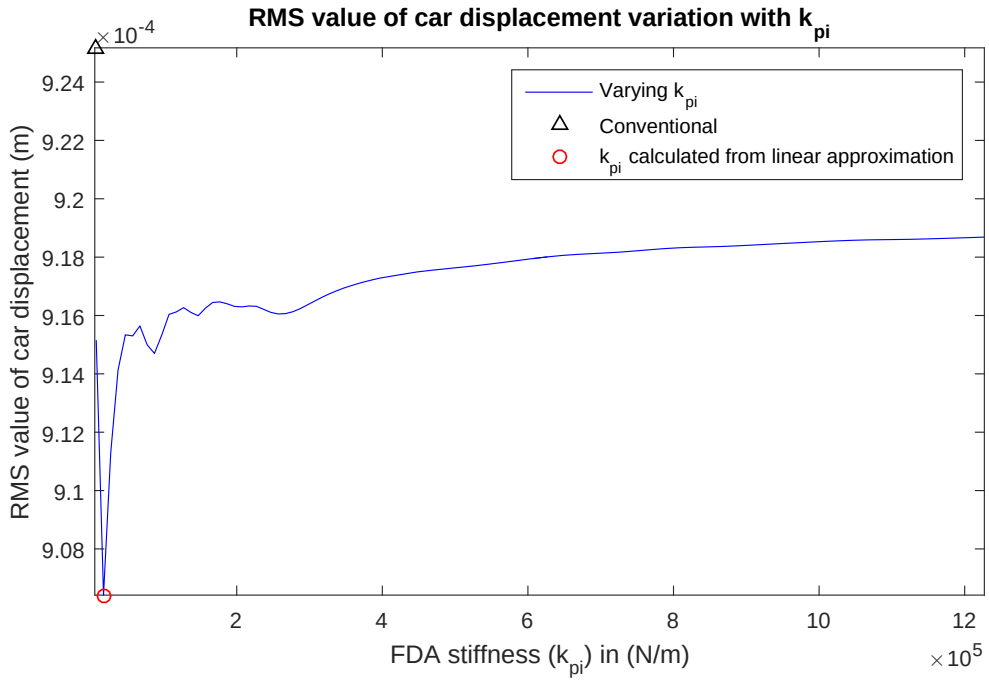

Figure 4.19: RMS carbody displacement for varying FDA stiffness

Chirp simulation tool

As seen in Section 3.5, the chirp simulation is carried out and compared with the transfer function calculated with the linearized approximation.

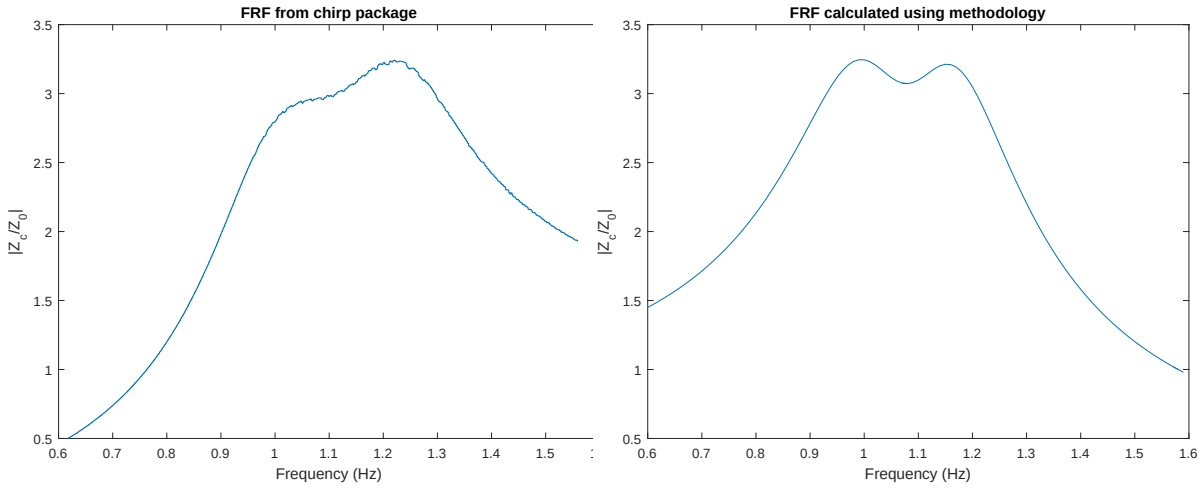

(a) Using chirp tool

(b) Using linearized approximation

Figure 4.20: Transfer function of carbody ($|\frac{Z_c}{Z_0}|$)

The ($Z_{pi} - Z_c$) value for the linearized approximation was taken as the value obtained from the chirp time simulation when the frequency is about 1.1 Hz (to compare the length of the peaks) . Comparing Figures 4.20a and 4.20b, there is a slight deviation in the

transfer function peaks but they are of similar magnitude. Therefore, the formulated design methodology is a reasonable method to calculate the optimal parameters for the Fluid Dynamic Absorber for the application.

4.4 New Generation Train running gear

4.4.1 Modelling

The Next Generation train (NGT)[17] quarter-car model is modelled with the following parameter values.

Table 4.10: Quarter-car parameters :Next Generation train

Parameter	**Value**
Mass of the wheel	916 kg
Mass of the bogie frame	2694 kg
Primary stiffness	4×10^6 N/m
Primary damping	1.24×10^5 Ns/m
Secondary stiffness	3.54×10^5 N/m
Secondary damping	1.3035×10^4 Ns/m
Mass of the carbody	12000 kg

The track model is the same as for the Manchester Benchmark model described in Section 4.3.1. Figure 4.21 depicts the time simulation quarter-car model of the Next Generation Train in the Dymola interface with a) conventional suspension b) suspension with the Fluid Dynamic Absorber.

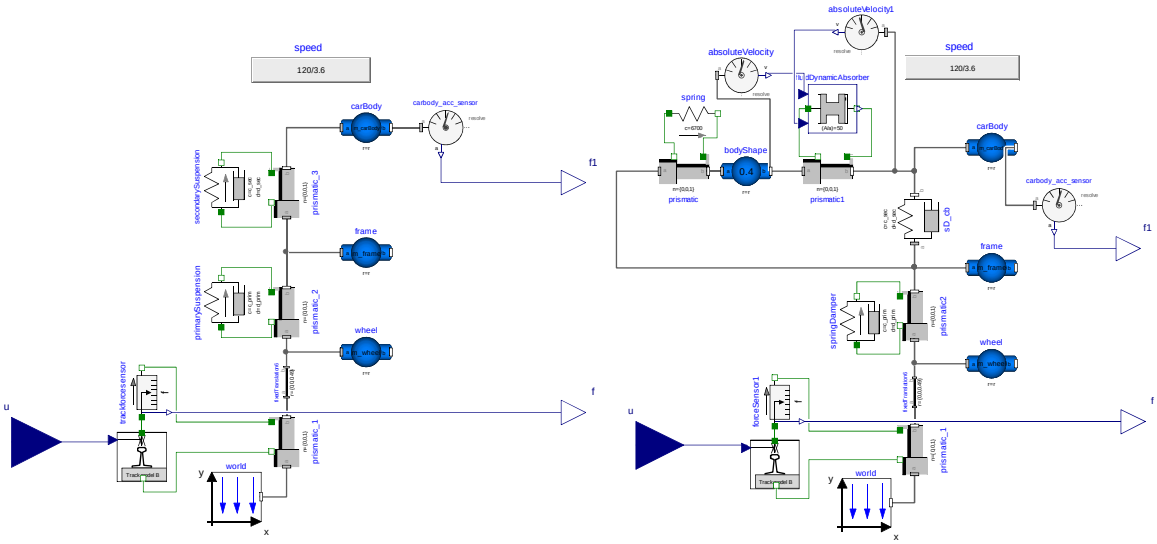

(a) Conventional suspension (b) With FDA in secondary suspension

Figure 4.21: Next Generation Train quarter-car model

4.4.2 Design parameters

The design parameters are calculated using the design methodology analogous to the way calculated for the Manchester Benchmark model. The Fluid Dynamic Absorber parameters calculated for an Area ratio (α) = 50 are:

Table 4.11: FDA parameters: Next Generation train

Parameter	**Value**
Area ratio(α)	50
Density of fluid	880 kg/m^3
Length of the stroke (2L+l)	0.732 m
L/l ratio (β)	0.72
Radius of the larger cross section (R)	0.071m
Piston mass (m_{pi})	0.2 kg
Piston spring stiffness (k_{pi})	6700 N/m

4.4.3 Simulation and results

The carbody acceleration and the track force can be seen in Figure 4.22 and Figure 4.23

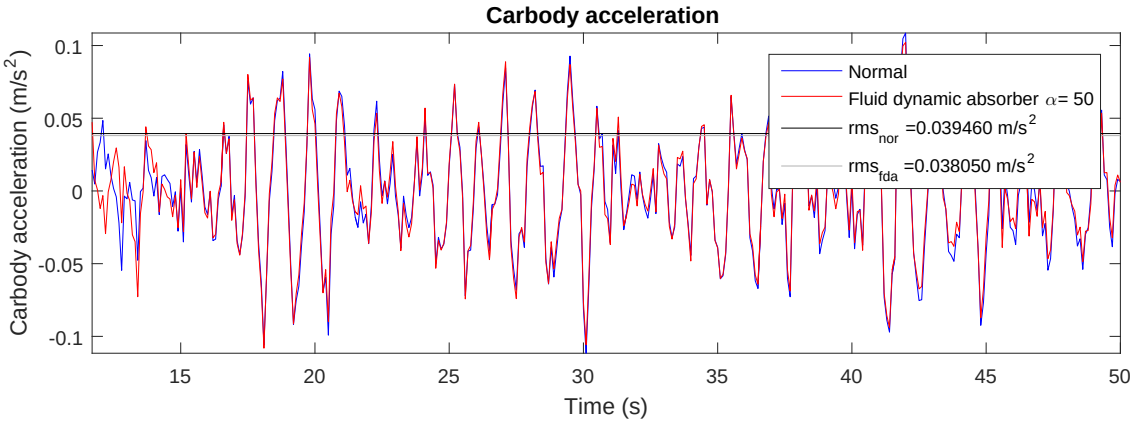

Figure 4.22: NGT: Carbody acceleration

Table 4.12: NGT: RMS acceleration of the carbody

Conventional (m/s^2)	**FDA** (m/s^2)	**Percent change**
0.0395	0.0380	-3.8%

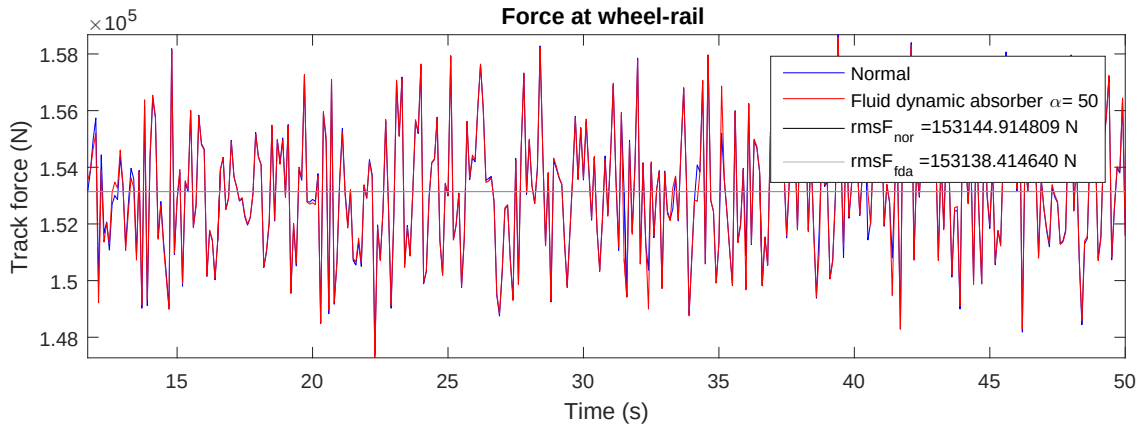

Figure 4.23: NGT:Wheel-rail force

The static load of the NGT running gear(F_0) is 152980 N for the conventional suspension and 153038 N for the one with the FDA.

Table 4.13: NGT:Wheel-rail force

Conventional (N)	$\frac{rms(F)}{F_0}$	**FDA (N)**	$\frac{rms(F)}{F_0}$
153145	1.001	153138	1.0006

The implementation of the Fluid Dynamic Absorber gives a reduction in the carbody acceleration of $\approx 4\%$ while the wheel-rail force remains almost the same.

5 Next Generation Train: Full-car model

The previous chapter covered the simulations of quarter-car rail vehicle models employing the Fluid Dynamic Absorber. In this chapter, the Fluid Dynamic Absorber will be implemented on a full car model in Simpack and simulations performed. For this purpose, the implementation of the Functional Mock-up Interface between Dymola and Simpack is discussed, points of application decided and the Functional Mock-up Unit designed. Finally, the results are discussed.

The main objective of the Functional Mock-up Unit to be built is to mimic the behavior of the device in a different environment. For this purpose, it is necessary to study the change in modelling conditions in both the environments so that it can be adapted and modelled for use in the target environment. In the Simpack interface, the Functional Mock-up Unit is a control element that accepts input signals and calculates the output signals. This control element can then be implemented in force elements with the magnitude of the output signals as the acting force.

The design procedure in Dymola and the implementation procedure in Simpack are discussed in the consequent sections.

5.1 Functional Mock-up Unit design in Dymola

Dymola v2015 consists of a plugin in its simulation tab which makes possible for model conversion to Functional Mock-up Units through its interface.

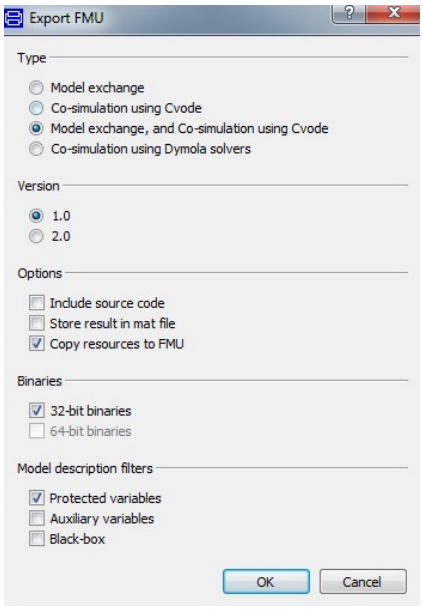

Figure 5.1: FMU tool: Dymola

When the Functional Mock-up Unit is generated, the quantity data (i.e. units like m, s signifying length and seconds respectively) are lost and so the input and the output fields in the unit need to be plainly considered as signals of the respective values. In Section 2.4.2, the modelling methodology of the Fluid Dynamic Absorber in the Dymola interface was discussed. The modelling procedure for the Functional Mock-up Unit will be a slight modification of the one in the Dymola interface. (compare Figure 5.2a and Figure 5.2b)

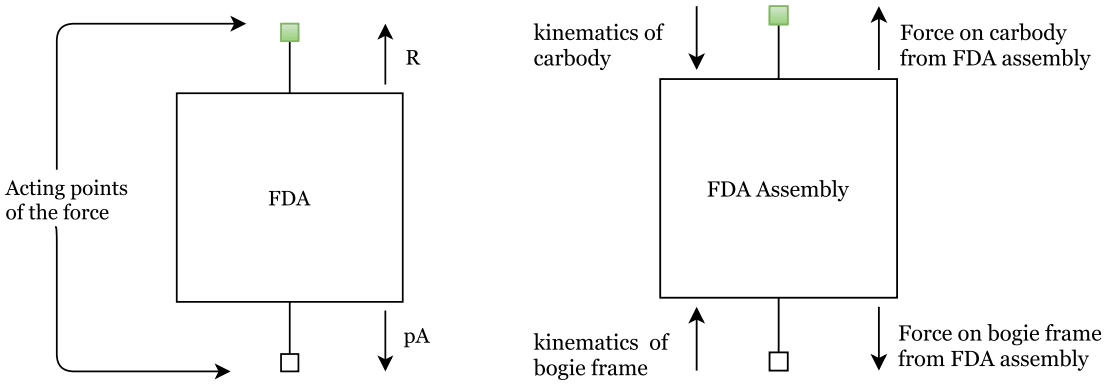

(a) Dymola from Section 2.4.2 (b) Functional Mock-up Interface

Figure 5.2: Designing method for FDA in different interfaces

Figure 5.2b describes the modification in the design procedure for the FMU. The Functional Mock-up Unit in Simpack will be used to generate forces on the acting bodies. It is hence necessary to calculate the forces at both the ends of the Fluid Dynamic Absorber assembly. This is achieved by the use of a force sensor from the Modelica's package. It calculates the magnitude of the force acting at the particular flange of the model returns the value. Figure 5.3 describes the schematic model.

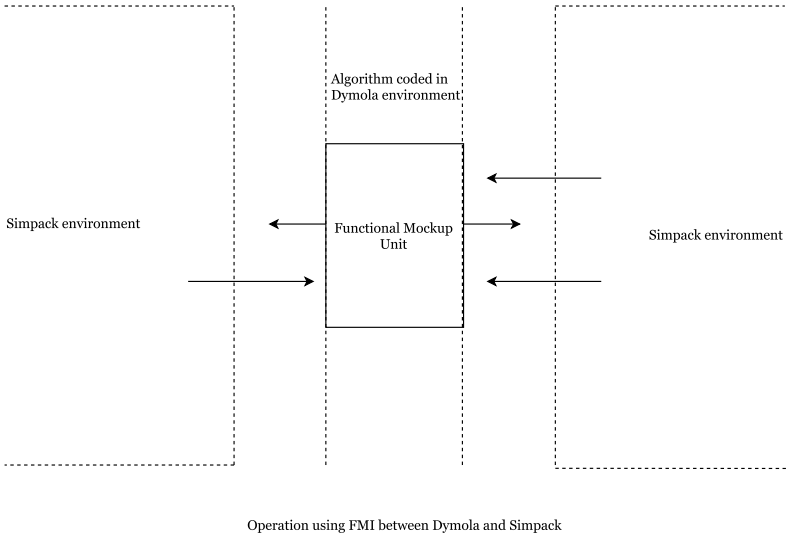

Figure 5.3: Schematic diagram of the FMU

The forces constitute the output signals of the Functional Mock-up Unit. But the Fluid

Dynamic Absorber requires the kinematic behavior of the bodies it acts on to calculate the forces. Otherwise, it will be equivalent to the Fluid Dynamic Absorber being unconstrained and hence no forces will be generated. For this purpose, the position vectors in the direction of action of both the bodies are input into the Functional Mock-up Unit as seen in Figure 5.2b. These input signals are to be generated from the vector points in the Simpack interface which will be described in Section 5.3.

The input signals are received by the Functional Mock-up Unit in the form of signals. These signals have to be converted to position vectors for the Dymola environment to understand. For this purpose, displacement sources are used from the Modelica's mechanics library. Apart from the position inputs, the velocity of the carbody is also input in the form of another signal for the Fluid Dynamic Absorber calculations. The Dymola model is illustrated in Figure 5.4.

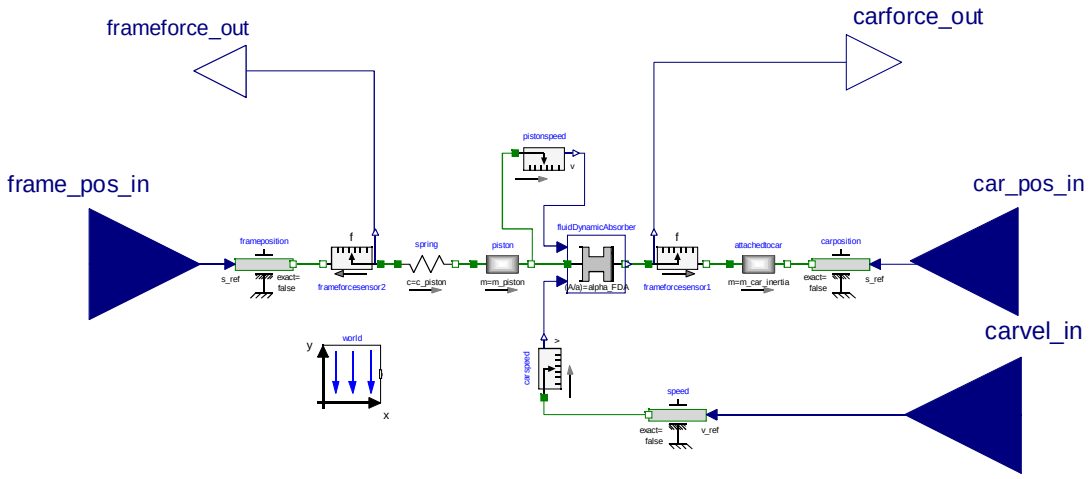

Figure 5.4: Functional Mock-up Unit in Dymola

The *frameforce_out* and the *carforce_out* represent the forces acting on the bogie and the carbody from the Fluid Dynamic Absorber assembly respectively. The *frame_pos_in* and the *car_pos_in* represent the position inputs from the bogie frame and the carbody to the Fluid Dynamic Absorber assembly respectively. The *carvel_in* represent the velocity inputs from the carbody.

5.2 Simpack model of NGT

To understand the application of the generated Functional Mock-up Unit on the full car model, a brief description about the geometric properties of the NGT car is given. The details of the different components used and the running conditions for simulation are discussed in the next section.

Figure 5.5 and Figure 5.6 depict the front car of the Next Generation train model and the bogie model in Simpack.

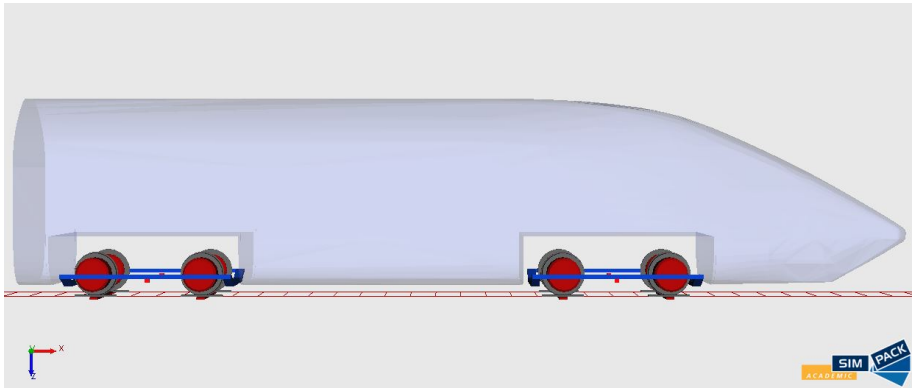

Figure 5.5: NGT:Leading car model in Simpack

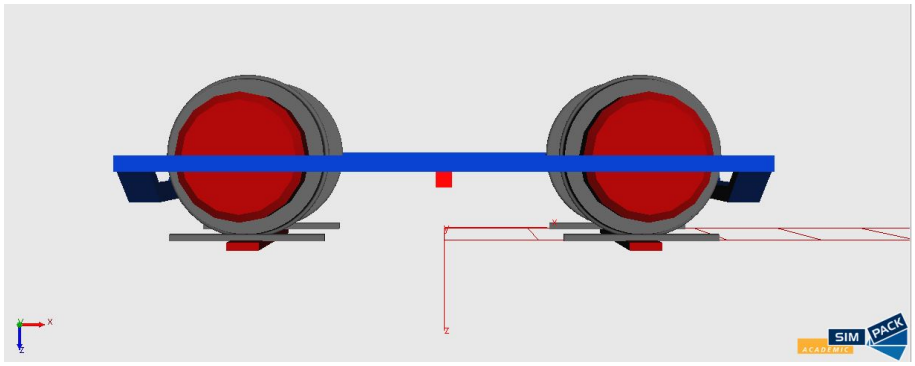

Figure 5.6: NGT:Bogie substructure in Simpack

The Fluid Dynamic Absorber will be applied in parallel to the secondary suspension at 4 points in the full car model. The positions of the application points of the secondary suspension are depicted for the full car and the bogie models with the spring-damper signs as shown in Figure 5.7 and Figure 5.8

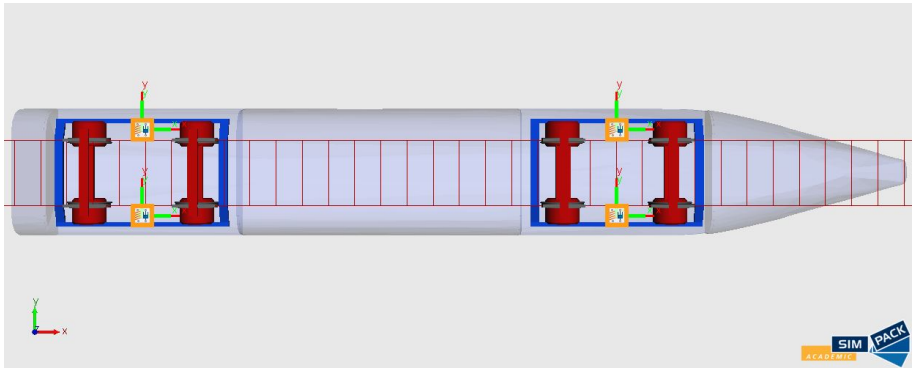

Figure 5.7: NGT:FDA placement postition on the car

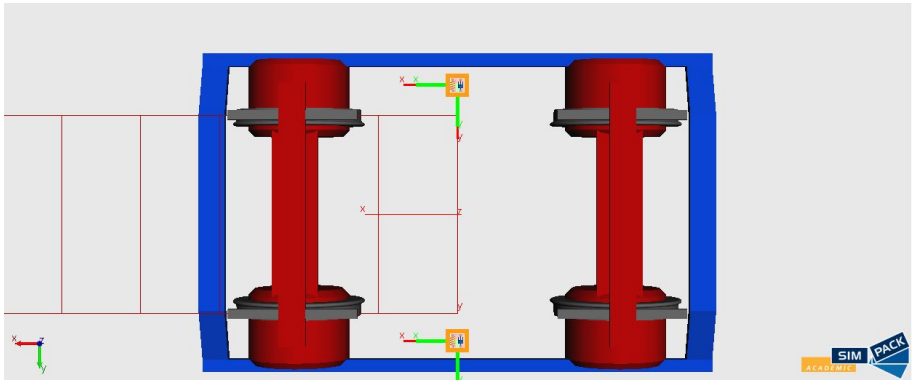

Figure 5.8: NGT:FDA placement position on bogie

The secondary suspensions are modelled as force elements linked to the carbody and the bogie frames at the markers. The markers identify the position vector where the suspension element acts. These markers will be utilized for the implementation of the Fluid Dynamic Absorber as a force element.

5.3 FMI interface in Simpack

The Simpack environment supports the use of Functional Mock-up Interface [30] for implementation of components modelled in other design environments (Dymola). It is implemented in the form of a control element type as shown in Figure 5.9.

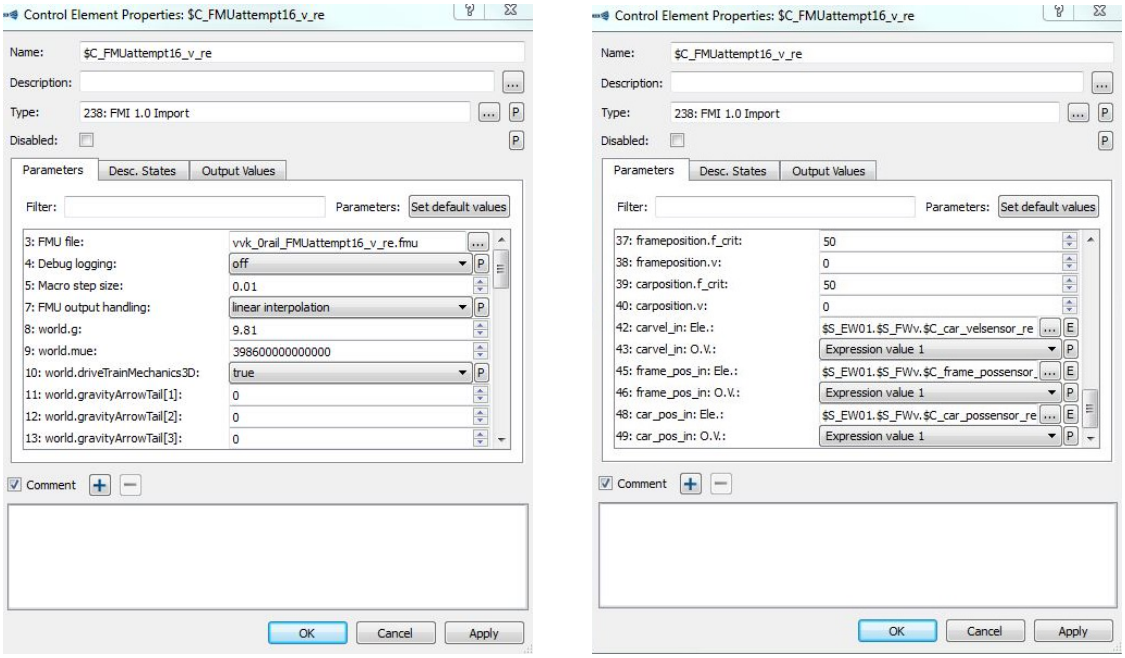

(a) FDA parameters in FMU

(b) FMU inputs

Figure 5.9: FMU:Control element in Simpack

The Functional Mock-up Unit consists of the input parameters modelled in the Dymola interface. The flow of information for the Fluid Dynamic Absorber operation through the FMU happens as seen in the schematic diagram (Figure 5.10).

The input channel to the Functional Mock-up Unit is assigned values with the help of expression sensors. The expression sensor is an efficient tool to design active systems in Simpack. Since Simpack does not have sensors to measure the velocity, position, etc of a particular body at a marker position, expressions are declared containing the desired vector. These expressions are then input in the expression sensors from the control element options.

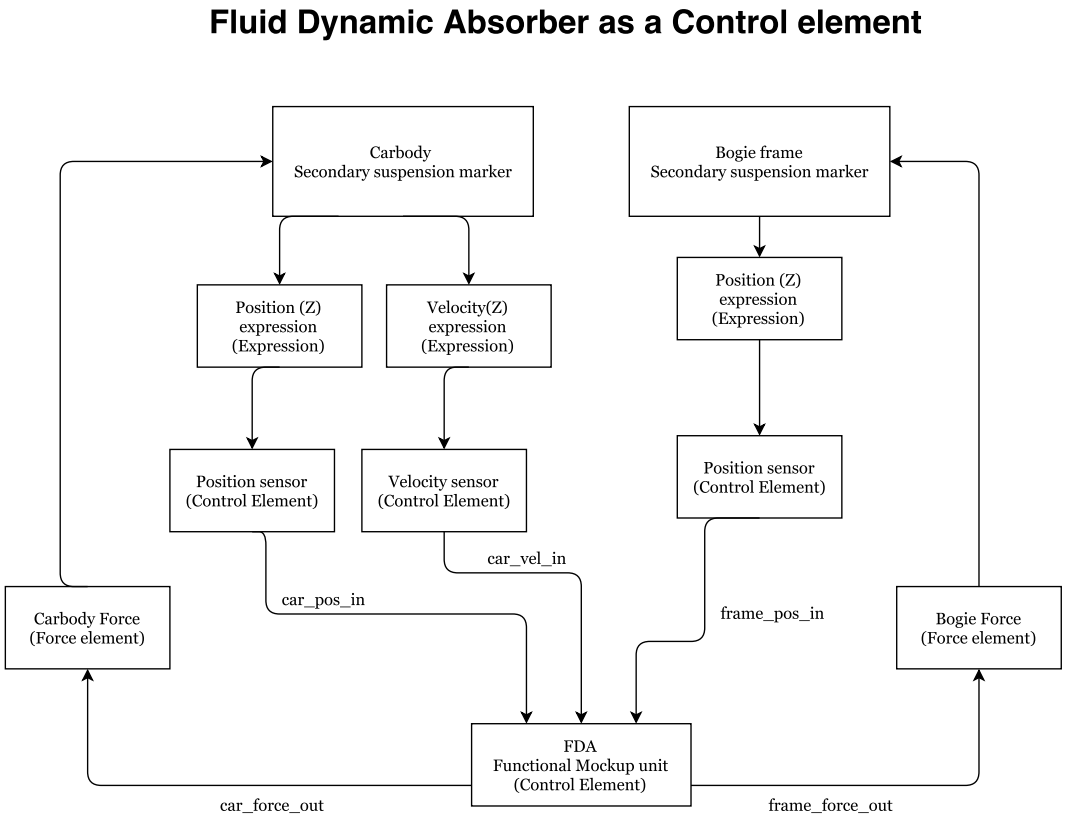

Figure 5.10: Working of the FMU as a control element

The outputs *frameforce_out* and the *carforce_out* from the Functional Mock-up Unit are implemented as force elements at the markers for the secondary suspension. The force elements in Simpack however work only when same magnitude of force is applied in both the directions from the Fluid Dynamic Absorber assembly. For this, a fixed mass point is created attached to the carbody with negligible mass and two force elements created with the bogie end having a value of *frameforce_out* and the carbody end with *carforce_out* as seen in Figure 5.11. Similarly, the Functional Mock-up Units are applied to all the four secondary suspension points (Figure 5.7) of the car.

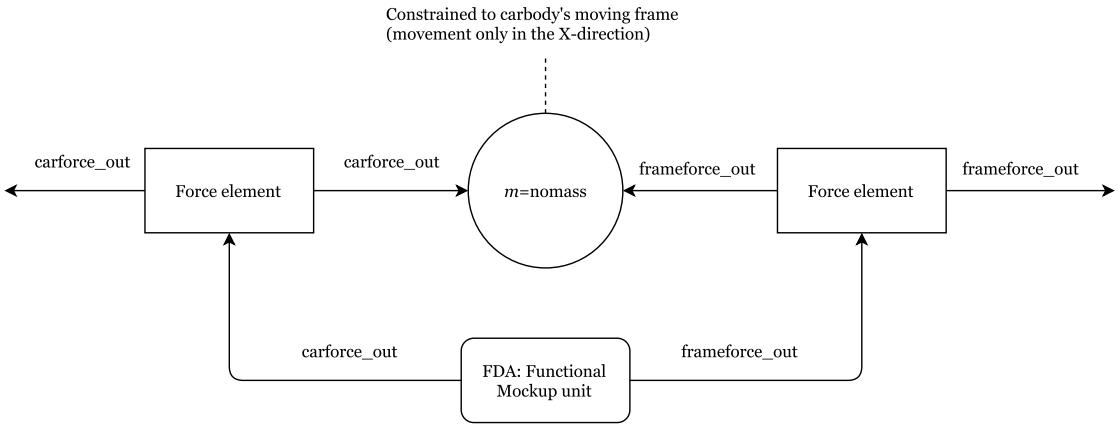

Figure 5.11: Force application

5.4 Simulation conditions

The track conditions for the time simulation in Simpack conforms with the Test track 3 scenario given in Appendix B. The train is run at a velocity of of 440 km/h in the specified track.

5.5 Comfort criteria

Wertungszahl (Wz) is a standard criterion used to evaluate comfort in rail vehicles [3]. The Wz criterion is evaluated from accelerations measured on the floor of the vehicle. They are calculated over defined time intervals or defined track sections. The Wz criterion is defined by the following equation:

$$Wz = [100B(f)a_0]^{0.3} \tag{5.1}$$

where: $B(f)$ is the frequency weighting function achieved through a filter,
f is frequency,
a_0 is acceleration amplitude (m/s^2)measured on the inner floor of the vehicle vertically. The filter functions are illustrated in [3]. Using the Wz criteria, the passenger is most sensitive to frequencies between 3 and 7 Hz for motion in the lateral and the vertical direction. The Wz criterion can also be expressed as a frequency weighted rms value of accelerations plotted on a logarithmic scale. The corresponding expression used to calculate Wz is:

$$Wz = 4.42(a^{wrms})^{0.3} \tag{5.2}$$

The relation between the comfort index and the sensitivity to vibrations is measured on a 1 to 4 scale, where Wz = 4 means that the vibrations level will have a harmful impact on the human body at a prolonged exposure.

The Simpack interface comes with the necessary filters for the calculation of Wz comfort criteria [28]. These filters are used to evaluate the comfort values in vertical direction.

5.6 Simulation

The design methodology used from Section 4.1 is used for the full car model as well to calculate the optimal combination of Fluid Dynamic Absorber parameters. In this case, the initial time simulation to calculate the s_{rel} (the relative motion between the FDA and the piston and the carbody) is performed in Simpack. The following cases were formulated for time simulation.

Table 5.1: NGT : Simpack simulation cases

Case	α	**Radius (R)**	**Stroke length (2L+l)**	ρ	**Control fluid mass** (m_F)	β	k_{pi}
	(no unit)	(m)	(m)	(kg/m^3)	(kg)	(no unit)	(kN/m)
Baseline	N/A	N/A	N/A	N/A	N/A	N/A	N/A
1	50	0.071	0.37	880	0.04	0.72	40
2	100	0.071	0.37	880	0.02	0.72	400
3	50	0.071	0.73	880	0.08	0.72	21
4	100	0.05	0.37	880	0.01	0.72	110
5	100	0.071	0.73	880	0.04	0.72	140

5.7 Results

The results of the simulation cases compared with the baseline models are listed in Table 5.2. The time history plots of carbody acceleration for the fourth case is plotted in Figure 5.12.

Table 5.2: NGT : Simpack simulation results

Case	**Dominant parameter** (α)	**Carbody** $acc_{rms}(z)$ (m/s^2)	**Wz Comfort Index**	% **reduction in** acc_{rms}
Baseline	N/A	0.1778	1.72	N/A
1	50	0.1729	1.7	2.74
2	100	0.1671	1.66	6.03
3	50	0.1727	1.69	2.86
4	100	0.1703	1.68	4.22
5	100	0.1656	1.66	6.86

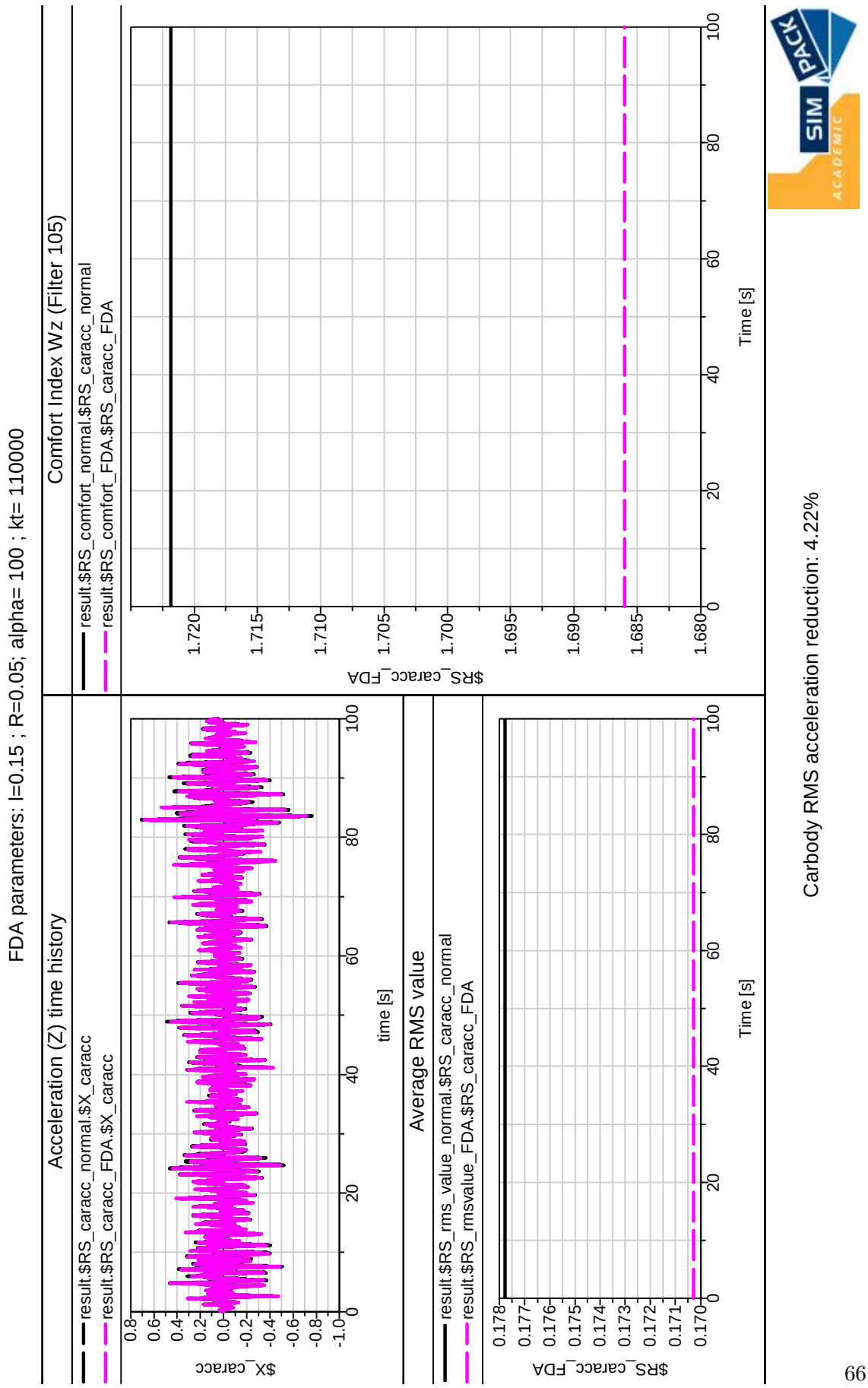

Figure 5.12: Results: Case 4

The effect of the Fluid Dynamic Absorber on the vertical dynamics of the full car model has been studied with help of time simulation in Simpack. The root mean square of the carbody acceleration reduces with increasing mass of the control fluid and the area ratio of the Fluid Dynamic Absorber construction.

Out of the cases simulated, cases 1 to 4 contain Fluid Dynamic Absorbers with parameters that can be added to the existing running gear from the literature survey [13], [16], [21] and [33]. Case 5 is designed to observe the possible improvement in the running behavior with the compounded effect of increased stroke length with a greater area ratio.

Furthermore, from the simulation cases, the parametric effect is studied through a simple comparison of the change seen in varying parameters.

Table 5.3: Comparison of the effect of changing different FDA parameters.

Cases and the corresponding changing parameter (I)	**Cases and the corresponding changing parameter (II)**	**Inference**
1 & 2 (α)	2 & 4 (A)	α has a greater effect on reducing the carbody acceleration than the area of the cross section (A)
1 & 3 ($2L + l$)	1 & 2 (α)	α has a greater effect on reducing the carbody acceleration than the stroke length of the Fluid Dynamic Absorber (2L+l)
2 & 4 (A)	1 & 3 ($2L + l$)	The area of cross section (A) has a greater effect in reducing the carbody acceleration than the stroke length of the Fluid Dynamic Absorber (2L+l).

With the comparison as illustrated in Table 5.3, one can increase the parameters for further improvement in the priority order of:

$$\alpha \quad > \quad A \quad > \quad 2L + l$$

The compounded effect of all the parameters will give the highest improvement as exemplified in Case 5. The first parameter is restricted by the change of fluid flow properties at higher speeds (for higher area ratios (α)) while the second and the third parameter (A) and (2L+l) are constrained by space requirements.

6 Outcomes

6.1 Meeting the objectives

The objectives mentioned in Section 1.2 are matched with the work done to achieve the same.

1. *Perform a comprehensive fundamental linear analysis using quarter-car models in order to expose promising design configurations, application fields and component layoffs*
    - The procedure involved in the linearization of the non-linear Fluid Dynamic Absorber has been discussed
    - The linearized model of the quarter-car model has been built using MATLAB and is used as a parameter calculator to find an optimal combination of parameters that gives the best performance
2. *Perform a literature and internet survey on the state of the art design and application of hydraulic dampers in railway running gears*
    - The literature survey has been done that provided with the information needed to design a Fluid Dynamic Absorber as per the existing dimensions of the dampers for railway running gears
3. *Development and non-linear multibody analysis of one exemplary application to DLR's Next Generation Train running gear*
    - The non-linear governing equations of the working mechanism of the device have been derived and documented as shown in Chapter 2
    - The non-linear quarter-car model has been developed for use in the Dymola interface with the Modelica language, time simulations performed and the resulting behavior documented (Chapter 4)
    - The non-linear Fluid Dynamic Absorber model in Dymola has been modified and exported for use in a full car model of Next Generation train's running gear and the performance studied (Chapter 5)

6.2 Conclusions

The Fluid Dynamic Absorber has been modelled and studied as a potential suspension device in railway vehicles. The non-linear device is applied with help of linearization techniques from literature [11], [29]. The main conclusion of the thesis work are:

1. The vertical dynamics of the rail vehicle improve with the addition of the Fluid Dynamic Absorber

- The ride comfort is improved by using the Fluid Dynamic Absorber in the secondary suspension. The root mean square value of acceleration for the carbody in the vertical direction is reduced between 4% to 6% of the nominal value
- The dynamic forces acting on the wheel-rail interface remain unchanged

2. The negligible effect of the Fluid Dynamic Absorber on the dynamic wheel-rail forces is attributed to the unsprung mass and the stiffer primary suspension.

3. The Fluid Dynamic Absorber gives a greater performance with a higher amount of oscillating fluid and a higher area ratio (α).

4. The simulations and the working principles point to a greater scope of improvement possible with more space being available for the device to be mounted.

5. The Fluid Dynamic Absorber performance changes with varying excitation conditions due to the non-linear behavior of the damping effect. This dependency on the excitation conditions is very important for the design of an optimum Fluid Dynamic Absorber.

6. The inertial mass effect is in comparison lower than the damping effect of the Fluid Dynamic Absorber in case of rail vehicles. This is due to the fact that the effect of the inertial mass being added to the carbody is constrained by the volume available for the amount of fluid in the Fluid Dynamic Absorber. With greater volume of fluid mass and greater area ratios the inertia effect due to the Fluid Dynamic Absorber is also increased.

7. The Fluid Dynamic Absorber designs used in the thesis cannot replace a conventional damper because of lower damping values in lower frequencies. But with greater area ratios and greater amount of oscillating fluid, it can replace a conventional damper as well.

8. The formulation of an initial design methodology of the Fluid Dynamic Absorber has been achieved.

6.3 Future Work & Recommendations

In Section 4.1, it is discussed that the working principle of the Fluid Dynamic Absorber is analogous to the liquid damper. One possible way to further increase the damping effect of the Fluid Dynamic Absorber is by increasing the pressure loss in the device. This can be achieved by combining the pressure-loss principles of both the Fluid Dynamic Absorber and the liquid damper (i.e) change in cross section area and an orifice. This will result in greater damping effect and at the same time, contribute to the inertial mass effect. The concept is shown in Figure 6.1a.

Another possible modification is to introduce an actively controlled cross section area such that the Fluid Dynamic Absorber adapts its effect according to the excitation characteristics. This actively changing cross section can be achieved by using a wedge inside the cross section that can move and hence change the cross section area and be actively controlled. It is illustrated in Figure 6.1b.

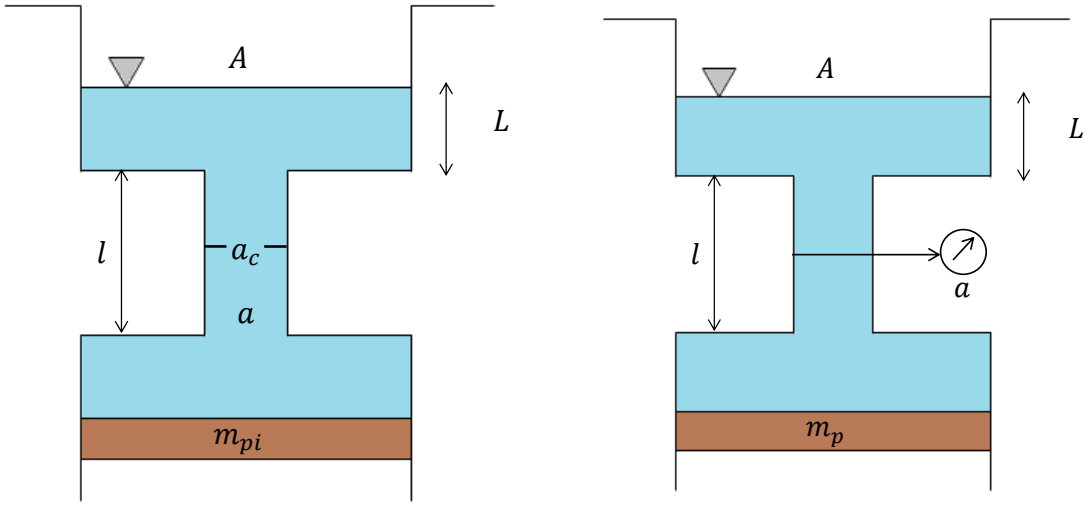

(a) FDA with an orifice

(b) FDA with actively controlled cross section area

Figure 6.1: Future work

A further study could also be conducted regarding the use of Fluid Dynamic Absorbers in improving dynamics in other degrees of freedom (e.g) yaw damping. The Fluid Dynamic Absorber's construction is in general lighter than a conventional damper of comparable dimensions. With greater area ratios, the Fluid Dynamic Absorber can be checked to see whether it can replace a conventional damper.

Non-linear optimization techniques

In this thesis work, the non-linear device was linearized for the specific application. The linear model has been then used to calculate the optimum parameters for the non-linear case. This approach has hence largely been linear with the non-linear model built to validate and observe the results.

Non-linear optimization of the Fluid Dynamic Absorber is another area of further work. It employs the tools for multiobjective optimization and can be applied to optimize more parameters simultaneously. This approach can potentially form the next step to the thesis work performed. The approach of multi-objective parameter optimization for a quarter-vehicle system (road) is described in [34]. It applies different algorithms such as Sequential quadratic programming, Genetic algorithms and Pattern search algorithms to achieve the optimization objectives. This utilizes multiple time simulations over a range of different varying parameters to calculate the optimal design. In the context of this thesis, work has been limited to proposing and testing an initial design methodology achieved through linear techniques. The non-linear optimization techniques can further improve the optimal design of the device.

Appendices

A Existing running gear

Diagrams of running gear used in contemporary High Speed Trains are given in this section.

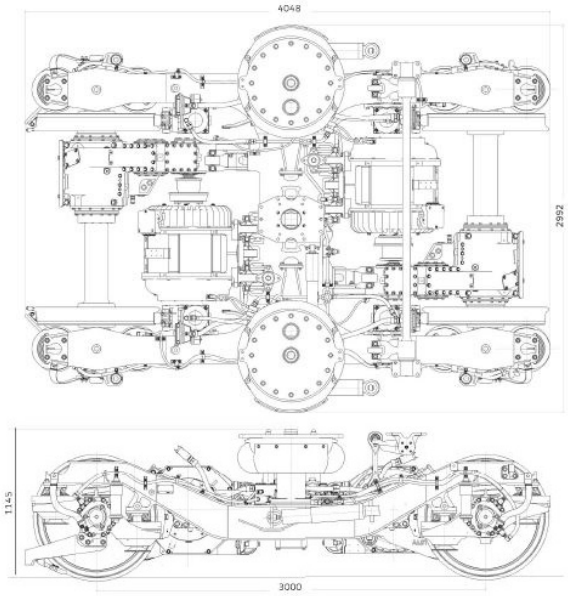

Figure A.1: Alstom *CL 334*, operating speed: 360 km/h [1]

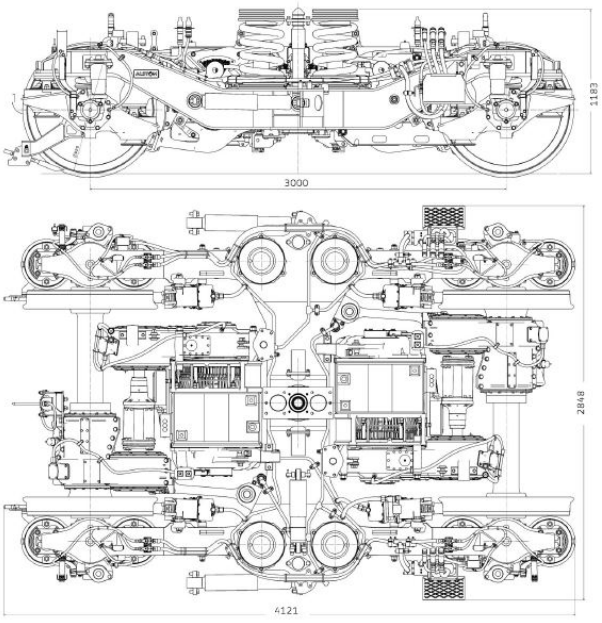

Figure A.2: Alstom *CL 511*, operating speed: 320 km/h [1]

,

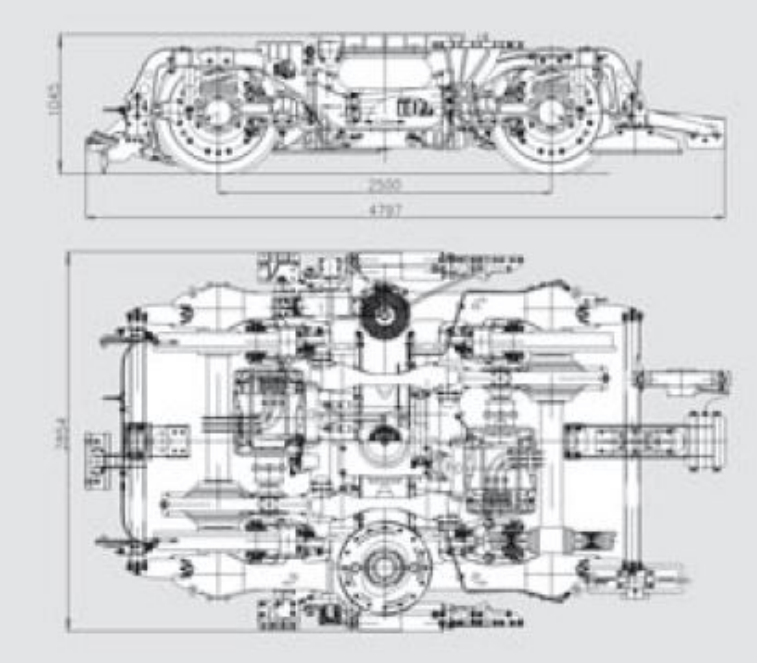

Figure A.3: Siemens *SF 500 TDG*, operating speed: 350 km/h [27]

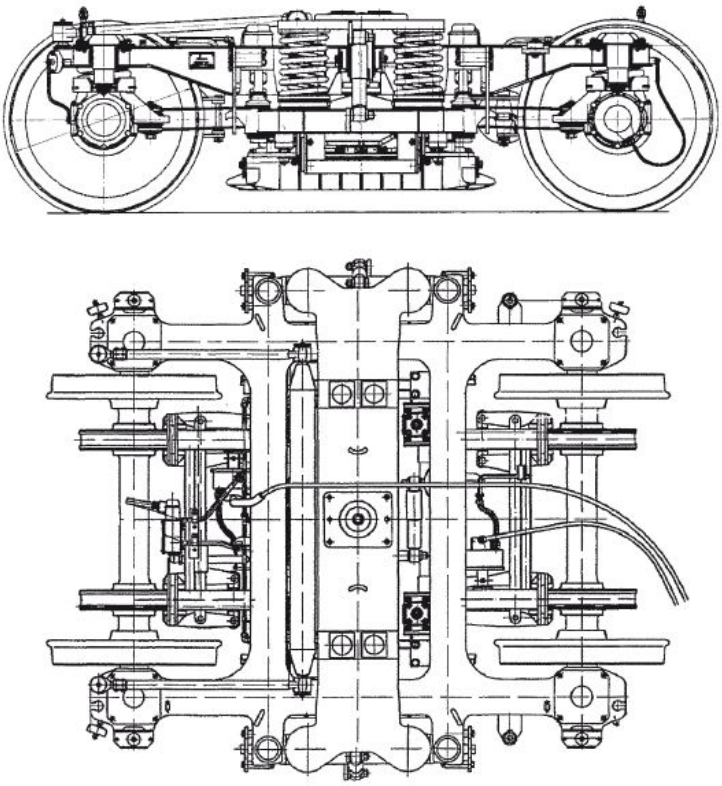

Figure A.4: Bombardier *Flexx fit*, operating speed: 160-280 km/h [7]

c

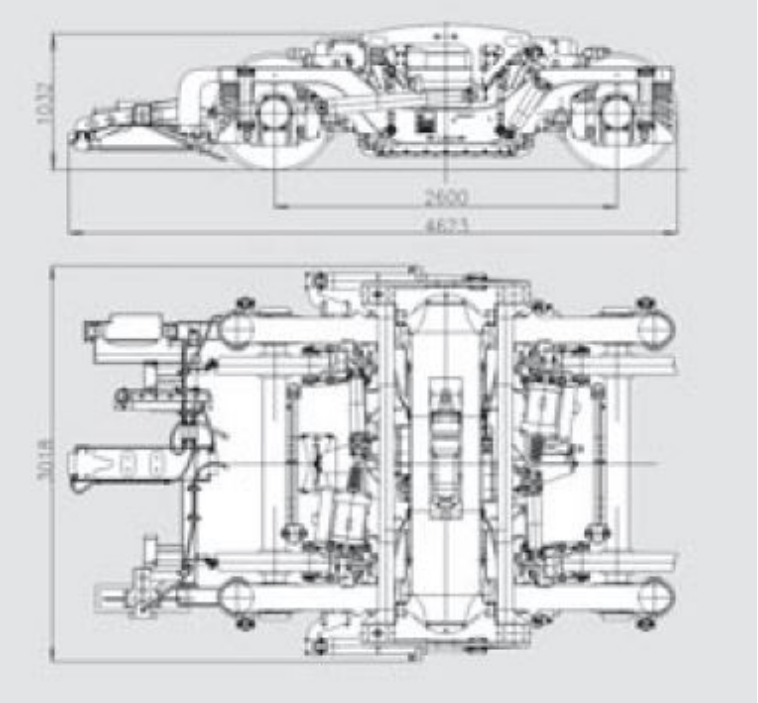

Figure A.5: Siemens *SF 600 TDG*, operating speed: 250 km/h [27]

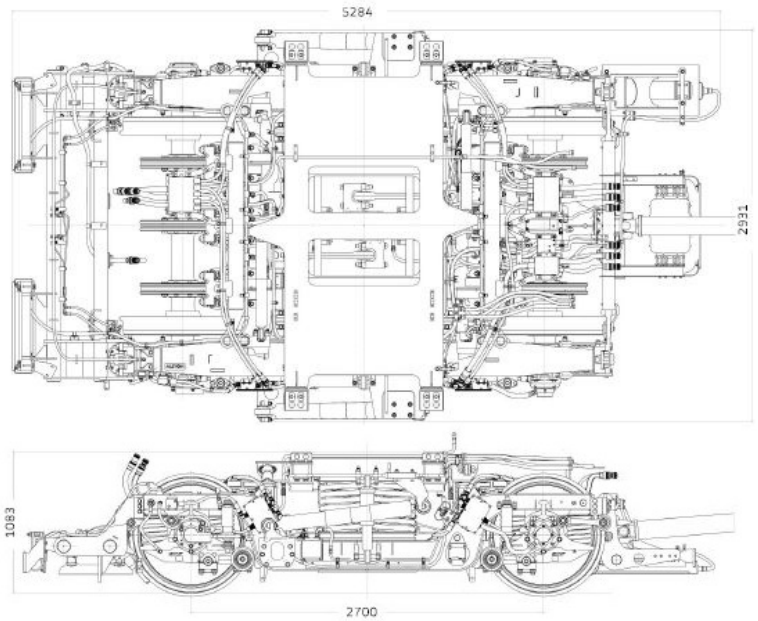

Figure A.6: Alstom *CL 624*, operating speed 225-250 km/h [1]

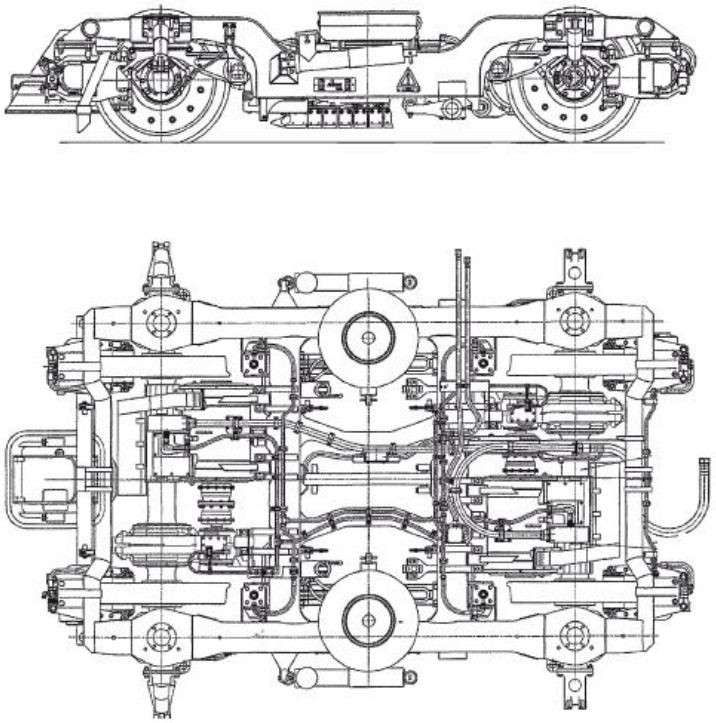

Figure A.7: Bombardier *Flexx link*, operating speed: 160-250 km/h [7]

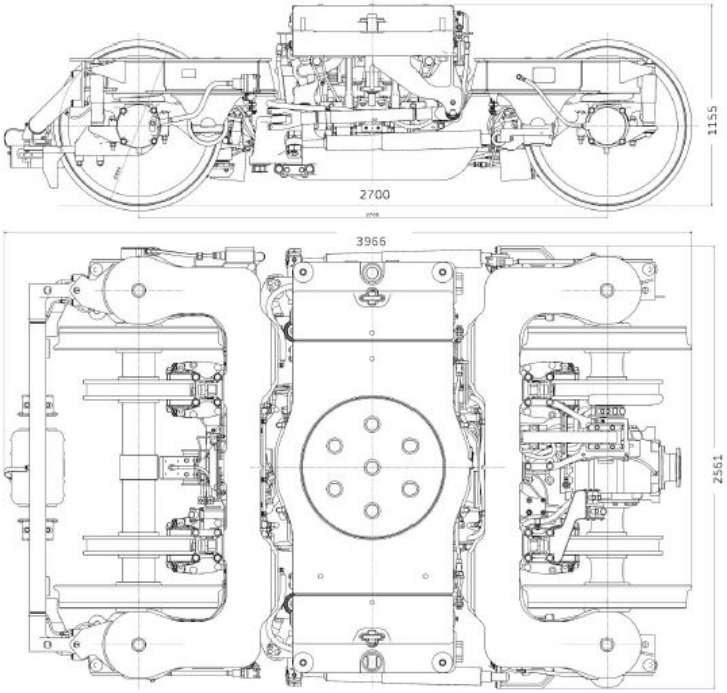

Figure A.8: Alstom *CL 623*, operating speed: 225 km/h [1]

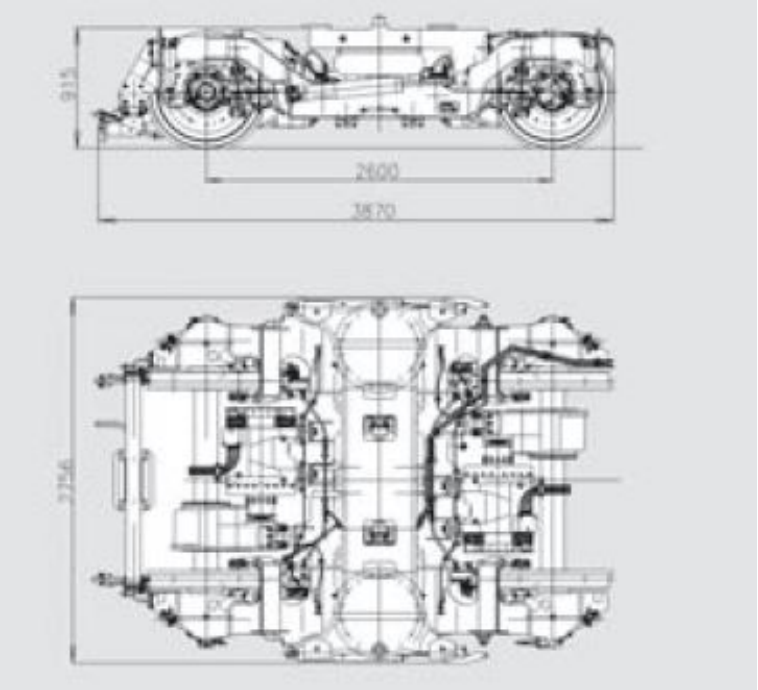

Figure A.9: Siemens *SF 5000 ETDG*, operating speed: 200 km/h [27]

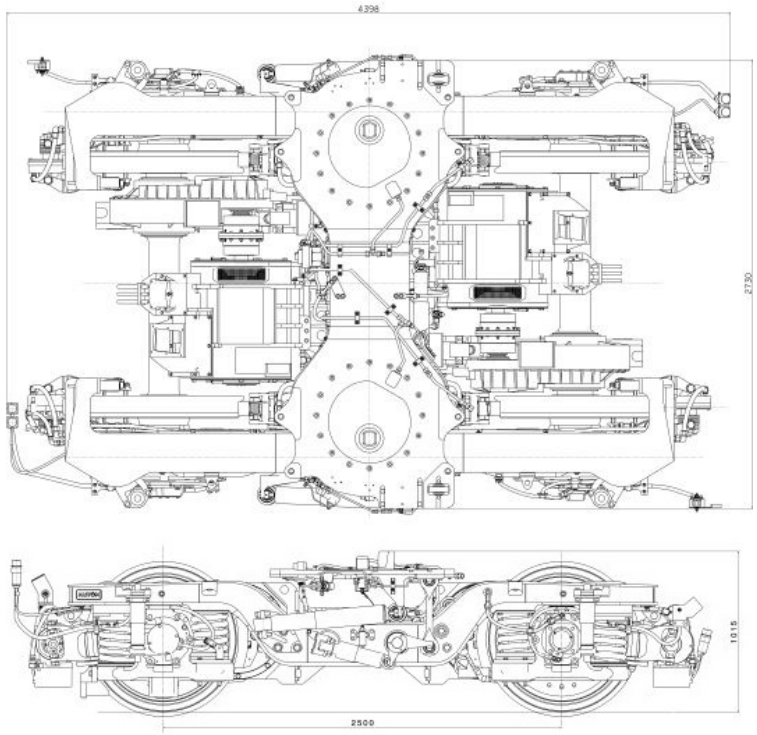

Figure A.10: Alstom *CL 347*, operating speed: 200 km/h [1]

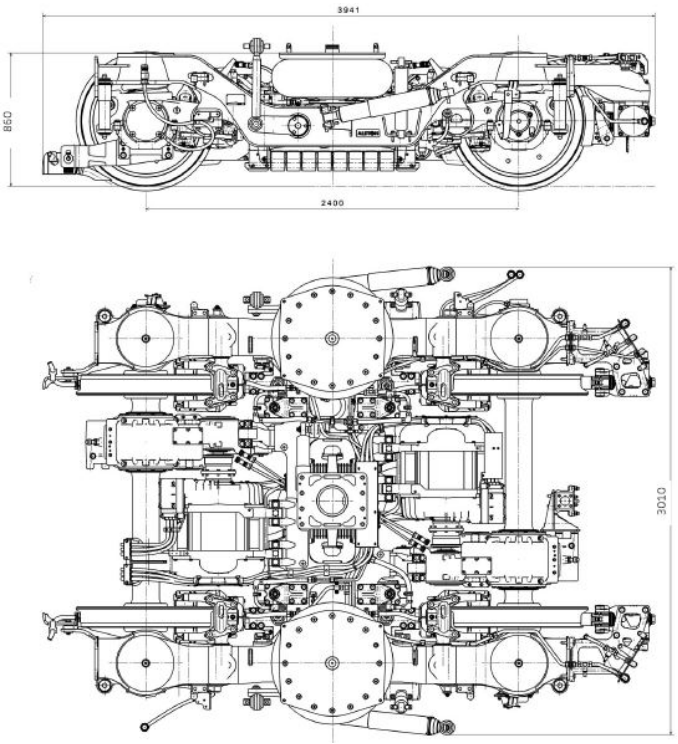

Figure A.11: Alstom *CL 541*, operating speed: 160-200 km/h [1]

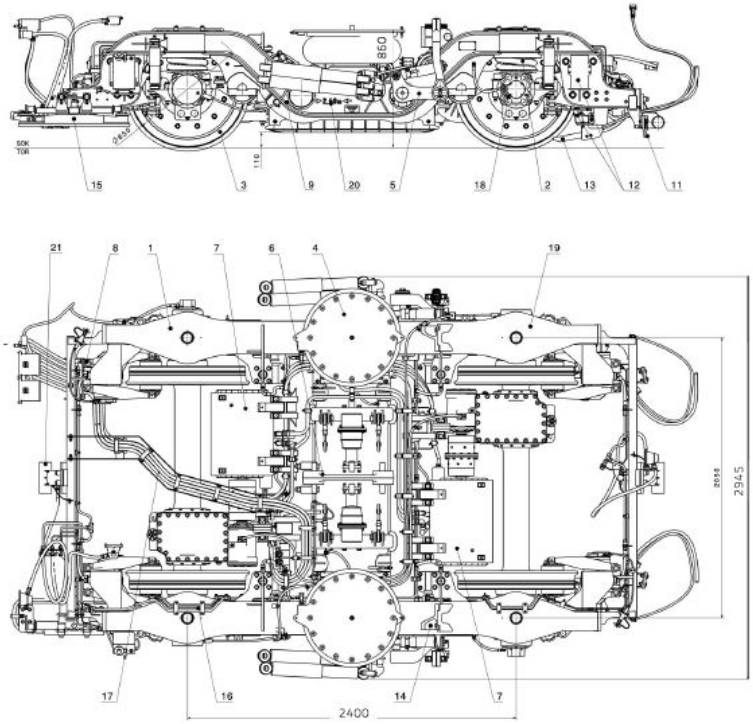

Figure A.12: Alstom *X 200*, operating speed: 160-200 km/h [1]

B Track data in Simpack simulations

The NGT is designed for operation on high speed lines represented by Test Track 3 [17]. At a running velocity of 400 km/h the track irregularities define the most serious challenge for the mechatronic track guidance. For Test Track 3 the irregularities generated using common PSD spectra are modified in order to meet the demands regarding the tracks for acceptance test in EN 14363.

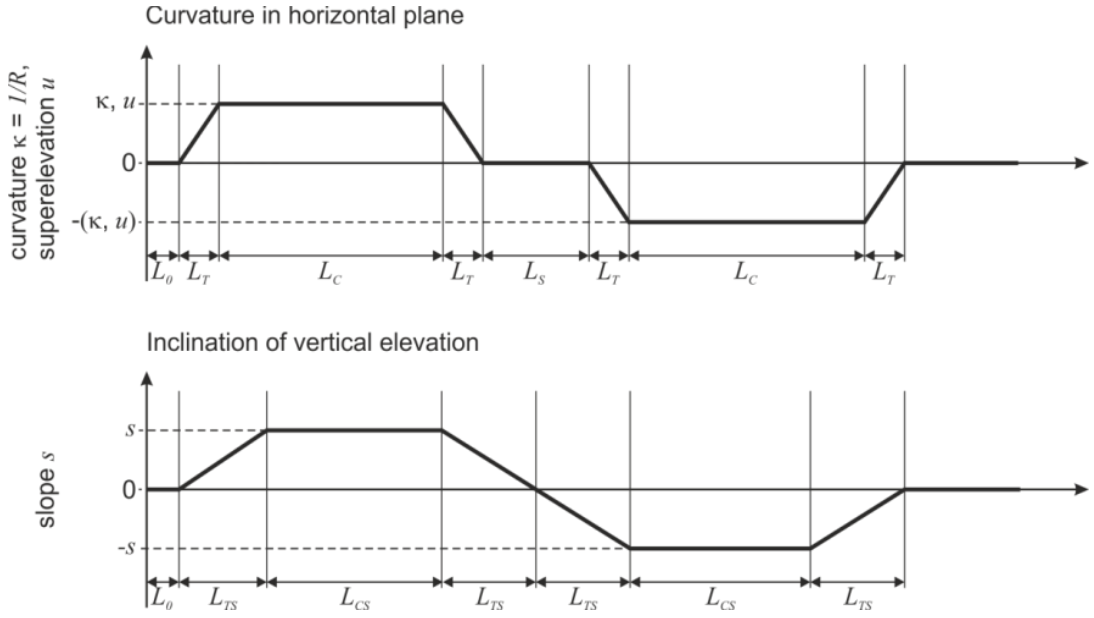

Figure B.1: Layout of the test track

Table B.1: Spatial parameters of FDA for railway secondary suspension

Parameter	**Value**
Speed (v)	400 km/h
Curve radius (R)	8500 m
Super elevation (u)	170 mm
Slope (s)	1%
Initial length(L_0)	260 m
Length of transition curve(L_T)	510 m
Length of constant curve (L_C)	3000 m
Length of intermediate straight section (L_S)	1350 m
Length of slope transition (L_{TS})	1200 m
Length of constant slope (L_{CS})	2295 m
Track irregularities	conforming to EN14363
Simulated time	100 s
Percentage of running distance	90

C Power spectral densities

C.1 Road

The tables from Simpack documentation [28] are used to generate Power spectral densities. These PSDs define road related irregularities in vertical direction and their unit is $m^2/(rad/m)$. The PSDs use a free factor $= 2\pi$ and are one-sided. The polynomials are defined as($\Omega = 2\pi F$):

$$S(\omega) = \frac{b_0}{a_0 + a_2\Omega^2 + a_4\Omega^4} \tag{C.1}$$

The coefficients are:

Table C.1: PSD for road irregularities

Road Type	b_0	a_0	a_2	a_4
Very good cement concrete	0.002129632	1.804124	453.5357	1
Good cement concrete	0.04521842	107.7899	9629.229	1
Good asphalt concrete	0.004627566	5.058896	917.2805	1
Good Macadam	0.003864958	2.339663	539.7142	1
Medium asphalt concrete	0.01696774	5.058896	917.2805	1
Medium pavement	0.04831402	38.09674	1454.728	1
Bad pavement	0.08305384	36.21485	1760.542	1
Very bad Macadam	0.1585651	7.058781	1164.409	1
Bad unfortified road	0.6648117	7.950653	1270.181	1
Very bad unfortified road	18.00072	7.950653	1270.181	1

C.2 Rail

The PSD units are $m^2/(rad/m)$ (horizontal and vertical) and $rad^2/(rad/m)$ (crosslevel).The polynomials are defined as($\Omega = 2\pi F$):

$$S(\Omega) = \frac{b_0 + b_2\Omega^2}{a_0 + a_2\Omega^2 + a_4\Omega^4 + a_6\Omega^6} \tag{C.2}$$

The coefficients are:

Table C.2: PSD for rail irregularities

Irregularity Type	b_0	b_2	a_0	a_2	a_4	a_6
Horizontal low	$1.440846{\cdot}10^{-7}$	0	0.00028855	0.6803895	1	0
Horizontal high	$4.164787{\cdot}10^{-7}$	0	0.00028855	0.6803895	1	0
Vertical low	$2.741619{\cdot}10^{-7}$	0	0.00028855	0.6803895	1	0
Vertical high	$7.343623{\cdot}10^{-7}$	0	0.00028855	0.6803895	1	0
Crosslevel low	0	$4.87399{\cdot}10^{-7}$	$5.535659{\cdot}10^{-5}$	0.1308172	0.8722335	1
Crosslevel high	0	$1.305533{\cdot}10^{-6}$	$5.535659{\cdot}10^{-5}$	0.1308172	0.8722335	1

D FDA Modelica code

```
model FDA "1D Fluid dynamic absorber"
 extends
    Modelica.Mechanics.Translational.Interfaces.PartialTwoFlanges
    ;
 extends Modelica.Blocks.Interfaces.SI2SO;
 parameter Modelica.SIunits.Density rho(min=0,start=1);
 parameter Real alpha "Area ratio";
 parameter Modelica.SIunits.Length length_small=0.1 "small
    length";
 parameter Real beta "Length ratio";
 parameter Real atf(min=100,start=100) "Arctan function
    compensation factor";
 parameter Modelica.SIunits.Length Radius_R= 0.05 "large
    radius";

 Modelica.SIunits.Force fR "Reaction force on frame";
 Modelica.SIunits.Force fP "Reaction force due to hydraulic
    pressure";
 Modelica.SIunits.Force damp_force "Damping force due to
    pressure loss";
 Modelica.SIunits.Force hydraulic_force
    "Hydraulic force due to the column of fluid";
 Modelica.SIunits.Pressure p_loss "Pressure loss in the
    column";
 Modelica.SIunits.Pressure p_0 "Hydraulic Pressure on plunger
    ";
 Modelica.SIunits.Velocity v_f1
    "speed of fluid column in the smaller cross section";
 Modelica.SIunits.Velocity v_f2
    "speed of fluid column in the expanded cross section";
 Modelica.SIunits.Velocity v_b "speed of flange_b";
 Modelica.SIunits.Velocity v_a "speed of flange_a";
 Modelica.SIunits.Velocity v_rel "speed of fluid column";
 Modelica.SIunits.Acceleration a_rel "relative acceleration
    bw a and b";
 Modelica.SIunits.TranslationalDampingConstant bT;
 Modelica.SIunits.Area area_small "control area";
 Modelica.SIunits.Position s_rel(start=0)
    "Relative distance (= flange_b.s - flange_a.s)";

 Real abso;
 Real absu;
```

```
equation
 area_small= (3.141592654*Radius_R^2)/alpha;
 s_rel= flange_b.s-flange_a.s;
 v_rel= der(flange_b.s-flange_a.s);
 v_a= u1 "Input of the velocity of plunger";
 v_b= u2 "Input of the velocity of FDA frame";

(alpha*area_small*v_a)-(area_small*(alpha-1)*v_b)=area_small*
   v_f1
    "Equation of continuity at contraction";
(area_small*v_f1)+(area_small*(alpha-1)*v_b)=alpha*area_small
   *v_f2
    "Equation of continuity at expansion";

 p_loss=((1-(1/alpha))^2+0.44)*0.5*rho*(v_a-v_b)^2*alpha^2
    "Pressure loss from contraction and expansion magnitude";
 p_loss= (bT*(v_a-v_b))/(area_small*alpha)
    "Equivalent linear damping coefficient";
 p_0= ((rho*length_small*der(v_f1))+(2*rho*beta*length_small*
    der(v_f2)))
    "Hydraulic pressure on the plunger using Bernoulli
       principle";

 abso= atan((v_a-v_b)*atf)*0.6335
    "Direction indicator of relative fluid flow w.r.t FDA
       frame";
 hydraulic_force= ((rho*length_small*der(v_f1))+(2*rho*beta*
    length_small*der(v_f2)))*area_small*alpha
    "Hydraulic force on plunger";
 damp_force= (p_loss*area_small*alpha*abso)
    "Damping force due to pressure losses";

 fR= (area_small*(alpha-1)*rho*length_small*der(v_f1))+(
    p_loss*area_small*alpha*abso)
    "Force acting on FDA frame";
 fP= (p_0*area_small*alpha)+(p_loss*area_small*alpha*abso)
    "Force acting on plunger/piston";

 absu= sign(v_a-v_b) " For comparing sign and arctan values";
 y=u2-u1;
 a_rel=der(y);
 flange_a.f= fP;
 flange_b.f= -fR;
 connect(y, y);
end FDA;
```

Bibliography

[1] Alstom Transportation: *Bogie Catalogue 2015*; http://www.alstom.com/products-services/product-catalogue/rail-systems/components/bogies/

[2] Andersson P.B.U,Kropp W: *Time domain contact model for tyre/road interaction including nonlinear contact stiffness due to small-scale roughness* ; Journal of Sound and Vibration 318 296–312 (2008)

[3] Anderson E,Berg M,Stichel S: *Rail Vehicle Dynamics*; Text book, Division of rail vehicles, Department of Aeronautical and vehicle engineering , KTH Royal Institute of Technology., Stockholm (2014)

[4] Awrejcewicz J, Olejnik P: *Numerical analysis of self-excited by friction chaotic oscillations in two-degrees-of-freedom systrem using exact Henón method.* sec.3; Machine Dynamics Problems, Vol.26, No 4, 9-20 (2002)

[5] Bansal R.K *A textbook of fluid mechanics and hydraulic machines*; Laxmi publications(2010)

[6] Berg.M ,Chaar.N: *Simulation of vehicle–track interaction with flexible wheelsets, moving track models and field tests*; Vehicle System Dynamics Vol. 44, Supplement,921–931 (2006)

[7] Bombardier Transportation: *FLEXX bogies*; http://www.bombardier.com/en/transportation/products-services/bogies/intercity-high-speed-trains.html

[8] Bruni S, Vinolas J, Berg M, Stichel S: *Modelling of suspension components in a rail vehicel dynamics context*; Vehicle system dynamics,49:7,1021-1072,DOI:10.1080/00423114.2011.586430 (2011)

[9] Bünte T: *Recording of Model Frequency Responses and Describing Functions in Modelica*; German Aerospace Center (DLR) Institute of Robotics and Mechatronics, Germany.

[10] Connor J and Laflamme S.: *Structural Motion Engineering*, pg. 260-272; DOI 10.1007/978-3-319-06281-5_5, Springer International Publishing Switzerland (2014).

[11] Corneli T, Pelz P.F *Employing Hydraulic Transmission for Light weight Dynamic Absorber* ; 9.IFK – Proceedings Vol.3(2014).

[12] Den Hartog J.P: *Mechanical vibrations*; Dover publications (2013)

[13] Hitachi Automotive Systems, Ltd: *Vertical damper*; http://www.hitachi-automotive.co.jp/en/products/aft/aft_04/01_pop.html

[14] Hundal M.S *Impact absorber with linear spring and quadratic damper*; Journal of Sound and Vibration 48(2), 189-1933 (1976)

[15] Iwnick.S : *Manchester Benchmarks for Rail Vehicle Simulation*; Vehicle System Dynamics, 30:3-4, 295-313, DOI: 10.1080/00423119808969454.(1998)

[16] Knorr-Bremse Systeme für Schienenfahrzeuge GmbH *Shock absorbers*; http://www.knorr-bremse.com/media/documents/railvehicles/product_broschures/brake_systems/Shock_Absorber_P_1259_EN.pdf

[17] Kurzeck B, Heckmann A, Wesseler C, Rapp M: *Mechatronic track guidance on disturbed track:The trade-off between actuator performance and wheel wear*; Institute of System Dynamics and Control, German Aerospace Center (DLR)

[18] Marano G.C, Greco R: *Optimization criteria for tuned mass dampers for structural vibration control under stochastic excitation*; Journal of Vibration and Control 17(5) 679–688 (2010)

[19] *Modelica- A Unified Object-Oriented Language for Systems Modelling Language Specification*; (https://www.modelica.org) (2014)

[20] *Next Generation train*; http://www.dlr.de/dlr/en/desktopdefault.aspx/tabid-10467/740_read-916/#/gallery/2043 (2016)

[21] Paulstra Railway Ferroviaire Eisenbahn *Catalogue of Rail vehicle suspensions and systems*; http://www.hutchinson-asia.com/uploads/anti_indus/Railway%20Catalogue/Railway%20catalogue_paulstra.pdf

[22] Pelz P.F,Cloos F, Corneli T, Hedrich P, Nakhjiri M. *Leichtbautilger für Fahrwerke*; VDI-Berichte Nr.2261 (2015).

[23] Pueube J.L: *Fundamentals of Fluid Mechanics and Transport Phenomena* Chapter.4; ISTE Ltd. (2009)

[24] Ramos J.C, Rivas A, Biera J, Sacramento G, Sala J.A: *Parametric study and simplified design of tuned mass dampers*; Applied Thermal Engineering 1836–1853, Elsevier Science Ltd (2005)

[25] Rana R, Soong T.T: *Parametric study and simplified design of tuned mass dampers*; Engineering Structures, Vol. 20, No. 3, pp. 193-204,Elsevier Science Ltd (1998)

[26] Savaresi S, Poussot-Vassal C, Spelta C, Sename O, Dugard L: *Semi-Active Suspension Technologies and Models*; Semi-Active Suspension Control Design for Vehicles (2010)

[27] Siemens mobility: *First Class Bogies*; http://www.mobility.siemens.com/mobility/global/sitecollectiondocuments/en/rail-solutions/components-and-systems/bogies-catalog-en.pdf

[28] Simpack GmbH *SIMPACK Documentation* pg.2419-2420(2015)

[29] Stutts S.D *Equivalent viscous damping*; Missouri State University (2013)

[30] T. Blochwitz, M. Otter, M. Arnold, C. Bausch, C. Clauß, H. Elmqvist, A. Junghanns, J. Mauss, M. Monteiro, T. Neidhold, D. Neumerkel, H. Olsson, J.-V. Peetz, S. Wolf: *The Functional Mock-up Interface for Tool independent Exchange of Simulation Models*; Proceedings 8th Modelica Conference, Dresden, Germany, March 20-22(2011)

[31] Thompson A.G; *Optimum tuning and damping of a vibration absorber applied to a force excited and damped primary system*; Journal of Sound and Vibration 77(3), 403-415 (1981)

[32] Thorby Douglas; *Structural Dynamics and Vibration in Practice: An Engineering Handbook*; Elsevier Ltd. (2008)

[33] ZF Friedrichshafen AG: *Damper Systems For Rolling Stock*; https://www.zf.com/corporate/en_de/products/further_product_ranges/rail_vehicles/chassis_rail_vehicles/chassis_index.html

[34] Zhongzhe C, Yuping H and Naterer G.F: *Design optimization of vehicle suspensions with a quarter-vehicle model*; No. 07-CSME-68, E.I.C. Accession 3037 (2008)